ISSN: 1863-5598

ZKZ 64717
06-26

Bodo´s Power Systems®

20 Years Anniversary

Electronics in Motion and Conversion

June 2026

ed-k
PULSED INDUCTANCE MEASUREMENT

POWER CHOKE TESTER DPG10/20 SERIES WITH 3-PHASE EXTENSION UNIT

Inductance measurement on 1~ and 3~ reactors from 0.1 A to 10 kA

3-PHASE EXTENSION UNIT

- Easy and quick measurement of 3-phase inductors
- Automatic measurement of all windings without reconnecting the terminals
- The software considers the different magnetic flux conditions in the core with 3-phase sinusoidal currents and corrects the measurement results
- The measurement result is equivalent to a conventional measurement with 3-phase sinusoidal mains voltage

KEY BENEFITS

- Very **easy and fast** measurement
- **Lightweight, small and affordable price-point** despite of the high measuring current up to 10000A
- **High sample rate and very wide pulse width range** => suitable for all core materials

APPLICATIONS

Suitable for all inductive components from **small SMD inductors** to **very large power reactors in the MVA range**

- **Development, research** and **quality inspection**
- **Routine tests** of small batch series and mass production

KEY FEATURES OF THE DPG10/20 SERIES

Measurement of the

- **Differential inductance** $L_{diff}(i)$ and $L_{diff}(\int Udt)$
- **Amplitude inductance** $L_{amp}(i)$ and $L_{amp}(\int Udt)$
- **Flux linkage** $\psi(i)$
- **Magnetic co-energy** $W_{co}(i)$
- **Flux density** B(i)
- **DC resistance**

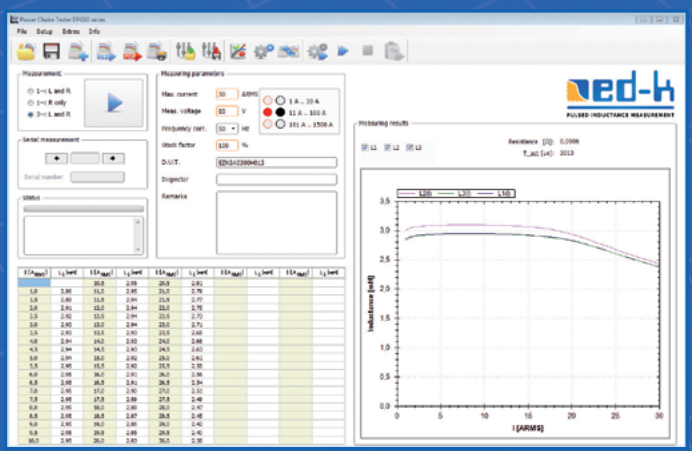

ed-k

Technological leader in pulsed inductance measurement for 20 years

www.ed-k.de

CAPACITORS BUILT TO ENDURE THE EXTREME.

Electronic Concepts
EST. 1969

pcim Please visit us at: HALL 7 BOOTH #300

INTRODUCING

UX3 SERIES HIGH TEMPERATURE UNLYTIC® 125°C

✓ 125°C operation with no voltage derating
✓ Low ESR and ESL
✓ High power DC applications

The UX31 / UX32 / UX34 / UX35 UNLYTIC HIGH TEMPERATURE UX3 SERIES represents the best choice for high power DC application featuring operation to **125°C** with no voltage derating and **acts as a drop in replacement** to existing standard polypropylene capacitors.

electronicconcepts.ie | sales@ecicaps.com | sales@ecicaps.ie

AS9100D CERTIFIED ISO 9001

ecicaps.com

Content

Supporters & Friends

WÜRTH ELEKTRONIK MORE THAN YOU EXPECT

YOU'VE GOT BETTER OPTIONS THAN THAT

Check out our Thermal Management Solutions

WE meet @ PCIM Europe
Hall 6 - 342

Thermal management is crucial for developing durable and efficient designs. Our gap filling, heat spreading, and hybrid solutions deliver optimal thermal management solutions, ensuring your design achieves maximum durability and efficiency. Paired with our expert services and custom solutions, we provide the perfect fit for your application. Ready to keep it cool?

www.we-online.com/thermalmanagement

#THERMAL

Highlights

- Gap filling, heat spreading and hybrid solutions
- Customized components for optimal fit
- Advisory services from technical experts

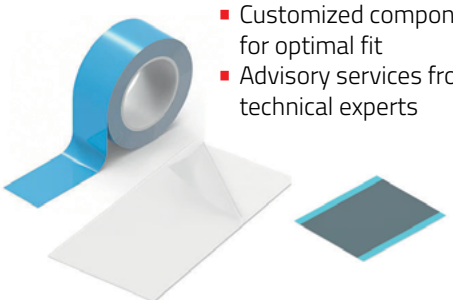

A Media
Katzbek 17a
24235 Laboe, Germany
Phone: +49 4343 42 17 90
Fax: +49 4343 42 17 89
info@bodospower.com
www.bodospower.com

Founder
Bodo Arlt, Dipl.-Ing.
bodo@bodospower.com

Editor in Chief
Alfred Vollmer, Dipl.-Ing.
alfred@bodospower.com

Correspondent Editor Bavaria
Roland R. Ackermann, Dipl.-Ing.
roland@bodospower.com

Editor China
Min Xu – xumin@i2imedia.net

US Support
Rusty Dodge
rusty@eetech.com

Creative Direction & Production
Bianka Gehlert
b.gehlert@t-online.de

Publisher
Holger Moscheik
holger@bodospower.com

Free Subscription to qualified readers Bodo´s Power Systems is available for the following subscription charges: Annual charge (12 issues) is 150 € world wide · Single issue is 18 €
subscription@bodospower.com

Printing by:
Dierichs Druck+Media GmbH & Co. KG
34121 Kassel, Germany

A Media and Bodos Power Systems assume and hereby disclaim any liability to any person for any loss or damage by errors or omissions in the material contained herein regardless of whether such errors result from negligence accident or any other cause whatsoever.

Ecology is free!

"Ecology is free!" is a quote from an interview I once had with the founding CEO of STMicroelectronics, Mr. Pasquale Pistorio, when I met him in Paris/France in 1995. This interview, that I performed for the magazine "Industry Week", mainly covered financials, profits, product roadmaps, management, market positions, investments, strategy etc. and he immediately gave an explanation, why he considered ecology to be "free": "Curing will be more dangerous and more costly than prevention. The companies that get their act together in environmental protection will come up with a strong competitive advantage."

Another aspect: Electrical power "generated" by wind, solar, hydro or tidal power plants does not depend on the prices of fossil fuels as the energy itself is provided free of charge by mother nature. Furthermore, renewables are not involved in the raw fossil energy logistical nightmares in terms of usability of sea passages etc. Therefore, renewables significantly increase the energy supply resilience while decreasing the impact of political dependencies.

This independence from fossil fuels is not just a matter of energy sourcing, but also drives broader technological change across the entire energy ecosystem. As electricity becomes the dominant energy carrier, innovations in power electronics play a key role in how efficiently it can be converted, controlled, and applied. This evolution is clearly reflected in railway traction systems, which have undergone a remarkable transformation over the past decades. By the way, already in 1923 the famous Ofoten Line to Narvik/Norway was electrified for greater efficiency.

However, even in 1995 you could still hear the clunking of notching up in locomotives, where large electromechanical devices switched high-power resistors to control/reduce the current, especially when the train started moving. Today, semiconductors in railway traction inverters have become a standard, and we all know the typical kind of humming. To hear a very special railway inverter sound, search for "musical scale taurus" on Youtube! Using SiC in the inverter enables engineers to increase switching frequencies, and in the long run locomotives will not be humming anymore. SiC inverters provide a higher efficiency, smaller size and weight and need less cooling. To learn more about SiC and GaN in many different applications, reserve December 1 and 2, 2026 for bodoswbg.com. If you don't want to wait that long, come to the Technology Stage in hall 4 at PCIM in Nuremberg on June 10 at 13:25 for SiC and on June 11 at 11:45 for GaN presentations.

Let me come back to trains for a second: Starting in Summer 2028 it will be possible to travel by train directly from Berlin/Germany (15 kV / 16.7 Hz) via Copenhagen/Denmark (25 kV / 50 Hz) and Gothenburg/Sweden (15 kV /16.7 Hz) to Oslo/Norway (15 kV / 16.7 Hz). Power electronics will enable us to travel emission free where before we had almost no choice but to take a plane.

For more than 20 years Bodo's magazine is delivered by postal service to all places in the world. It is the only magazine that spreads technical information on power electronics globally. We have EETech as a partner serving our clients in North America. And don't miss our Chinese version at bodospowerchina.com. An archive of every issue of the magazine is available for free at our website bodospower.com.

My green tip of the month: Consider using a train for both business and for private travel; I often work on the train, but I also enjoy reading, relaxing and streaming a movie. In Europe, you can even get North of the arctic circle by train – directly from Stockholm, which is well connected to Gothenburg.

Alfred Vollmer

Events

GaN Marathon 2026
Florence, Italy June 7 – 10
https://ganmarathon.com

PCIM Expo & Conference 2026
Nuremberg, Germany June 9 – 11
https://pcim.mesago.com/nuernberg

Sensor+Test 2026
Nuremberg, Germany June 9 – 11
www.sensor-test.de

EV Tech Expo Europe 2026
Stuttgart, Germany June 9 – 11
www.evtechexpo.eu

PEDG 2026
Viña del Mar, Chile June 21 – 24
www.pedg2026.com

The Smarter E 2026
Munich, Germany June 23 – 25
www.thesmartere.de

CWIEME Shanghai 2026
Shanghai, China June 24 – 26
www.coilwindingexpo.cn

WPTCE 2026
Halifax, Canada July 6 – 9
https://ieee-wptce.org/

PCIM Asia 2026
Shenzhen, China August 26 – 28
https://pcimasia-shenzhen.cn.messefrankfurt.com

Highest performance for highest bandwidth applications

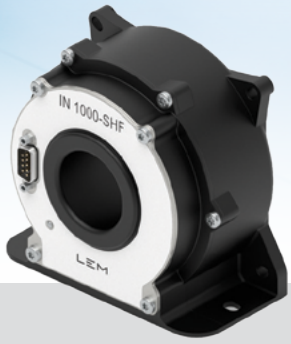

IN 1000-SHF

As industries push performance boundaries—from medical imaging to EV powertrains—precision high-speed current sensing is essential.

LEM's IN 1000-SHF delivers 2.5 MHz bandwidth, sub-nanosecond response time, ultra-low noise, minimal offset, and excellent thermal stability, enabling engineers to monitor fast-switching environments like traction converters and SiC/GaN systems. Designed for electronic measurement of 1000 ARMS (DC, AC, pulsed...), it ensures galvanic isolation between primary and secondary circuits for safe, accurate operation.

As the latest evolution of the IN series, the IN 1000-SHF redefines dynamic performance, unlocking new possibilities for control, efficiency, and reliability in demanding applications.

www.lem.com

- **Closed loop current sensor using extremely accurate zero flux detector**
- **Bandwidth of 2.5MhZ-3dB**
- **Metal housing for optimized immunity to EMC and power dissipation**
- **Operating temperature -40°C to 85°C**

LEM

Life Energy Motion

European Project develops next Generation of On-Board Chargers

The HiPower 5.0 consortium, overseen by the Fraunhofer Institute for Reliability and Microintegration IZM, has produced a 22 kW OBC (on-board charger) with a total volume of four liters, which is far smaller than the current market average of twelve liters. This OBC is based on bidirectional GaN semiconductors from Infineon. The goal of the HiPower 5.0 consortium is to harness the advantages of modern GaN and wide-bandgap semiconductors in market-ready products within a fully European value chain. In addition to the automotive sector, the consortium is also addressing applications in the marine shipping industry. The HiPower 5.0 project brings together partners from ten European nations, including two OEMs, 21 tier-1 and tier-2 suppliers, six specialists for power electronics, ten universities, and seven research institutions. From August 2025 to June 2028, they have been working on six use cases, supported by 33.7 million Euro in funding from the EU and its member states. The German Federal Ministry of Research, Technology, and Space is contributing 5.74 million Euro and the Free State of Saxony is contributing 0.12 million Euro.

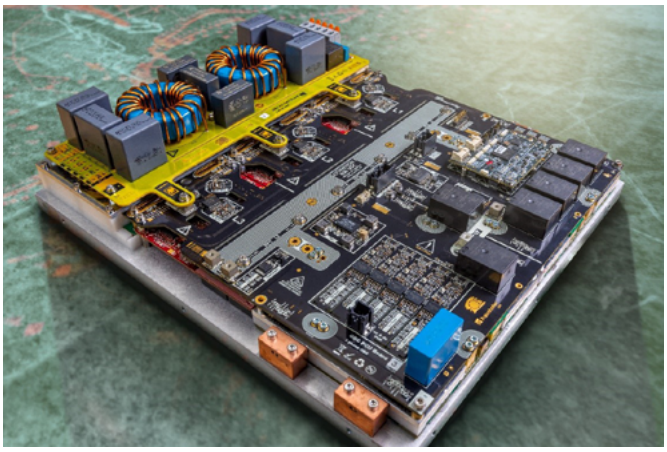

www.izm.fraunhofer.de

Pooling Microelectronics Expertise in Northern Germany

With the launch of the Northern Chip Network e.V. (NCN) at DESY in Hamburg/Germany, companies, universities, research institutions, and innovation partners from the Hamburg and Schleswig-Holstein region are pooling their expertise to strengthen collaboration, initiate partnerships, and further enhance the region's competitiveness, innovative abilities, and visibility. The network aims to more closely link existing strengths in research, education, and industry. Northern Germany possesses expertise across the entire microelectronics value chain – from university education and basic research, through process, product, and technology development, to industrial semiconductor manufacturing. At launch, the NCN includes global industrial companies such as Nexperia, NXP Semiconductors, Semikron Danfoss, Vishay Siliconix Itzehoe GmbH, and X-FAB MEMS Foundry Itzehoe. In addition, there are research partners such as the DESY, the Fraunhofer Institute for Silicon Technology (ISIT), universities such as Kiel University (CAU), the Kiel University of Applied Sciences, and the Hamburg University of Technology (TUHH); as well as key regional innovation and sustainability partners such as the Itzehoe Innovation Center (IZET), the Hamburg Renewable Energy Cluster (EEHH), and the Schleswig-Holstein Society for Energy & Climate Protection (EKSH). As an open network, the Northern Chip Network invites other interested companies, universities, research institutions and regional stakeholders to contribute to its future work.

www.northernchipnetwork.de

Fast Charging Company gets Funding and expands into India

Nyobolt announced it has raised $60 million in funding to accelerate its development pipeline and bring its power performance solutions to the autonomous machines that need them most. The round was led by Symbotic, a company in AI-enabled robotics technology for the supply chain, with participation from IQ Capital, Latitude (Phoenix Court), Scania Invest and CBMM. In data centers GPU racks running large-scale AI workloads generate intense transient power demands that legacy UPS infrastructure was never designed to handle. Nyobolt's fast charging technology is built for these environments, where downtime is not an option and performance cannot be compromised. For example, in Symbotic's SymBot™ autonomous mobile robots Nyobolt's performance battery delivers six times more energy capacity than the ultracapacitors previously used, while is 40% lighter, and achieves at least ten times the cycle life of traditional Lithium-Ion technology, enabling continuous, high-intensity 24/7 operations across Symbotic's warehouse deployments. Nyobolt is also expanding its footprint into India, signing a Memorandum of Understanding with the state of Rajasthan to bring more than 100 MW of off-grid AI data centers and power management infrastructure to one of the world's fastest-growing digital economies. The Rajasthan partnership marks the first of what Nyobolt expects to be a broader presence across multiple Indian states, with a particular focus on renewable energy integration and grid-independent energy storage.

www.nyobolt.com

Electronics for the Future

ROHM
SEMICONDUCTOR

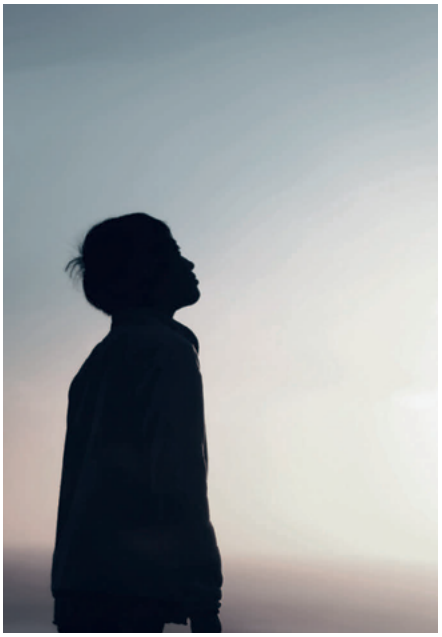

CONGRATULATIONS ON YOUR ANNIVERSARY!

For 20 years, Bodo's Power Systems has been representing technical excellence and high-quality reporting in power electronics.

We thank you for the long-standing, trust-based cooperation and wish you continued success and inspiration!

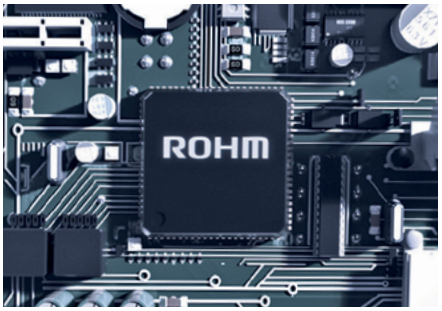

pcim

Let's Meet in Nuremberg
Hall 9 | Booth 318

www.rohm.com

Expanded Capacity for Validation and Services in China

Würth Elektronik eiSos Group opened the Laboratory Phase II at its Asia Quality Design Center (QDC Asia) in Shenzhen, China. Established in August 2008, QDC Asia spans approximately 4,700 m², with a dedicated testing area of 1,700 m² housing over 300 pieces of high-precision testing equipment. Operating in strict compliance with ISO/IEC 17025 and ISO/IEC 17043 standards, the center holds accreditations as a testing laboratory, a proficiency testing provider, and a lab recognized by VDE (TDAP), UL (WTDP), and IEC (CTF2). Initially focused on pre-shipment product inspection for production, the Laboratory has evolved into a comprehensive testing center offering a wide range of services including product incoming inspection testing, design change validation, reliability testing, product conformity judgment, material compliance, failure analysis, etc. However, with existing lab space maximized and approaching saturation, expansion became imperative to support the Group's growing business needs. The newly added 352 m² laboratory is a strategic response to this demand. Primarily designed for environmental and electrical performance testing, the facility is equipped with an energy-efficient VFD chiller featuring magnetic bearing technology, as well as a scalable electrical system capable of meeting peak load demands. A total of 38 testing devices will be gradually deployed across phases to align with actual business needs: 19 units on the ground floor, followed by an additional 19 on a second level. The expansion thus lays the foundation for a significant increase in capacity: In future, throughput for environmental testing is expected to grow by 170 percent compared to current capacity.

www.we-online.com

OCP and Current/OS: Strategic Alliance to Enable DC Adoption in AI Data Centers

The Current/OS Foundation highlights the progress of its strategic collaboration with the Open Compute Project Foundation (OCP), concluded through the signing of an alliance aimed at accelerating the development of Direct Current-powered data center architectures. The foundation aims to drive industry alignment around DC solutions for AI-driven infrastructures, reflecting a shared ambition to transform digital infrastructures into more efficient, sustainable, and high-performance systems, and to establish new standards for the electrical architecture of next-generation data centers. The collaboration is structured around several key deliverables including a comprehensive white paper, Data Center Facility – Low Voltage Direct Current Power Distribution, detailing architectures and best practices for scalable AI infrastructure. It is complemented by a training program available in the OCP Academy to educate engineers and professionals on open-standard system design and deployment and it also includes a formal specification document defining technical requirements, interfaces, and interoperability standards to enable vendor-agnostic innovation. The alliance between Current/OS and OCP aims to promote the adoption of open standards for DC architectures in data centers and to unite an ecosystem of industrial, technological, and academic stakeholders around this transition, addressing the growing challenges of power consumption, performance, and sustainability. The two organizations will work to reduce electrical conversion stages, increase power density for AI workloads, and enhance infrastructure resilience while simplifying electrical architectures. The initiative also aligns with open and interoperable standards to foster innovation, industrial adoption, and compatibility across the ecosystem.

www.currentos.org

Strategic Collaboration for 900 V EV Platforms

Onsemi announced an expanded strategic collaboration with NIO to power next-generation electric vehicle (EV) platforms. Building on a multi-year partnership, the companies are more closely engaging to accelerate NIO's transition from 400 V to 900 V architectures by using onsemi's EliteSiC M3e technology. The expanded collaboration builds on a partnership, which began with onsemi's EliteSiC technology supporting NIO's 400 V platforms and has evolved into a strategic, system-level alignment. Today, onsemi's EliteSiC technology underpins NIO's transition to 900 V architectures, including its latest flagship SUV, the ES9, and additional model. The companies' collaboration reflects a broader shift in the auto industry toward closer alignment between automakers and semiconductor companies, as vehicles become more power-intensive. By supporting system-level integration, onsemi is helping customers bring scalable, higher-performance electric vehicle platforms to market more quickly and efficiently while reducing development complexity and accelerating execution. This approach is becoming increasingly important as automakers transition to higher-voltage architectures and more advanced electric drive systems.

www.onsemi.com

WE **ENGINEER** POWER ELECTRONICS **FOR A BETTER FUTURE**

SEMIKRON DANFOSS

High-power SiC IPM

Addressing the 1500V_{DC} Challenge on System Level

Visit us at

PCIM Expo

Nuremberg, 9 - 11 June
Hall 7, Booth 459

SKiiP® 4

500kW up to 3MW

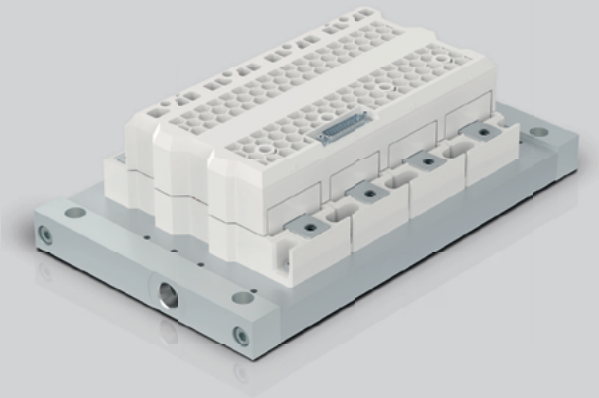

Focus on your innovation – powered by SiC, ready as a system-level building block.

Whether you are advancing Power-to-X and green hydrogen production, optimizing high-efficiency motor drives, designing for 1500 V_{DC} grid architectures, or improving power quality and active filtering – you need reliable, high-performance power. We deliver it. Across renewable energy and industrial power conversion applications, SKiiP 4 SiC 2 kV is your advantage.
The power tool built for the 1500 V_{DC} challenge.

Features

- 2kV SiC MOSFETs
- Half-bridge and multi-phase configuration
- System-level design interface
- Driver, sensors, heatsink
- Optimized performance and short-circuit control
- Self-protecting system
- 100% burn-in tested
- 500kW to 3MW

SiC Silicon Carbide

semikron-danfoss.com

Intelligent Power Modules from India

In presence of India's Prime Minister, Mr. Narendra Modi, Alpha and Omega Semiconductor (AOS) has officially inaugurated its Kaynes Semicon's OSAT facility in Sanand, Gujarat. Now AOS' proprietary IPM5 manufacturing process is implemented at the Sanand facility. The IPM5 (Intelligent Power Modules) integrate 17 different dies into a single package, providing the core "intelligence" for next-generation motor controls and energy-efficient appliances. From groundbreaking to product delivery it took 14 months to establish the facility.

www.aosmd.com

President of ESIA elected

The General Assembly of the European Semiconductor Industry Association (ESIA) elected Erik Rein, Executive Vice President and Board Member Mobility Electronics responsible for semiconductor business at Bosch, as the organisation's new President. He succeeds Michael Budde, who has stepped down from the ESIA Presidency following his recent change of responsibilities within Bosch. Erik Rein has worked in semiconductor-based mobility solutions, manufacturing, purchasing, and quality management. In his position, he is responsible for Bosch's global semiconductor and sensor business.

www.eusemiconductors.eu

Senior Vice President and GM appointed

OmniOn Power (OmniOn) has appointed Brian Korn as the new Senior Vice President and General Manager of its Core Products business. Korn brings more than 20 years of experience in power products spanning board mounted, front end, and specialized power solutions for data center, telecom, and network infrastructure applications. At OmniOn Power, Korn will be responsible for defining the strategic direction, driving the operational execution, and overseeing the long-term performance of the company's Core Products business. Korn joins OmniOn from Advanced Energy, where he held senior leadership roles overseeing embedded and front end power products for key growth industries. Earlier in his career, he led product and business teams at Cisco Systems, Equinix, Sun Microsystems, and Silicon Graphics.

www.omnionpower.com

Starting with Automotive Components: Production Start for third Generation of SiC Devices

Bosch has started to introduce its third-generation silicon carbide chips and is supplying samples to global automakers. Bosch has invested around 3 billion euros in semiconductors as part of Europe's IPCEI (Important Projects of Common European Interest) funding programs for microelectronics and communication technology. Its wafer fab in Reutlingen, Germany, develops and manufactures the third generation SiC chips on 200-millimeter wafers. In September 2023, Bosch acquired a second fab for SiC chip manufacturing in Roseville, California, and is currently equipping it with production facilities. The company is investing an additional 1.9 billion US-Dollar in the U.S. plant, which plans to manufacture and deliver its first SiC chips this year – initially as samples for customer trials. Originally developed for sensors, the so-called "Bosch process" enables manufacturing of high-precision vertical structures in silicon carbide. This design increases the chips' power density – a decisive factor for the third generation's performance. Analyses by the market research and consulting company Yole Intelligence forecast that the global market for SiC power semiconductors will grow from 2.3 billion U.S. dollars in 2023 to around 9.2 billion U.S. dollars by 2029, driven primarily by electromobility.

www.bosch.com

Fuji Electric
Innovating Energy Technology

8th Generation IGBT Modules

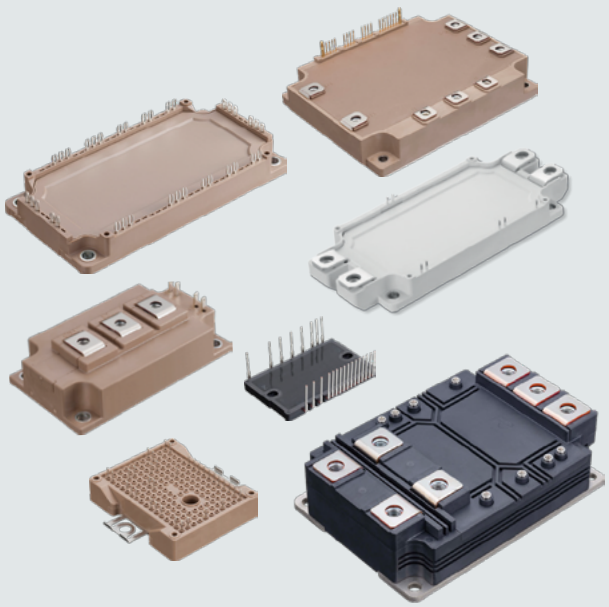

MAIN FEATURES

- Power loss reduction through optimized chip technology
- Improved reliability at high temperatures
- New solder material enables to operate at case temperature Tc=150 °C
- System cost reduction by increasing power density

10-15% reduction in total power losses

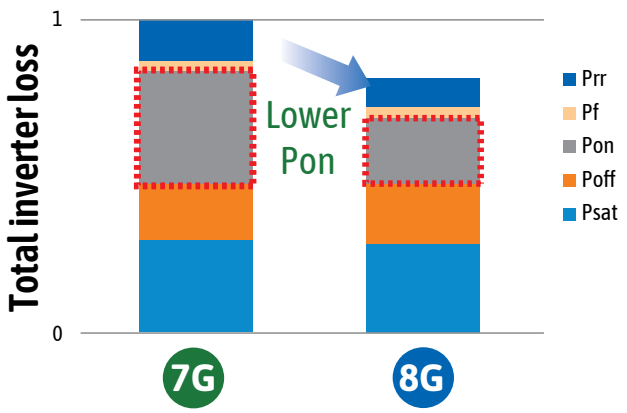

1200V device, fc=4kHz, recovery dv/dt(10-90%)=4kV/µs, continues operation

pcim
9 –11.6.2026
NUREMBERG, GERMANY

www.fujielectric-europe.com

300 mm Fab: First Tool Move-In in Itzehoe

At Vishay's facility in Itzehoe/Germany the first tools have moved in – kicking off with fully automated wet chemistry equipment from Siconnex. Using spezialized equipment, the Siconnex equipment were set into their final footprints in this 300 mm fab. Vishay is setting up a fully automated production line dedicated to automotive MOSFETs. By taking this strategic step in Europe, Vishay is sending a decisive signal regarding supply security for the European automotive sector. In an era where "supply chain sovereignty" has become the defining priority, this expansion is set to create approximately 150 new jobs at the facility. The systems, custom-tailored for Vishay, are specifically configured for metallic etching (AlCu) and post-dry-etch polymer removal. Siconnex got this position primarily due to its BATCHSPRAY® technology, which delivers in critical areas like footprint efficiency, resource management as well as automation & safety.

www.siconnex.com

Joint Supply Chain Intelligence Initiative

The Global Electronics Association and CalcuQuote, Elisa Industriq announced a partnership to deliver timely, actionable supply chain intelligence for the electronics industry. The collaboration combines the Association's global industry perspective with CalcuQuote's real-time sourcing and supply chain data to give companies clearer visibility into market shifts and greater confidence in sourcing decisions. The partnership will translate aggregated market signals into practical insights that help companies identify emerging pressures earlier, reduce sourcing risk, and respond more quickly to shifting conditions. All insights and reporting will be generated from aggregated and anonymized data to protect confidentiality. Global Electronics Association points out that the value of this partnership goes beyond any single presentation or dataset and that this collaboration further strengthens the Association's global data programs as it continues building insight across the full electronics supply chain. CalcuQuote, Elisa Industriq emphasizes that no single company has a complete view of the supply chain and that real progress comes from combining perspectives. The initiative is expected to include market reports, trend analysis, and other intelligence resources designed to help stakeholders across the electronics supply chain monitor risk, interpret market developments, and make faster decisions. The organizations will share additional details on the initiative's research focus and planned deliverables as the collaboration progresses. Global Electronics Association is the voice of the electronics industry, working with more than 3,000 members, thousands of partners, and dozens of governments to ensure a more resilient supply chain and drive industry growth. Formerly known as IPC, the organization serves a $6 trillion market and has offices across Asia-Pacific, Europe, and North and Latin America.

Global Electronics Association™

www.electronics.org

Call for Nominations for 2027 Global Energy Efficiency Award

Recognizing that energy efficiency is critical for addressing climate change and advancing sustainability, PSMA has started the call for nominations for its 2027 Global Energy Efficiency award on Earth Day. Nominations must be submitted by September 8, 2026 by visiting the 2027 Global Energy Efficiency Award web page at www.psma.com/technical-forums/energy-management/energy-efficiency-award. There is no cost for submissions, and nominees do not need to be PSMA members. The 2027 winner will be awarded at APEC 2027. PSMA (Power Sources Manufacturers Association) established its annual Global Energy Efficiency Award in April 2024 to recognize breakthrough innovations that deliver meaningful energy savings across industries and applications. Eligible nominees include any company or organization worldwide that designs or manufactures electrically powered systems. Award criteria focus on energy efficiency (rather than renewables or electrification), appliances and equipment (rather than building codes) and high global impact. So the award seeks to spotlight solutions that go beyond incremental improvements, showcasing advancements that prioritize energy efficiency in appliances and equipment while demonstrating a high potential for global impact. Furthermore, the award is intended to be an inspiration for continued innovation within the power electronics community because energy efficiency is more than respecting the environment or meeting regulations. PSMA explicitly points out that it makes a key difference in the lives and business of customers in terms of utility bills, longer battery life, lighter portable devices, longer system lifetimes, reduced cooling and maintenance, and higher reliability due to lower thermal stress. These benefits make energy-efficiency solutions indispensable—and worthy of recognition by our industry.

www.psma.org

Japanese precision since 1935

HIOKI

Precision Current Clamps for every application

2 to 2000 A max

DC to 2 MHz

⌀ 50 mm max

up to 0.07 % accuracy

shop.hioki.eu/current-clamps

HIOKI EUROPE GmbH | Helfmann-Park 2 | 65760 Eschborn | hioki@hioki.eu

What a Journey!

Bodo in his young days

I was born after World War II and grew up in peace, but I missed my Grandpas and Uncles, as they were taken by the wars. It was the time when hard working parents made the "Wirtschaftswunder" in Germany. My older Brother ignored his Märklin train set. So I got my hands on the trains at the age of five and was fascinated by the technology. That was the beginning of my love of engineering. From before Christmas up to Easter, I turned our living room into a HO miniature wonderland, where my duty also included the full cleaning of the living room.

Finally, I became an engineer and worked in design for rotogravure and other industrial projects like contact lens manufacturing equipment.

My most exciting time was working for RCA and later Harris introducing the MOSFETs and IGBTs to the European market. Working with Frank Wheatley, the inventor of the IGBT and his boss Don Burke together with Fred Lokuta gave me a deep insight into power electronics. There are more friends from Mountaintop that helped my journey. Gary Dolny, Chris Rexer, Harald Ronan, Wallace Wiliams and others who taught me to understand semiconductors from the very basics.

That took a quarter of a century and now another quarter has passed by as an editor.

So, 20 years ago I started to publish my own magazine, which now enjoys a world-wide distribution with an added Chinese franchise.

Bodo's Power Systems is celebrating its 20th anniversary. And the journey continues. Holger, as part of my family, will take it into the future, and Alfred will continue to support us. I will have time to work on my train layout, take my 1974 beetle convertible for a ride and enjoy life as usual.

Here are some little anecdotes from the past:
After a Spoerle party (now Arrow) in Dreieich near Frankfurt my colleges and I returned to our hotel. The following day was my Birthday and so we had a midnight party in my hotel room, having fun and emptying the mini bar. Next morning the lady at the front desk asked me if I had something from the mini bar and I answered one. She said "What?" and I said "The mini bar!".

Visiting Chicago in 2001 for PCIM I had booked a Radisson hotel. On arrival it was familiar to me and I asked the young lady behind the front desk if it had been a Sheraton. She answered "yes of course before I was born". That gave me a good indication of my age!

Again in Chicago working for Reed, this time as the editor in chief of the PCIM Magazine. Reed had a booth and a girl handling all the publications that had been laid out. I arrived and looked at all of them. The girl said you can take away as many as you like. I took the whole pile of PCIM magazines and walked away. I walked through the exhibition halls and talked with people on their booths and left a magazine with each of them. Returning to the Reed booth, I picked up the next pile of PCIM magazines, which made the girl look at me. So I opened page four in the magazine and she said "oh, that picture is of you and you are the editor".

These were the days of safe travel with no war. Now we have the world on fire. Too many battles are ongoing. There are no leaders in the world to find safe solutions. Is there too much personal profit involved that too many young people must die? We must all work and vote for a peaceful future for our Kids and Grandkids.

I always enjoy reading Bodo's Power magazine. It's a very informative magazine, with excellent articles and useful advertising. There's no other power electronics magazine that's as useful, and I'm a big fan of Bodo's Power.
I am very much fascinated about the content you provide in your monthly magazines. It is well organized with very useful content.

thank you for a great magazine. Besides a local Swedish magazine Elektroniktidningen, Bodo Power is the only magazine we read at work.

I am now retired from the electronic business. I spent wonderful times reading your precious articles. Thank you so much. Take care and long life to your mag.

Just wanted to tell you that I loved your Viewpoint in the latest issue of Bodo's Power Systems. (I showed it to my wife, who also was impressed by it.) Although the vast majority of human beings are good people, there are too many who harbor hate or fear of those who are different' from them, even though, in truth, they are not very different.

I have been a regular and devoted reader of Bodo's Power for many years. I just wanted to let you know how I appreciate your magazine and am always pleased to receive a new copy.

I work for ABB, where your journal helps me keep up with new developments, both in detail and on a generalist level. It also satisfies my private interest as in an earlier job I was involved in designing tests for IGBTs. This interest has remained with me since. I would like to thank you for the valuable publication and hope you will keep publishing it for a long time. I also wanted to take the chance to congratulate with you and your team for the excellent job you do every month. The magazine, website…fantastic resources for electronic engineers (and more).

It's my first time reading through the magazine, and I'm glad I took the time! It was well written and contained several helpful and interesting articles.

I still enjoy thumbing through your magazine each month to get a feel of what is going on in the world of power electronics. I've been retired for over 7 years now and am looking forward to my 78th birthday in a week. Still keep in touch with a few of the old RCA crew. We meet for lunch every few months. Jack W., whom I'm pretty sure you remember, is one of them.

Being a Power Electronics engineer, it gives always a feeling of pleasure, everytime I see your email on market updates. May it be A new driver, new design, new Sic device by leaders like Infineon, EPC, ST, Cree and all .or even updates on Exhibition, or design Webinars.

I was glad to read your recent editor's page "Working for Peace". You did really a great job in committing yourself to the idea of a world that works without the pain and fear of war and the soulless brains seeing Warcraft as a legitimate act of power conservation and even a future-oriented planet. I am sure that not all of your customers and business contacts welcome your clear statement. However, I my eyes, a peaceful world is the only solution and also the way of sense. I wish you much success and hope that you "stay mature enough", as you put it.

I'm used to read all of your editorials and I like your monthly green advice. I'm probably not the only person to write you regarding your October's editorial. My message is meant to counterbalance things others might tell you. While several of your comments will upset many people in various industries, I personally found your stance very courageous. You did not avoid the risk of losing a few readers who put more value in profit than preserving human life and its habitat. Instead, you chose putting forward a strong message of humanity. The shock for me was not the message but into which magazine it is published ! By comparison, other magazines act as if their editors had no involvement at all in the well being of the planet and its inhabitants. "Science sans conscience n'est que ruine de l'âme" wrote Rabelais. It's good to see that you care about this motto. Congratulations mister Arlt.

High Resolution 10kV Modular Measurement System for Solid State Transformer Testing

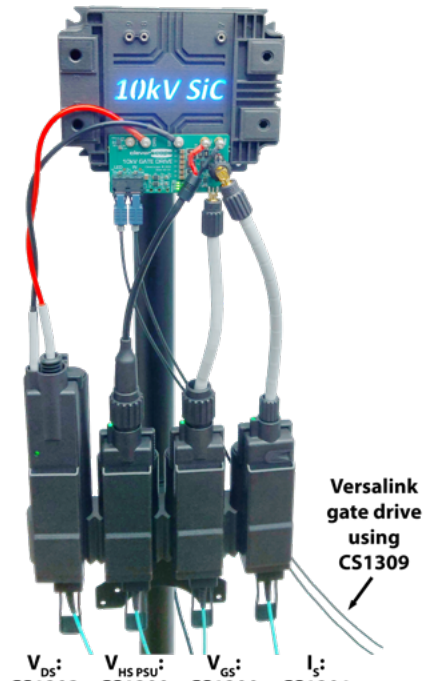

CS508 Oscilloscope

The rapidly increasing power required for Data Centers and Electric Vehicle Charging is driving development of Solid-State Transformers (SSTs). Migrating from 50/60Hz Transformers to higher frequency SSTs for converting medium-voltage (13.8 – 35 kV_{AC}) to 400 V_{DC} or 800 V_{DC} introduce benefits such as lower operating currents, improved efficiency, with smaller form factors, weight, scalability and bi-directional operation. The new CS1203 10 kV Digitizer is the latest addition to the Solid-State Transformer Test Solution from Cleverscope. It is precisely designed to support researchers and engineers in pushing the blocking voltages of power MOSFETs to 10 kV. Increasing the blocking voltage of the transistors from 3.3 kV to 10kV decreases the number of stages in the SST with improved reliability and lower costs.

The Challenge of measuring Efficiency in Multi-Level Solid State Transformer

Decreasing the number of stages imposes new requirements for measuring efficiency when trying to reach >99 %. With individual stage offsets up to several tens of kV, the need for high common mode voltage resilience paired with measuring smallest signals like V_{GS-ON} on tens of kV floating potential, becomes more challenging with blocking voltages rising beyond 3.3 and up to 10 kV. Also, R_{DS-ON} values are roughly the same compared to 1.2 or 3.3 kV modules to keep the conduction losses minimal. The implication is that VDS-ON will be a smaller fraction of the 10 kV blocking voltage than of 3.3 kV, resulting in a higher resolution and accuracy needed compared to testing legacy modules. And this brings new challenges for the test instrumentation, because the accuracy of the instruments needs to be higher than before.

Optical Isolation for precise and safe measurements

The Cleverscope CS1203 digital fiber isolated digitizer has a 14 bit ADC, 1.25 V resolution in the 10 kV measurement range and common mode rejection ratio (CMRR) of >100 dB at 50 MHz. This enables precise insight into the Drain-Source Voltage analysis during ON- and OFF-phases of a switching cycle. Paired with the CS1201 digital fiber isolated digitizer for current measurements of I_S up to 630 A, high precision switching and conduction loss analysis can be performed with excellent accuracy. The CS1200 fiber isolated remote digitizer completes the set for testing V_{GS} during a Double Pulse Test for optimization and reliability testing.

All signals are digitized directly in the remote digitizers, hence at the test point, and then sent digitally to the CS548 oscilloscope for lowest noise performance. The CS1203 is specially equipped with high voltage silicone insulated wire connections. For safe and easy control of the gate drivers, the CS1309 Fiber Isolated Digital Output Pod in combination with CS548 control oscilloscope can be utilized. PWM control can be set to drive a Single, Half-Bridge, Full-Bridge or Double Pulse Setups. The CS1309 connects via industry standard Versatile Link 1 mm fibers to the Device Under Test.

This modular system with Remote Digitizers & Digital Output Pods is controlled via the CS548 Oscilloscope from Cleverscope. It can be operated on any modern PC with the free of charge software or directly be implemented into a customer written automated test software.

Banner Specifications:

- CS1203 Input Ranges V_{DS}: ±1 kV & ±10 kV
  - Voltage Resolution: 125 mV in ±1 kV range & 1.25 V in ±10 kV range
  - Noise: 375 mV_{RMS} in ±1 kV range & 3.75 V_{RMS} in ±10 kV range
  - High Voltage silicone insulated wire connection
- CS1200 Input Ranges V_{GS}: Probe attenuation dependant
- CS1201 Current Ranges: up to ±630 A pulsed and higher options available
- ADC Resolution: 14 bit
- CMRR: >100 dB @ 50 MHz
- Analog Bandwidth: 200 MHz
- Common Mode Voltage: >30 kV
- Fiber cable length: 1 - 30 m
- The CS1200, CS1201 and CS1203 are used with CS548 oscilloscope from Cleverscope.

Controlled by the powerful Cleverscope UI, or use our driver to create your own custom test system application in C, MatLab, VB.Net, Python or Labview.

www.cleverscope.com

Taste Japan.

Talk to our power semiconductor experts and
experience Japanese craftsmanship with all senses.

Meet us at
PCIM Expo 2026
Hall 7, Stand 409

Exhibition preview & meeting requests:
semis.info@meg.mee.com
www.pcim.meu-semiconductor.eu

MITSUBISHI ELECTRIC
Changes for the Better

DC/DC Power Modules: Intelligent Switching for efficient Applications

DC/DC power modules provide massive advantages in industrial and predictive maintenance applications. The ability to adapt dynamically to different load conditions saves energy. This not only leads to extended battery life, but also to a reduction in thermal stress, which increases the reliability and service life of an entire application.

By Timur Uludag, Senior Technical Marketing Manager, Würth Elektronik eiSos Group

Conveyor belts, presses, chipping machines, etc. have been an integral part of industrial plants since the industrial revolution. However, every machine needs to be serviced from time to time. Depending on the intensity and duration of use, wear occurs, and some machine components wear out faster than others. However, the wear and condition of a machine is often not directly visible from the outside. Poorly maintained machines lead to rejects, wasted resources and increased production costs. Not to mention the fact that even minor machine malfunctions can quickly lead to long production line downtimes and even safety risks.

Common practice is to service the machines at regular intervals as defined by the machine manufacturer to avoid breakdowns, regardless of whether there is a specific problem or not. The digitalization of industrial production, known as Industry 4.0, relies on the networking of machines, devices and sensors with people. The data about the status of the machine is transparent and can be called up at any time. Industry 4.0 thus enables a "predictive maintenance" strategy for machine maintenance.

Figure 1 shows a typical application in an industrial environment for a sensor concept supporting "predictive maintenance".

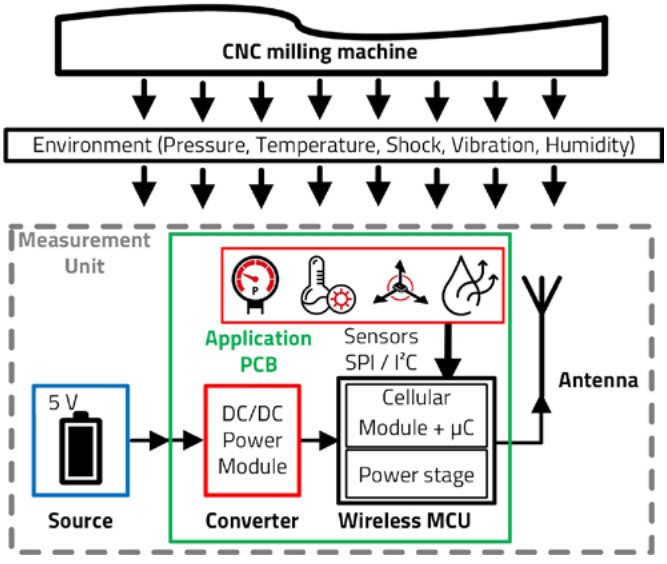

Figure 1: CNC milling machine with predictive maintenance structure

The wireless MCU (cellular module with µC + power stage) records the values of temperature, vibration, shocks and humidity according to a defined time interval and sends them as a data packet to a server, which then processes the data further. The data serves as the basis for "predictive maintenance" to determine the status of the machine and then decides whether maintenance needs to be carried out. The transmitter is supplied via a DC/DC power module with 3.3 V, which draws its energy from a battery. The measurement unit consists of the components / functional units shown in Figure 1. A DC/DC power module, transmitter and sensors are placed on a single circuit board. The battery and the antenna are in a housing together with the circuit board. It is precisely at this point that the power supply plays a critical role.

To get the longest lifetime out of a battery you need a highly efficient power supply. This involves both efficiency in terms of the current drawn from the battery and the heat generated by the power module, which can have a negative impact on the service life of the battery. As industrial application environments can have high ambient temperatures, the power module's thermal derating must start as late as possible to ensure full and efficient operation.

The trend in the field of DC/DC power modules is moving away from specialization towards an "ultimate approach". This means that the power modules no longer have just one outstanding feature that they need for use in a specific application but have a myriad of features that make them indispensable for a wide range of applications.

Each of the applications described places specific requirements on the DC/DC converter supplying the power. This article looks at the individual requirements and provides an overview of how a DC/DC power module from the WPME-VDMM series can fulfil them.

If we look at the requirements for the DC/DC converter in the applications described, they can be summarized by the following four criteria:

- Load Optimized Switching
- Efficient Use of Energy
- Power sequencing
- Full power over the entire temperature range

Load Optimized Switching

Battery-powered applications, such as the one described, do not always operate under full load conditions. A measurement application, for example, has a higher power requirement during measurement and a lower power requirement between measurements.

The different load conditions can be described as follows:

- The application operates in idle or standby mode →
  Very low power consumption µA - range
- The application operates in light load mode →
  Low current consumption mA range
- The application operates under rated power →
  Normal current consumption mA-A range

Optimum switching behaviour for a DC/DC power module should adapt dynamically to the load requirements.

Erik Rehmann, GVA expert for Quality Management

MEET THE EXPERTS:

pcim

EUROPE

9. – 11. June 2026 in Nuremberg
Hall 9 · Stand 432

gva-power.de

„WHERE INNOVATION GOES IN SERIES: GVA"

Our Development, Production and Quality departments are separated by one floor and two flights of stairs – nothing else. Because all GVA experts share the same systemic understanding and the latest know-how. That´s why we are able to mass-produce innovative developments in the shortest possible time. With guaranteed quality – and gladly also for you!

Your GVA expert:
Daniel Bonanno
+49 (0)621 / 78992-27
d.bonanno@gva-power.de

YouTube

GVA
POWER ELECTRONICS EXPERTS

Switching losses and line losses are the two most important influencing factors when considering the optimum switching behaviour of the power module. Using the example of a buck converter, switching losses occur during the ON phase. Line losses, on the other hand, occur during the OFF phase when the load is supplied with power.

At low loads, the power module should switch little or not at all, as switching is the main cause of losses. To achieve this, adaptive switching behaviour is required. Furthermore, an intelligent system must be able to switch automatically between these modes depending on the current load requirement.

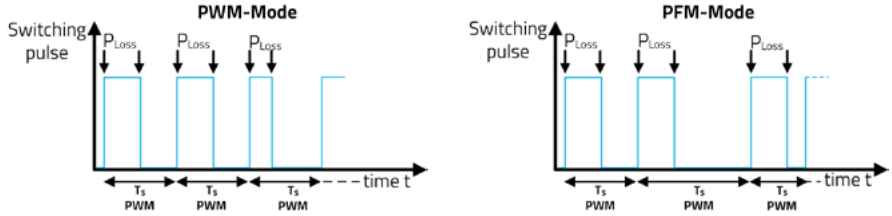

Figure 2: Different load conditions require different switching behaviour: PWM mode at full load (left) and PFM mode at low load (right).

Figure 2 (left) shows the "typical" behaviour expected of a standard buck converter operating in pulse width modulation (PWM) mode. A variable pulse width is generated while the switching frequency remains fixed. The period duration T_S is the same for all cycles. PWM mode is widely used and is found in most industrial power supplies. This mode is satisfactory for the type of applications that operate under heavy load conditions for most of their operating life. However, applications such as sensors have a different load behaviour. Here, light load operation is the predominant operating situation. The switching behaviour must therefore be adapted so that it functions optimally in this load situation. In pulse frequency modulation (PFM) mode, the frequency varies. If you compare PWM mode and PFM mode, as shown in Figure 2 (right), it becomes clear that PFM mode offers greater efficiency, as fewer switching operations take place over time and therefore the switching losses are lower. During the idle time in PFM mode, the module does not produce any losses compared to PWM mode.

The VDMM 1710x560 power modules automatically transition between both modes of operation based on the load conditions. In light load conditions the module operates in PFM mode. This mode is characterized by reduced current consumption which leads to higher efficiency. For the following explanation, a buck converter as shown in Figure 3 is used as the basis.

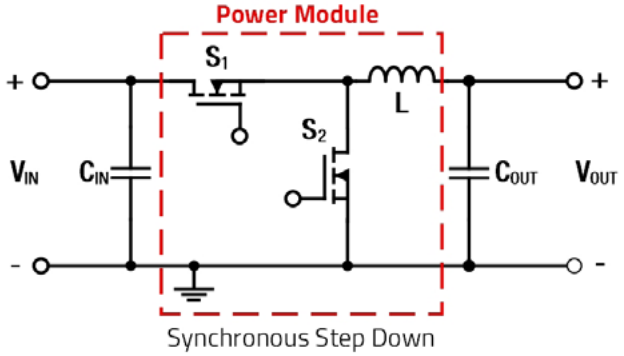

Figure 3: Synchronous Step-Down basic circuit.

In PFM mode, the power module begins by switching S1 and S2 as in PWM mode for a short period of time to charge the output capacitor. When the threshold for the output voltage is met, the device stops switching, leaving both S1 and S2 off, and the load is supplied entirely by the output capacitor. During this time, there are no switching or conduction losses within the power module.

While the load is being supplied, the output voltage slowly decreases according to the power consumed. The module monitors the output voltage and when a certain limit value is reached, another burst of switching is triggered, and the cycle is repeated. As the load current increases, the idle time decreases and the switching time increases until the idle time reaches a minimum threshold where the module switches to PWM mode.

Efficient Use of Energy

The efficiency curves in the data sheet for the power modules 171010560, 171020560 and 171030560 show various combinations of V_{IN}, V_{OUT} and I_{OUT} in the "TYPICAL PERFORMANCE CURVES" [1].

How does the efficiency of a power module affect an application that is powered by a battery or rechargeable battery? The lifetime of a rechargeable battery is significantly influenced by two primary factors: by the number of discharges and charges as well as by the battery temperature.

The lifetime of a lithium-ion battery is strongly influenced by the number of charging cycles. A charging cycle is defined as the discharging and subsequent recharging of a total of 100 % of the battery capacity, regardless of whether this is done in one or more partial discharges. In general, the capacity of a lithium-ion battery decreases with the number of charging cycles. This means that the battery can store less energy with each charging cycle. Decreasing the number of charging cycles must be the goal for battery-driven applications to reduce costs by decreasing maintenance intervals.

Based on the power consumption shown in Figure 4 of a sensor application with a cellular module, the time after which the battery must be recharged at a specified measurement interval is calculated as an example. This is based on different efficiencies of the power module.

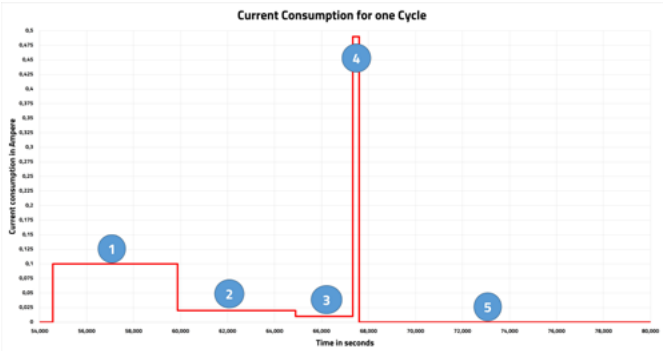

Figure 4: Typical power consumption of a cellular module over time.

The cellular module consists of a microcontroller (MCU) that offers integrated functions for wireless communication. It combines the computing power of a microcontroller with wireless communication protocols such as LTE, Bluetooth, Wi-Fi or others. Wireless MCUs are often used in applications that require wireless data transmission, such as predictive maintenance, the Internet of Things (IoT) and industrial control systems. They enable devices to communicate with each other without physical cables, which increases flexibility and ease of use in many applications.

The following is a brief description of the progression over time shown in Figure 4, described as the various modes of the MCU and the LTE modem:

Section 1: MCU is ready to collect data, LTE modem is establishing a connection

Section 2: MCU acquires the sensor data (here the temperature as an example), LTE modem is in IDLE mode

Intelligence in every battery cell

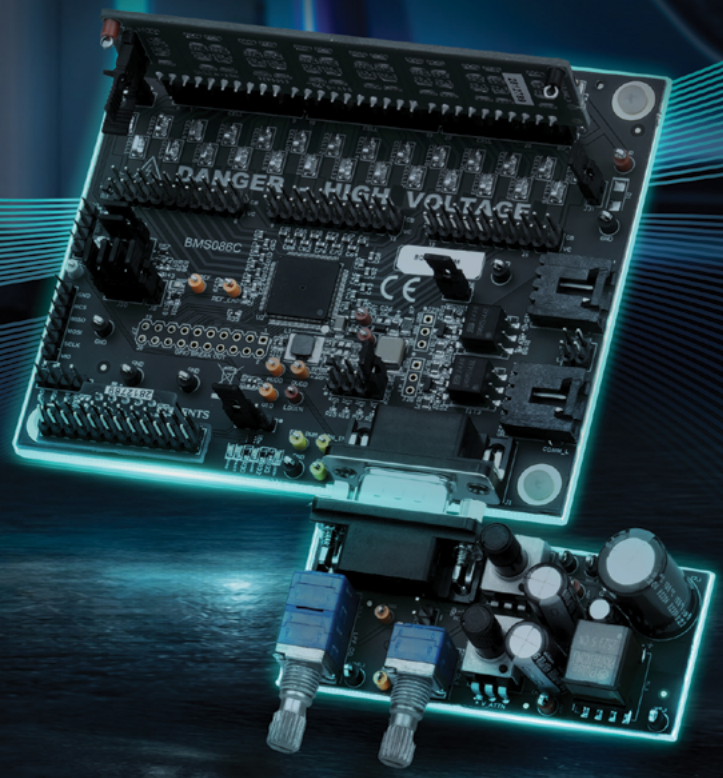

Visit the Texas Instruments booth at PCIM to see how we're innovating what's next in power

Hall 7 | Booth 652

Texas Instruments

70 years in Europe
est. 1956

Section 3: MCU and LTE modem are in IDLE mode and waiting for the transmission interval
Section 4: MCU sends the data to the LTE modem and the LTE modem sends the data to the remote station
Section 5: MCU is in shut-down mode and the LTE modem is in deep sleep mode

Each section is represented here by an electrical charge in ampere hours (Ah). The sum of these values gives the total requirement in Ah for a complete cycle. Based on this value, it is possible to calculate how many cycles can be run before the battery will be fully discharged.

Calculation example:
- Battery with 2800 mAh (2.8 Ah) capacity
- Load current of the application of Figure 4
- Power module output voltage 3.3 V
- Efficiency of the DC/DC converter

The table shows the measured values of the application shown in Figure 1. The values for the power requirement of the power module and the efficiency are based on real measurements. The corresponding values for the required charge are based on the following equation.

$$Q = I_{IN} \cdot t_{IN}$$

I_{IN} – Input current of the power module typ. [A]
t_{IN} – Duration of the input current of the power module [h]

Section	Charge [Ah]	Input current cellular module typ. [A]	Input current power module typ. I_{IN} [A]	Efficiency power module typ.[%]
1	0,00010464	0,10	0,0709	93,3
2	0,00002008	0,020	0,0144	91,4
3	0,00000494	0,010	0,0073	90,0
4	0,00002629	0,49	0,347	93,5
5	0,00000090	0,000009	0,000068	10
∑	0,00015683			

Each cycle with a duration of approximately 70 seconds according to Figure 4 therefore requires 0.00015683 Ah. If we now assume a measurement interval of 60 measurements per minute, 8 hours per day for a 5-day week, this will result in a consumption of 0.376403023 Ah per week.

For a battery with 2800 mAh = 2.8 Ah, this means that it would have to be recharged after approximately 7.4 weeks. To see the effects of efficiency on the time until a recharge would be necessary, the operating efficiencies of each section will be decreased by 2 %, 5 % and 10 % and shown in Figure 5, which clearly shows that the maintenance interval is strongly influenced by the efficiency of the power module.

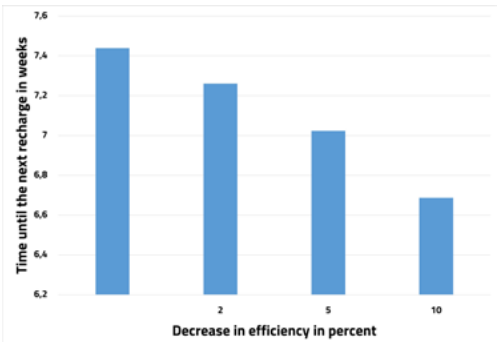

Figure 5: Dependence of the recharging time on the efficiency of a DC/DC converter.

Efficiency impacts more than just charging intervals in a battery-powered system. If the efficiency in a system decreases, more energy will be dissipated as heat. In a space-constrained application this could mean the entire system is operating at a higher temperature. Batteries are highly susceptible to heat, directly impacting service life. At high temperatures, the chemical reactions within the battery accelerate, which leads to faster ageing of the cells. This can lead to a reduction in capacity and increased self-discharge. It can also lead to degradation of the electrolytes and damage to the internal structures of the battery. In the long term, this can reduce the number of charging cycles that the battery can go through before its capacity decreases to an unusable level. To maximize the service life of a battery, it should ideally be operated and stored at moderate temperatures.

Choosing a power module with the highest efficiency provides benefits in the short-term, as shown in the time between recharges in Figure 5, as well in the long-term by decreasing aging and stress on the battery.

Power sequencing

In systems that require several voltages, such as microcontrollers and DSPs, the voltages often must be provided in a specific time sequence. Figure 6 shows an example of this behaviour.

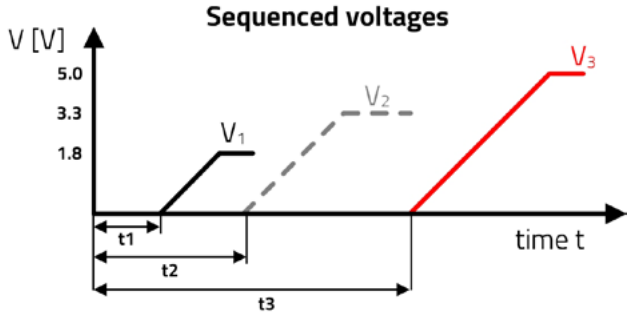

Figure 6: Sequential ramp-up of supply voltages.

The three voltages V_1, V_2 and V_3 are not applied to the load at the same time. Each of the voltages is required after a certain time period. V_1 is switched on after the time t_1. The second voltage V_2 starts to rise after V_1 has reached its nominal value. V_3 is switched on last, waiting for V_2 to reach its nominal value.

To realize this type of voltage sequencing, the power module requires two functions – an enable function and a power-good-function: The enable function specifies that the converter starts switching when the threshold value at the EN pin is reached. As soon as V_{OUT} is above a certain threshold value, e.g. 90 %, the PG pin (Power Good) switches to high state.

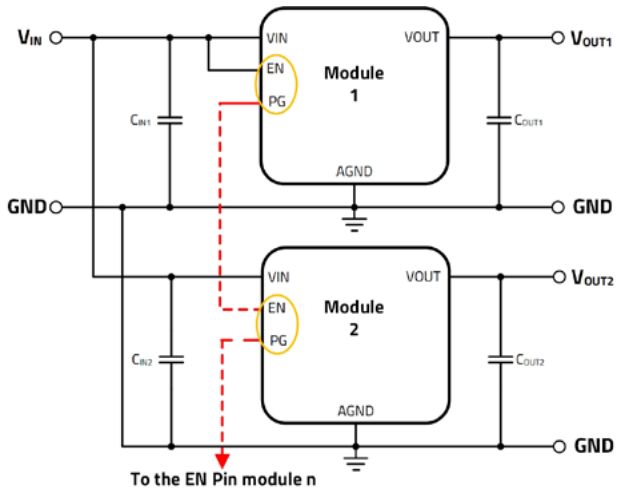

Figure 7: Typical simplified circuit for sequential start-up of the supply voltages using the 1710x0560 power module family.

Ideally, you'd stick to PLECS

But sometimes reality needs a little SPICE

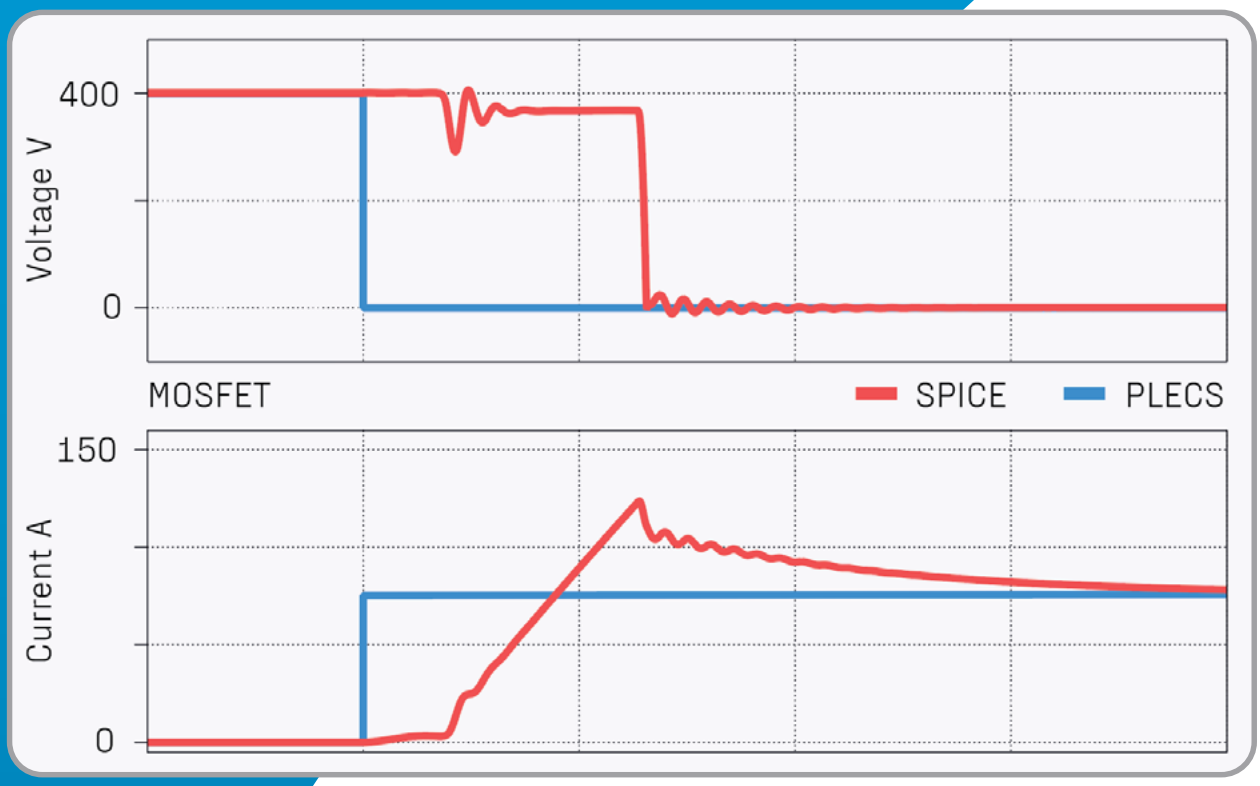

Now you can use SPICE models in PLECS

plexim
electrical engineering software

Advert

Figure 7 shows power module 1, which is switched on via the EN pin connected to V_{IN}. As soon as the output voltage V_{OUT1} of module 1 has reached power good threshold, the PG pin switches to high state. If the PG pin of module 1 is now connected to the EN pin of module 2, the PG signal from module 1 switches module 2 on. Module 2 then begins to regulate V_{OUT2}, realizing a sequential start-up of two separate output voltages.

Another positive effect of switching the modules on sequentially is that the peak input current supplied by the upstream supply, V_{IN}, is reduced. If the modules were put into operation at the same time, their input currents would add up and possibly exceed the limit value of the upstream source.

Thermal Derating and Heat Dissipation

Thermal performance and efficiency go hand in hand as every percent decrease in efficiency shows up as heat that must be safely dissipated. Just having a sufficient path for the heat to move away from the module is not always enough, as introducing more heat into the entire system increases the temperature stress on the surrounding components. Hence, the thermal behaviour of a DC/DC converter in a space-constrained application is a critical design parameter. A comparison of the derating curves of the VDMM 171010560 with those of an LDO (low drop-out regulator) in a similar housing design illustrates the negative influence of losses on performance (figure 8).

Figure 8 shows the negative influence of the power loss on the output current capacity of the LDO. The LDO used for the comparison is designed for V_{IN} = 5 V and I_{OUT} = 1 A. The derating of the LDO already starts at an ambient temperature of 45°C. At this conversion ratio, the power losses within the LDO are too high to allow for the full output current to be supplied above 45°C, despite its rating as a 1 A device. Unlike the power module, additional cooling must always be provided for the operation of an LDO at higher ratios of V_{IN} to V_{OUT}.

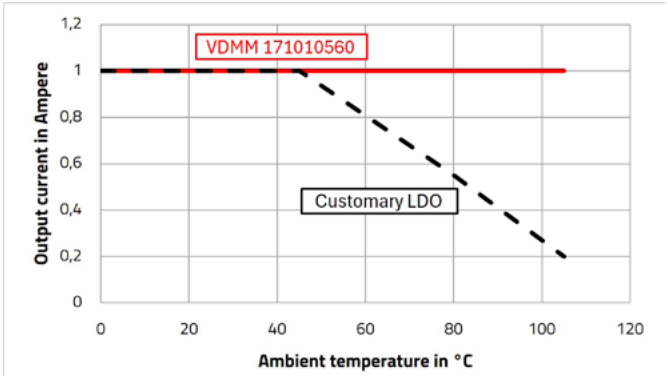

Figure 8: Derating comparison between WPME-VDMM 171010560 and an LDO.

In contrast, the VDMM 171010560 shows no derating up to 105°C with an output current of 1 A for VIN = 5 V to VOUT = 3.3 V, which means that the size, weight and cost of the solution is much smaller compared to a solution based on an LDO.

Over 95 % of the power fed into the 171010560 is used to supply the application. In comparison, the LDO uses only 66 % of the input power for this task, which is illustrated in the following calculation:

$\eta = \frac{P_{out}}{P_{in}} = \frac{V_{OUT} \cdot I_{OUT}}{V_{IN} \cdot I_{IN}} \; for \; I_{OUT} = I_{IN}$	V_{IN} = *Input voltage [V]* V_{OUT} = *Output voltage [V]* I_{IN} = *Input current [A]* I_{OUT} = *Output current [A]*
$\eta = \frac{V_{OUT}}{V_{IN}} = \frac{3{,}3V}{5V} = 0{,}66$	

34 % of the power in the LDO is converted into heat, which must be dissipated by the device. The problem arises from the fact that the input and output currents of the LDO are the same and therefore the voltage drop across the LDO with its current must be completely realized as power loss.

Operation with low efficiency leads to the following disadvantages:

- Additional supply energy requirements for operating the application
- Additional cooling either passively (increasing solution size) or active (further increasing supply energy)
- Lower reliability due to the higher temperature load on the system
- Higher development effort and higher costs for thermal management

In conclusion, the use of DC/DC power modules provides massive advantages to industrial and predictive maintenance applications. The ability to adapt dynamically to different load conditions enables these modules to work optimally under both full load and light load conditions. This not only leads to extended battery life, but also to a reduction in thermal stress, which increases the reliability and service life of the entire application. The VDMM series (171010560, 171020560 and 171030560) from Würth Elektronik combines these advantages and thus offers a versatile power supply solution.

Reference

[1] Data Sheets for the MagI³C-VDMM MicroModules from Würth Elektronik: https://www.we-online.com/en/components/products/MAGIC-VDMM_

[2] MagI³C-Modules in the online simulations-Platform RedExpert: https://redexpert.we-online.com/re/5vUzzckU

CAPACITORS BUILT TO ENDURE THE EXTREME.

Electronic Concepts
EST. 1969

INTRODUCING

UX3 SERIES

HIGH TEMPERATURE UNLYTIC® 125°C

The UX31 / UX32 / UX34 / UX35 UNLYTIC HIGH TEMPERATURE UX3 SERIES represents the best choice for high power DC application featuring operation to 125°C with no voltage derating and **acts as a drop in replacement** to existing standard polypropylene capacitors.

SCAN ME

TO LEARN MORE

VETERAN OWNED

CONTACT US

ecicaps.com

sales@ecicaps.com | sales@ecicaps.ie

Designing a 30 kW 3-phase Interleaved T-Type Vienna PFC for AI Server Power Supply

How topology, device strategy, and real-time control shape the next generation of AI power supplies

By Sam Abdel-Rahman, System Architect Server PSU, David Meneses, Principal System Application Engineer, and Yennam Raghuvaran Reddy, System Application Engineer, all Infineon Technologies

As AI server rack power continues to rise, substantial changes in server rack architectures evolve as shown in Figure 1. Current generation racks (Gen 1) contain both power delivery components as well as backup power and IT payload, leveraging single-phase PSUs of increasing wattages. As rack power levels go beyond 250 kW the next generation (Gen2) architecture is shifting towards dedicated sidecar racks for power delivery and backup power, with PSUs shifting toward three-phase AC input, HVDC distribution and power levels up to 30 kW (Figure 1, [1]).

The scope of this article is to demonstrate the 3-phase PFC evaluation board design and exceptional efficiency and power density to enable next generation PSUs.

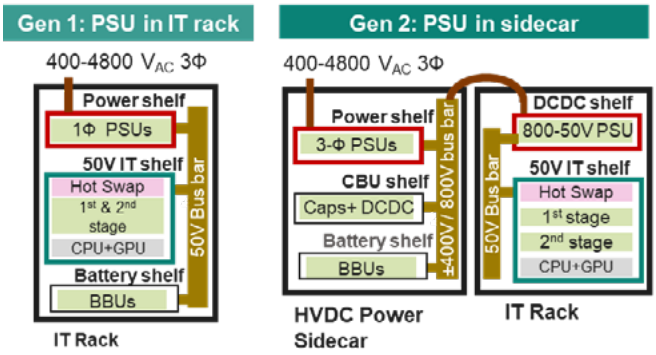

Figure 1: Power evolution for AI server rack architecture and PSUs

Board specifications

The newly developed EVAL_30KW_TTYPE_PFC (Figure 2) demonstrates a 30 kW, three-phase interleaved T-Type Vienna PFC front end for AI server power supplies in 1U form factor. The platform combines 650 V CoolGaN™ Bidirectional Switch (BDS) in the back-to-back path of the T-type Vienna, 1200 V CoolSiC™ MOSFETs in the high-voltage rectifier path, and PSOC™ Control C3 Performance Line for full digital control.

Design specifications	
Input voltage range	360 V_{AC} ~ 528 V_{AC} line to line voltage (3 phase)
Output voltage	890 V_{DC} nominal
Output current	33.33 A
Output power max	30 kW
Efficiency	> 99%
Power factor (load > 10%)	PF > 0.98, 20% ➞ 80% load iTHD < 10%, 20% ➞ 80% load
Temperature ambient	-5°C to 45°C (OCP)
Size	133 x 342 x 40 mm

This evaluation board is designed to naturally fit into the complete PSU, where it can feed a downstream DC-DC stage, which is an arrangement that becomes relevant once the architecture moves toward next generation PSUs with three-phase input and HVDC output ([1]).

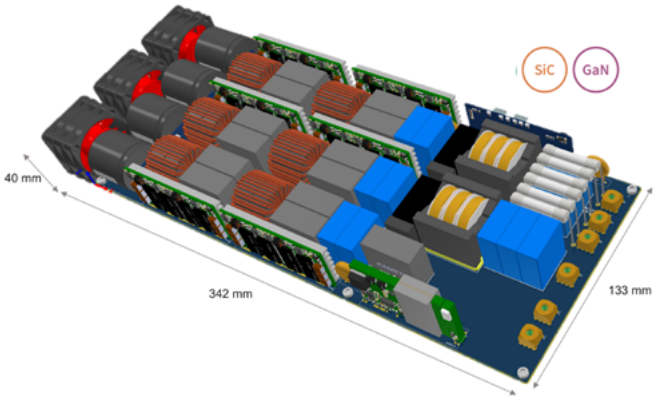

Figure 2: Board and component overview

Interleaved 30 kW T-Type Vienna front end

At 30 kW, the PFC stage is crucial to reach the required efficiency, power density and thermal behavior, of an AI server PSU. The design is no longer only about scaling up the power; it is about choosing a topology that can handle three-phase input, establish a high-voltage DC bus efficiently, and fit in the specified server PSU form factor.

The board presented is valuable because it makes practical design trade-offs visible. At this power level, conduction loss, choke design and current ripple, gate-drive quality, control design, and the use of wide-bandgap devices all have a direct influence on the electrical and thermal behavior of the platform.

The interleaved architecture of this board was chosen because it addresses several board-level requirements at once:

- **Low height fitting in 1U server power shelves form factor.** In the interleaved implementation, the current in each inductor choke is equal to half the phase current, resulting in smaller inductor size.
- **Manageable input filtering effort.** The presented design implements two CH270060GT cores with 28 turns for each of the interleaved stages. The switching frequency associated with each choke current is 72 kHz, while the effective ripple frequency per phase is 144 kHz. Figure 3 illustrates the effect of ripple cancellation at the phase current side. Leading to EMI filter reduction.
- **Better thermal management.** Interleaving also helps by distributing power losses of switches and magnetics across different areas of the board, which leads to more flexible and relaxed ther-

JOIN US AT PCIM EUROPE 2026

Vincotech

Visit our booth and discover Vincotech's latest products and solutions.

As a chip-independent power module manufacturer, we empower you to find the best-fit solutions for your needs – whether in motion control, renewables, or power supplies. Meet our experts, explore our dedicated customer stations, and put your speed to the test for a good cause with our charity challenge.

Power up your knowledge

Tuesday | 09 May, 10:50 | Exhibitor Stage
„Enhanced Power Module with Si_3N_4 Substrate and Reliable High-Temp Operation for Next-Gen PV and PCS Systems“

Tuesday | 09 May, 14:30 | PCIM Conference
„Integrated Interphase Transformer and dv/dt Filter Analysis for Interleaved SiC Motor Drives“

Tuesday | 09 May, 15:30 | PCIM Conference, poster session
„Smart Paralleling of SiC-MOSFETs in Power Modules“

Wednesday | 10 May, 13:25 onwards
Bodo's panel „Riding the SiC Wave Efficiently“

VINCOTECH @ PCIM EUROPE 2026 BOOTH 7-469

www.vincotech.com/PCIM

Vincotech congratulates Bodo's Power Systems on its 20th anniversary.

Thank you for two decades of inspiring the power electronics community with insight, innovation, and excellence.

mal solutions and heat sinks design, and avoids concentrating the full thermal burden in one local region of the layout.

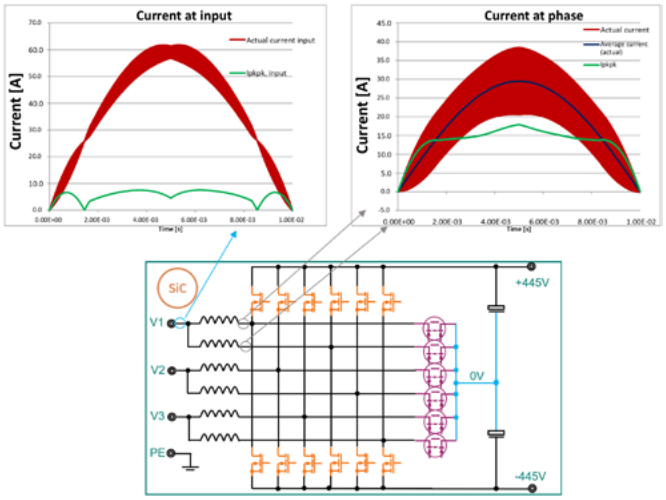

Figure 3: Interleaving rationale: phase current vs. input current, ripple reduction, and EMI implication

PSOC™, SiC, and GaN BDS on the board

As mentioned earlier, the board architecture (Figure 4) is built around three elements:

- 650 V CoolGaN™ BDS in the bidirectional switching path
- 1200 V CoolSiC™ MOSFETs in the higher-voltage rectification path
- PSOC™ Control C3 Performance Line for digital control

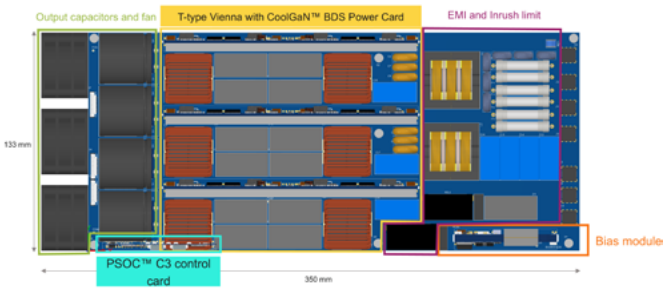

Figure 4: Board distribution of EVAL_30KW_TTYPE_PFC

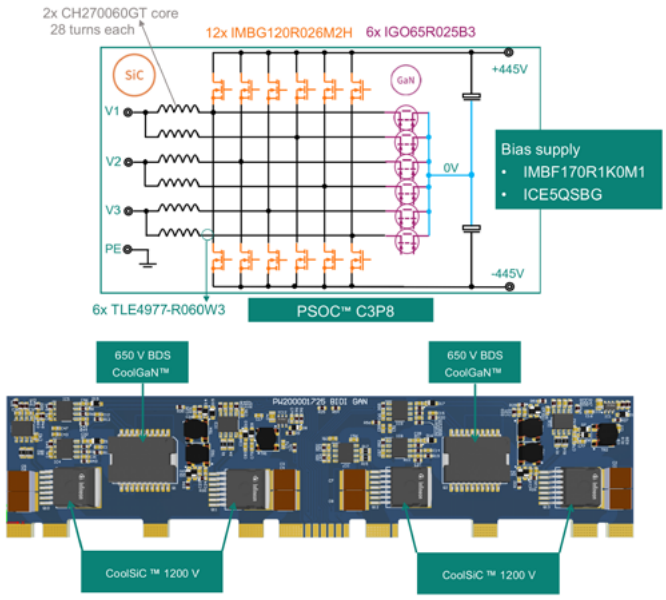

Figure 5: Power card with the power semiconductors to implement an interleaved T-type Vienna rectifier

Together, these elements define how the platform reaches its efficiency, controllability, and density targets at 30 kW. The GaN BDS path is fundamental to the T-type Vienna implementation, as it realizes the bidirectional switching function in a compact and efficient way. Each phase implements a power card with the interleaved stages as shown in Figure 5. The back side of the power card is empty of components and a heatsink is mounted to cool down the power semiconductors in bottom side cooled SMD packages.

The power stage includes IMBG120R026M2H and IGO65R025B3, with 1EDB9275F and 1EDB7275F gate drivers, TLE4977 R060W3 current sensors, and a dedicated bias implementation based on IMBF170R1K0M1 and ICE5QSBG.

The PSOC™ Control Performance Line implementation is one of the strongest differentiators of the board. The control architecture uses a three-CPU system (PSC3P8), which enables clustering the different functions needed to implement the power conversion in interleaved T-type Vienna rectifier. The main CPU subsystem is not used in the present implementation and it could be conveniently used for housekeeping and communications functions as well as telemetry and black box functions in the final application. The real-time power-conversion tasks are implemented in the Programmable Power Control Accelerator (PPCA). In the current partitioning, CPU0 handles PFC1 current-loop control, modulation, and PLL, while CPU1 handles PFC2 current-loop control, modulation, and the voltage loop (Figure 6). This gives each interleaved channel a clear control role and makes the implementation more scalable and easier to optimize.

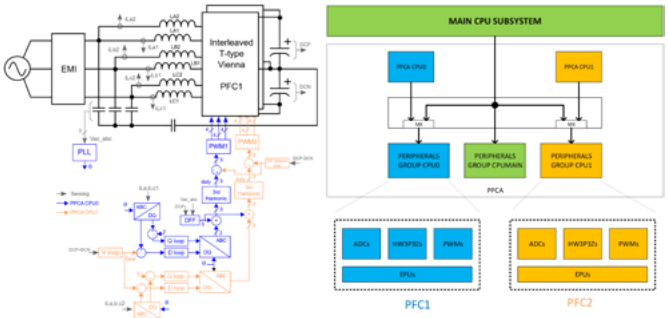

Figure 6: Digital control block diagram

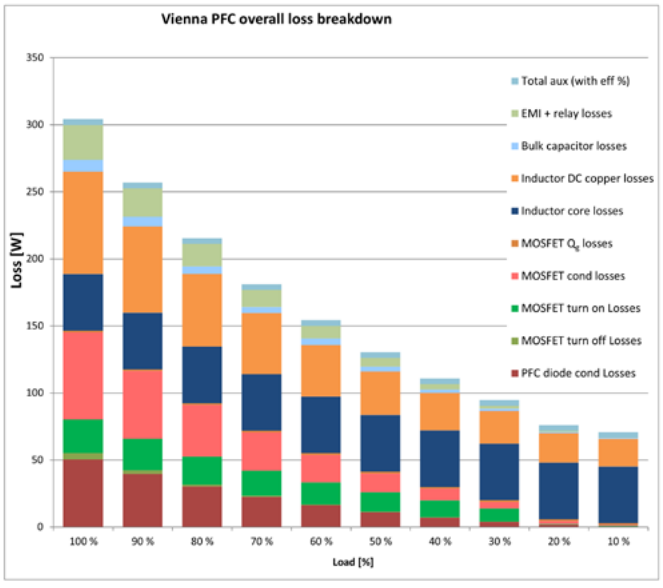

Figure 7: Breakdown of power losses at different load conditions

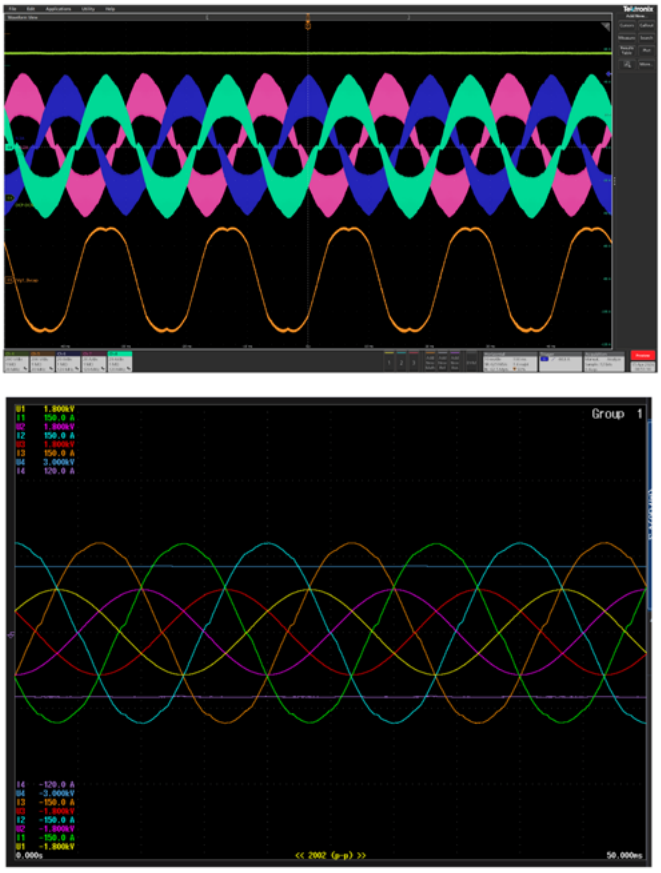

Figure 10: PFC stage waveforms (top to bottom): Output DC voltage (dark green)–, PFC choke currents in one of the interleaved stages (green, pink, blue), grid to AC virtual neutral (Orange), zoomed in PFC choke currents (orange, green, blue), and input AC waveforms (yellow, purple, red).

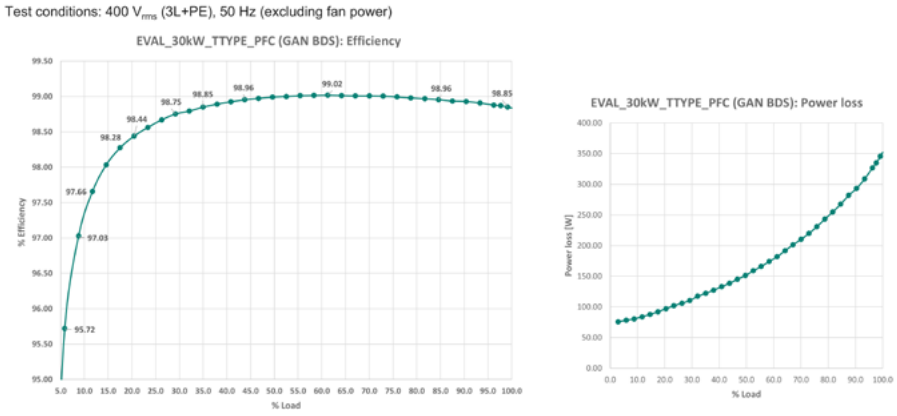

Figure 8: Measured efficiency and power loss

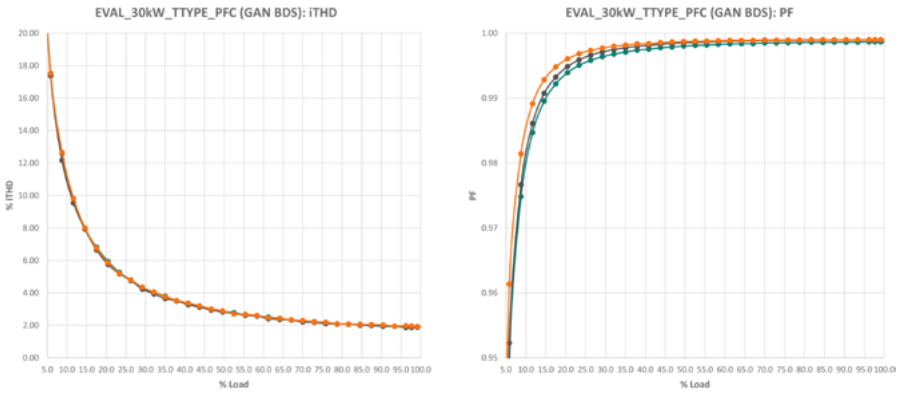

Figure 9: Measured iTHD and power factor

Power loss distribution

At 30 kW, the power stage cannot be judged by efficiency alone. We also must understand where the losses sit, how they shift with load, and what that means for magnetics, thermal spreading, and the next round of optimization. In our nominal operating view at 415 V_{AC} line-to-line and 890 V_{DC}, the dominant full-load contributions come from conduction losses in the CoolGaN™ BDS path and from core and conduction losses in the inductor. At lighter load, the inductor core losses become predominant. Figure 7 shows a breakdown of all power losses at different load conditions.

Measured results

The measured results show that the board operates as intended. Testing on the EVAL_30kW_TTYPE_PFC platform with 650 V CoolGaN™ BDS was carried out at 400 Vrms line-to-line voltage and 50 Hz, excluding fan power. Under those conditions, efficiency rises from roughly 92% at low load to a peak of about 99% near 60% load, and remains at 98.84% at full load. Full-load power loss is approximately 352 W, Figure 8.

Input-current quality is equally outstanding across the operating range, PF is well above 0.99 at 20% load and above, with a THD well under 6% from the same load point, Figure 9.

Figure 10 shows stable output DC voltage, defined grid-to-virtual-neutral behavior, and the expected choke-current behavior in one interleaved stage, alongside clean input AC waveforms.

Summary

The 30 kW 3-phase PFC evaluation board from Infineon demonstrates the next evolutionary step in AI power. High-efficiency and power density are achieved by adopting wide-bandgap devices. The PSOC™ digital controller offers the capability and resources needed for an interleaved T-Type PFC converter. To learn more about how Infineon is powering AI from the grid to the core, visit https://www.infineon.com/technology/ai/we-power-ai/psu?utm_campaign=202606_glob_en_pss.a.dc&utm_medium=3rdptmedia&utm_source=bodospowersystem_technicalpublicationarticle&utm_content=website_technologypage&utm_term=pcim_psu&uid=ci0122620002&aid=ai012262

References

Infineon Technologies AG: Evolving power supplies and rack architectures to meet AI server demand; whitepaper; October 2025; (https://www.infineon.com/gated/infineon-evolving-power-supplies-and-rack-architectures-to-meet-ai-server_8ae9cd21-516d-4a3a-a681-84449d100fee?utm_campaign=202606_glob_en_pss.a.dc&utm_medium=3rdptmedia&utm_source=bodospowersystem_technicalpublicationarticle&utm_content=website_technologypage&utm_term=pcim_psu&uid=ci0122620001&aid=ai012262)

www.infineon.com

A Three-Phase GaN QFN Module for High Power-Density Motor Drives

The EPC91132 evaluation board is a 3-phase BLDC motor drive inverter board featuring the EPC33110 module, which integrates three monolithic gallium nitride (GaN) half-bridges, each with gate drivers, bootstrap circuits, and level shifters. Its form factor is optimized for the small joints of humanoid robots and for 20 mm drone motors.

By Marco Palma, VP of Marketing and Systems, and Simone Scano, Applications Engineer, both Efficient Power Conversion (EPC)

Gallium nitride (GaN) power devices are enabling a new generation of high-efficiency, high-power-density motor drive systems, allowing motor drive inverters to operate at higher switching frequencies. As a result, motor inverters based on GaN technology can achieve switching frequencies well above 100 kHz while reducing both conduction and switching losses. These characteristics enable smaller passive components, improved efficiency, and more compact system designs. These characteristics are particularly important when dealing with miniature motors, such as those mounted in small and medium-sized drones and in the arms of a humanoid robot. These motors have very low inductance (tens of µH) and resistance (hundreds of mΩ), and the higher switching frequency of GaN devices enables higher-bandwidth motor control and better dynamic performance and efficiency. With the increasing demand for miniaturization, the monolithic integration of the inverter's essential function within a GaN integrated circuit has become a stringent requirement. While the integration poses a significant challenge for semiconductor manufacturers, it allows designers to simplify their layouts and their application boards.

EPC91132 description

The EPC91132 reference design board is a complete platform tailored for humanoid robot joints and small drone applications. The board can operate with a wide DC input voltage range of 10 V to 60 V, accommodating various power sources typical in robotics and drones. EPC91132, shown in Figure 1a, is equipped with all the features and functions of a complete motor drive inverter, including a microcontroller, regulated off-line power supplies, DC voltage sensing, on-board magnetic encoder for rotor shaft position and speed control, and current sensor ICs with embedded overcurrent fault signal triggered at 30 A. The inverter is controlled by the on-board microcontroller, which can be programmed via a dedicated connector and operated in real time via an RS-485 port.

The EPC91132 outline has been designed with the breakout board concept to fit two different motors. With the external PCB ring, the EPC91132 can be mounted in a Lingkong MG8008E-i9 motor for a humanoid joint motor, as can be depicted in Figure 2a [2]; removing the external PCB ring, the entire inverter fits on a small board with a 23 mm diameter and can be mounted in the drone motors made by Vertiq 23-06 220KV and 23-06 2200KV (Figure 2b) [3].

EPC33110 three-phase GaN module description

The pulsating heart of the EPC91132 is the EPC33110 module from Efficient Power Conversion. The EPC33110 is a three-phase module in gallium nitride (GaN) technology and represents the latest innovative solution in power electronics for motor drive applications (Figure 1b). GaN monolithic integrated circuit technology enables the EPC33110 to deliver exceptional performance in a compact form factor.

Efficient Power Conversion GaN IC technology enables the integration of logic functions and gate drivers on the same substrate as the power FETs, thanks to the lateral conduction of the power devices, thereby enabling the realization of monolithic power half-bridge chips. The EPC33110 implements the co-packaging of three half-bridges, keeping the excellent electrical and thermal performance of GaN devices, while optimizing the overall size of the inverter [4]. Each half bridge integrates gate drivers, bootstrap circuits, and level shifters. The EPC33110 simplifies system design by eliminating the need for discrete gate drivers and transistor compo-

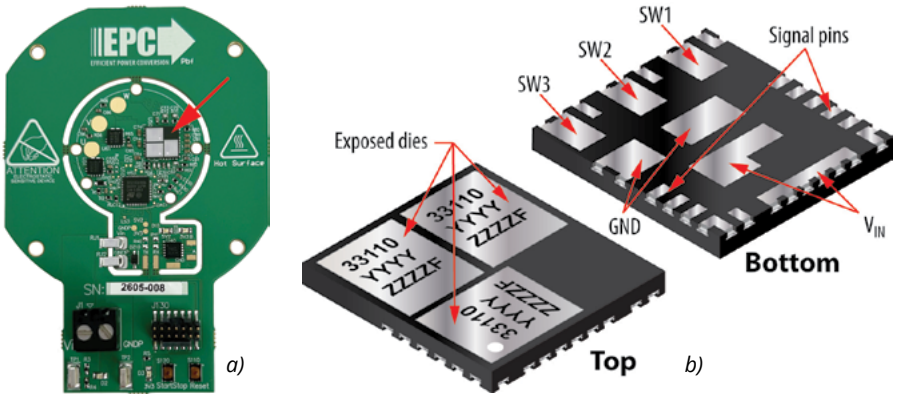

Figure 1: a) Overview of EPC91132 board – three-phase inverter for drones and humanoid motor joints; b) Top and bottom view of EPC33110 module

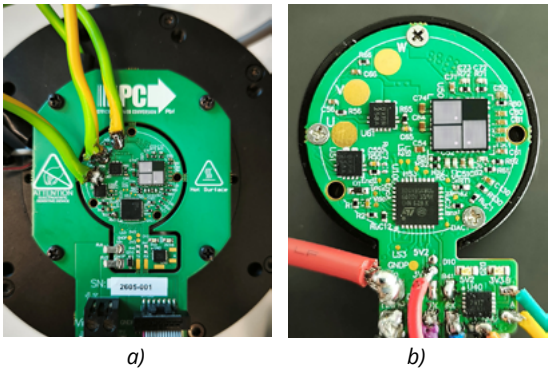

Figure 2: a) EPC91132 with outer PCB ring mounted in a humanoid joint motor; b) EPC91132 mounted in a drone motor

Powering Innovation, Driving Performance

Dependable, High-Voltage Solutions for Every Application

Our broad portfolio of high-voltage products and solutions deliver the performance, scalability and reliability needed to power innovation across industries. From electric vehicles and renewable energy systems to industrial automation and aerospace applications, our solutions are designed to meet the demands of industrial, automotive, aerospace and other critical applications.

Key Features

- **Extensive and Scaleable Portfolio** High-voltage silicon, IGBT, and SiC technologies available in discrete and module configurations tailored to your power needs
- **Superior Efficiency** Proprietary technology for optimized thermal management and reduced power losses
- **Field-Proven Reliability** Hi-Rel and automotive-qualified with HV-H3TRB capability for harsh environments
- **Accelerated Development Workflow** Comprehensive tools, software and technical support to simplify design and speed up your time-to-market

Whether you're designing for automotive, industrial or energy systems, Microchip is your trusted partner for high-voltage solutions that drive success. Explore our portfolio today and take your designs to the next level.

MICROCHIP

microchip.com/PickYourPower

The Microchip name and logo and the Microchip logo are registered trademarks of Microchip Technology Incorporated in the U.S.A. and other countries. All other trademarks are the property of their registered owners.
© 2026 Microchip Technology Inc. All rights reserved.
MEC2651A-UK-05-26

nents. Embedding the critical power components within a 6x6.5 mm² module allows designers to use only a minimal set of external components. Co-packaging three integrated half-bridge ICs enhances power density and delivers good thermal performance thanks to the excellent top-side cooling provided by the exposed dies.

EPC33110 performance in EPC91132 mounted in a humanoid joint motor

EPC33110 performance was tested in a humanoid joint motor application at 48 V input voltage, with load conditions up to 11 A_{RMS} continuous phase on a dynamometric bench. Operating at 60, 80, and 100 kHz PWM with 20 ns dead time, the board delivered a continuous phase current of 11 A_{RMS}, with a temperature increase of 70 °C. The measures were conducted with and without the motor cover case on top of the EPC91132. The motor case served as a heat sink, and there was no forced-air cooling.

Figure 3 shows the increase in the EPC33110 temperature vs. the ambient temperature and the phase rms current, which can be continuously delivered to the motor. Each point on the graph was measured once thermal equilibrium was reached, after approximately 10 minutes. During these measurements, the motor speed was 100 RPM.

For the motor used in the tests, which had a torque-per-ampere constant of 2 Nm/A_{RMS}, the 22 Nm maximum load corresponded to 11 A_{RMS} current in each leg of the inverter.

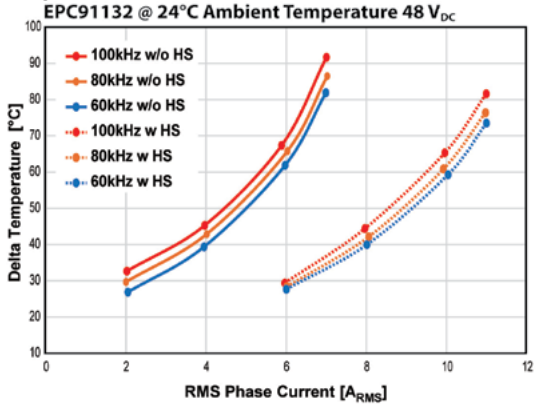

Figure 3: Output current capabilities of EPC33110 operated at 100 kHz PWM in a humanoid robot joint.
DcBus = 48 V, PWM frequency = 60, 80, 100 kHz. Without (left) and with (right) the motor case as heatsink for the module

The temperature measurements were taken by attaching a thermocouple to the top of the EPC33110 module in both cases, with and without the motor cover serving as a heatsink. The temperature was also recorded using a thermal camera, and, for measurements with the motor cover, a square hole was engraved to enable internal temperature monitoring.

While in the case of humanoid robot joints, natural convection cooling is the only option, in drone applications, the propellers generate strong airflow, providing thrust and effective cooling for the entire system, thereby increasing the inverter's current capability.

EPC33110 performance in EPC91132 mounted in a drone motor

EPC33110 performance was also evaluated in a drone application, using the Vertiq 23-06 220KV motor equipped with a 12-inch underactuated propeller. The tests were performed from 1000 rpm to 3400 rpm, which is the maximum achievable speed of this motor under these load conditions at 24 V input voltage.

For each speed, the device temperature was measured by attaching a thermocouple to the top of the EPC33110 module and waiting approximately 10 minutes until thermal equilibrium was reached. The average input power required at each speed was measured (Figure 4), and the propeller torque was estimated at each speed (Figure 5).

The drone motor was driven at a switching frequency of 100 kHz with a 20 ns dead time. The maximum temperature increase of the device was about 4°C (with an ambient temperature of 26°C).

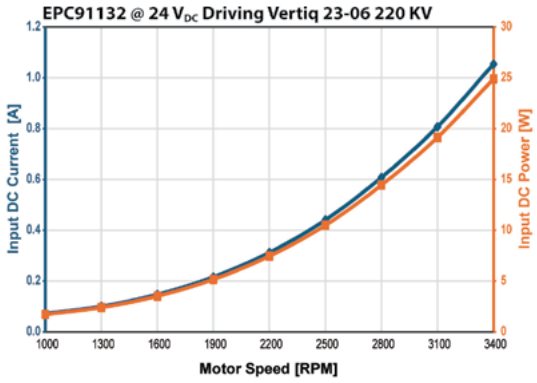

Figure 4: Input DC current and power required by the motor to sustain the torque generated by the propeller vs. motor speed

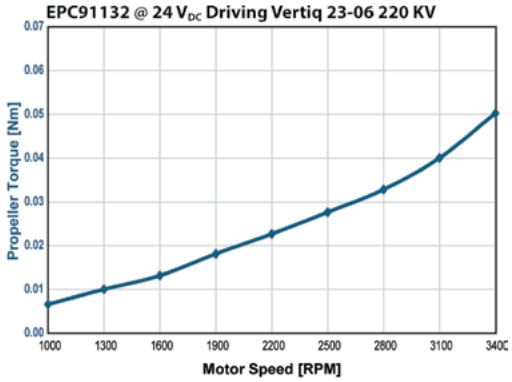

Figure 5: Propeller torque vs. motor speed

Conclusion

The EPC91132 is a 23 mm small-motor-drive inverter reference design for humanoid wrists and hands, as well as drones. The heart of the EPC91132 is the EPC33110 GaN module based on Efficient Power Conversion GaN monolithic integrated circuit technology. The EPC33110 is a compact three-phase module in a 6x6.5 mm QFN package that integrates three GaN half-bridges with built-in gate drivers, bootstrap circuits, and level shifters, optimized for motor control. A single 5 V power supply can power the module to operate up to 80 V with a typical on-resistance of 11.7 mΩ, supporting 3.3 V or 5 V logic inputs.

The EPC33110 is designed to drive three-phase permanent-magnet motors commonly used in drones and humanoid robots. The EPC91132 reference board supports these applications with a wide 10–60 V input range and includes complete motor drive features.

Thanks to top-side cooling optimized by the exposed dies, EPC33110 can deliver up to 11 A_{RMS} continuously per phase, as verified in steady-state tests on a humanoid joint motor mounted on a dynamometer bench.

Reference

[1] "GaN Power Devices for Efficient Power Conversion", Fourth Edition – by Alex Lidow, Michael de Rooij, John Glaser, Alejandro Pozo Arribas, Shengke Zhang, Marco Palma, David Reusch, Johan Strydom.
[2] LKMTECH, MG8008-i9v3 (2026, May 1), http://en.lkmotor.cn/ProDetail.aspx?ProId=265
[3] Vertiq, 23-06 G1 Module (2026, May 1), https://www.vertiq.co/23-06-g1
[4] Three-Phase Module Based on Monolithic GaN Half-Bridge ICs, in Bodo's Power Systems December 2025, pages 24-26, by Federico Unnia, Marco Palma.

HITACHI

IGCT highest power density for most compact equipment

The IGCT is the semiconductor of choice for demanding high-power applications such as wind power converters, medium-voltage drives, pumped hydro, marine drives, co-generation, interties and FACTS.
Hitachi Energy's range of 4500 to 6500 V asymmetric and reverse conducting IGCTs deliver highest power density and reliability together with low on-state losses.

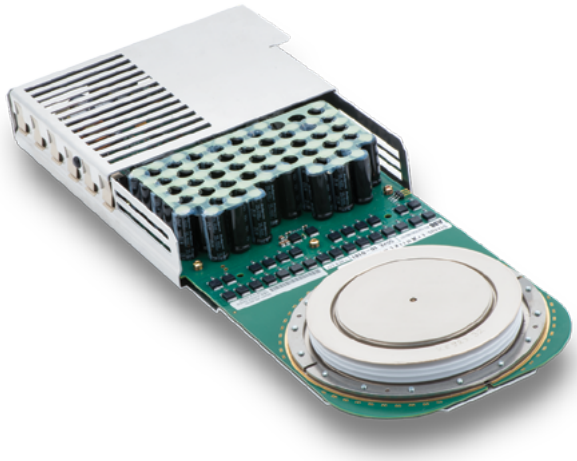

hitachienergy.com/semiconductors

Enhanced Power Module for PV and PCS/ESS Applications

Inverter technology continues to evolve through system-level optimizations. However, innovations at the power-module level enable the greatest gains in power density and cost reduction. This article presents two key module-based technologies that further improve inverter performance – robust silicon nitride (Si_3N_4) substrate ceramics and power devices built to operate at junction temperatures of up to 175 °C.

By Matthias Tauer, Sr. Technical Marketing Manager, Vincotech

Modern power conversion systems must increase power density and reduce per-kilowatt cost, yet maintain inverters' current footprints. Several developments at the system level support these goals. Inverters can deliver more power without requiring larger conductors or modules if they can be made to operate at higher DC and AC voltages while retaining similar maximum phase currents. Optimized switching strategies such as discontinuous pulse width modulation (DPWM) can reduce switching losses significantly, in some cases by more than 30 %, enabling more efficient operation. Mechanical and thermal improvements, including advanced heatsink structures and heat-pipe integration, extend the allowable dissipation capacity and push inverter designs closer to their theoretical performance limits.

While system-level optimizations deliver valuable gains, further increases in performance require advances within the power module itself – specifically, a transition to Si_3N_4 substrates and operation at junction temperatures of up to 175 °C. These two improvements significantly expand what is thermally and electrically achievable within a given module's footprint.

Si_3N_4 substrates have lower thermal resistance and are more rugged than conventional materials, so they improve overall thermal conductivity and mechanical robustness. They also support higher output power without requiring changes to the power module or the inverter's mechanical envelope.

The capacity to operate at junction temperatures of up to 175 °C increases thermal headroom. Higher allowable junction temperatures expand the safe operating area, provide tolerance for transient overload conditions, and extend lifetime under demanding mission profiles. The greater thermal headroom enables designers to make the most of higher voltages, improved switching strategies, and optimized thermal paths without compromising reliability.

flow E3BP and *flow* E3BP$^+$ at a glance

Vincotech's *flow* E3BP$^+$ module builds on the *flow* E3BP platform (Figure 1). This enhanced version supports junction temperatures of up to 175 °C and incorporates Si_3N_4 ceramic substrates, while maintaining full compatibility with the compact 110 mm × 62 mm outline. Its Si_3N_4 substrates reduce thermal resistance by 26 % compared with equivalent Al_2O_3-based DCB layouts.

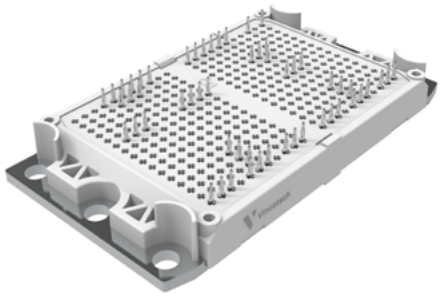

Figure 1: flow E3BP

This module comes in a CTI600 plastic housing with isolation flaps around the heatsink mounting screws to meet insulation requirements for 2 kV applications. It also offers an optional 15 mm mounting height to ensure adequate creepage and clearance distances.

The 3 mm convex copper baseplate eliminates local concavities along both the longitudinal and transverse edges to distribute pressure uniformly and maximize contact with the heatsink surface. This controlled curvature provides consistent, long-term stable thermal resistance and mitigates phase-change TIM (PC-TIM) pump-out. The recommended PC-TIM is qualified for continuous operation at temperatures up to 150 °C. It is available pre-applied to the baseplate to streamline assembly.

Reliability considerations

Table 1 summarizes the coefficient of thermal expansion (CTE) for different copper–ceramic–copper stack-ups. The overall CTE depends on the CTE of the ceramic material, the relative thicknesses of the ceramic core and the copper layers. Thinner ceramic layers and/or thicker copper foils increase the stack-up's effective CTE.

Material	Thickness [mm]	CTE [ppm/K]
Al_2O_3	0.38	9.2
	0.63	8.3
Si_3N_4	0.32	6.9

Table 1: CTE of different substrate materials and thicknesses

For a ceramic thickness of 0.32 mm, Si_3N_4 substrates exhibit an effective CTE that aligns closely with common semiconductor materials – specifically silicon (≈2.6 ppm/K) and silicon carbide (≈4 ppm/K). This excellent CTE match, combined with high fracture toughness, makes Si_3N_4-based substrates well suited for power modules that require long power-cycling lifetimes, as illustrated in Figure 2.

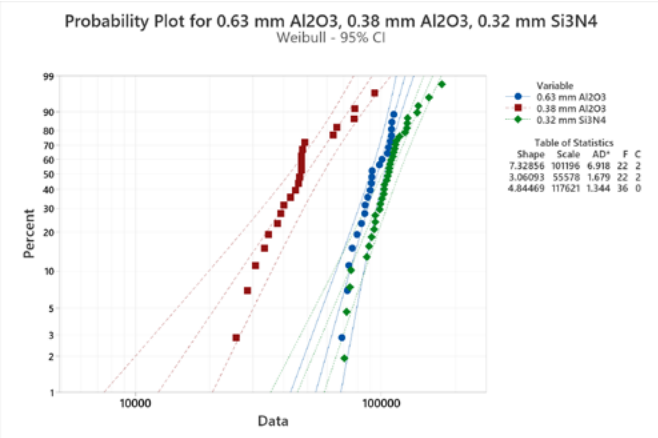

Figure 2: PCsec reliability comparison between Al_2O_3 (0.63 and 0.38 mm) and Si_3N_4 (0.32 mm), Test conditions: Si IGBT, ΔT=100 K, $T_{j,max}$=150 °C, t_{on}=0.5 s

PRECISE & ERGONOMIC

Current Clamp by Danisense

DC to 1MHz Bandwidth – Best in Class Accuracy and Phase Shift

Congratulations on the 20TH ANNIVERSARY of Bodo's Power Systems! We wish you much continued success and many further inspiring stories.

DANISENSE

info@danisense.com I danisense.com

The green dots in Figure 2 mark failure events for the 0.32 mm Si_3N_4 substrate, which lasts more than twice as long as the 0.38 mm Al_2O_3 substrate. The 0.63 mm Al_2O_3 variant, represented by the blue dots, follows closely. Although this thicker ceramic performs well in terms of reliability, designers generally do not select it for baseplate-equipped modules because of its higher thermal resistance. In terms of thermal performance, the 0.38 mm Al_2O_3 substrate is preferred. However, it is far less reliable, as indicated by the red dots.

A PC-TIM pump-out (PCmin) reliability assessment was conducted to evaluate thermal resistance (R_{th}) stability under thermo-mechanical cycling. The device under test (DUT) was oriented vertically, introducing a gravitational shear component in the thermal interface material to accelerate TIM migration and represent a worst-case condition for pump-out.

The test matrix comprised *flow* E3BP assembled with PCTIM, *flow* E3BP assembled with standard thermal grease, and a competitor's baseplate module assembled with the same grease. Table 2 indicates the defined failure thresholds and cycle counts for each configuration.

A direct comparison of the two grease-based assemblies shows that *flow* E3BP achieves more than twice the number of cycles. This improvement stems from the optimized baseplate geometry, which reduces mechanical movement and thereby minimizes TIM pump-out.

The durability of *flow* E3BP and the phase-change TIM's high pump-out resistance improve long-term reliability. Together, they create a robust thermal interface with just 12 % R_{th} drift after around 23,000 cycles. The test was discontinued because the chamber was scheduled for subsequent campaigns; the DUT had already exceeded the required 20,000-cycle qualification threshold, and degradation remained minimal.

DUT	TIM type	R_{th} limit	Cycles	Comment
flow E3BP	PC-TIM	12 % increase	23k	Test discontinued
	Grease	20 % increase	14.5k	
Competitor	Grease	20 % increase	7k	

Table 2: Comparison of R_{th} drift and cycle lifetime for different TIM types and module, Test conditions: t_{on}=1 min, ΔT=100 K, const I, vertical orientation

Application example

The application example highlights the benefits of reduced thermal resistance and higher allowable operating temperatures in modern power electronics. The two graphs in Figure 3 show the transient thermal behavior of the buck IGBT in an NPC (neutral-point-clamped) topology implemented in the *flow* E3BP$^+$ module under different load conditions. In the first graph, representing normal operation at 50 Hz line frequency, the junction temperature shows a periodic thermal swing, peaking at approximately 152 °C. This

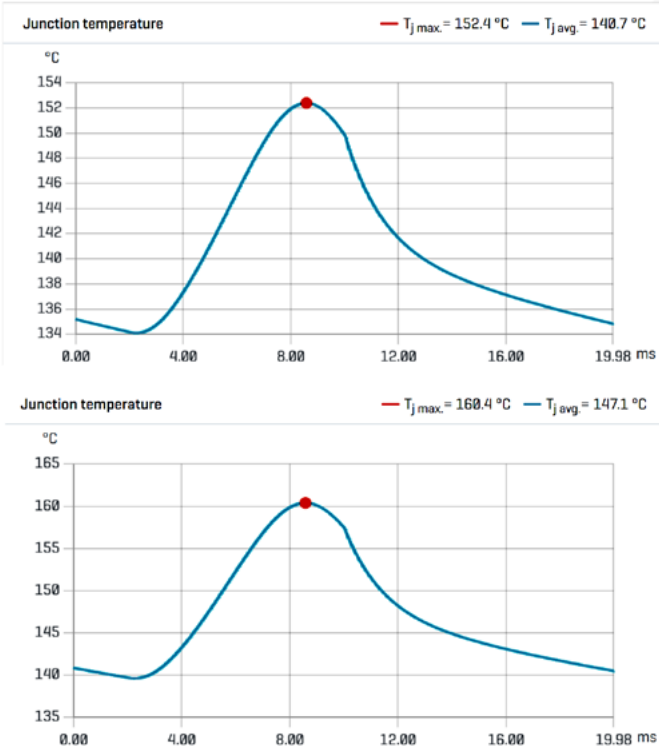

Figure 3: 465 kW PV inverter buck switch temperature at normal operation (top) and overload (bottom) (V_{dc}=1500 V, $V_{ac,ph}$=577 V, I_{ph}=269 A, cosphi=0.8, f_{sw}=16 kHz, R_g=4.7 Ω)

reflects the cyclic thermal loading typical of photovoltaic inverter applications.

The second graph in Figure 3 shows the buck IGBT's junction temperature under an overload condition at 1.1 × nominal output power. While the overall waveform remains similar, the higher output current increases conduction and switching losses, raising the peak junction temperature to approximately 160 °C.

These results underscore the benefits of the Si_3N_4 substrate used in the *flow* E3BP$^+$. Its R_{th} is around 26 % lower than that of conventional substrates. This improves heat spreading and reduces junction temperature peaks under both nominal and overload conditions.

Conclusion

Si_3N_4 substrates and 175 °C junction-temperature capability increase power density and expand operating margins in modern inverter designs. The former's superior thermal conductivity and mechanical robustness remove major bottlenecks at the substrate level. The latter provides critical thermal headroom, giving designers greater flexibility to handle transient overloads and demanding mission profiles without compromising reliability. Together, these technologies increase power density, improve robustness, and make more efficient use of existing power-module platforms.

www.vincotech.com

Bodo's Power Systems®
Electronics in Motion and Conversion
Follow us on LinkedIn:
linkedin.com/company/bodo's-power-systems

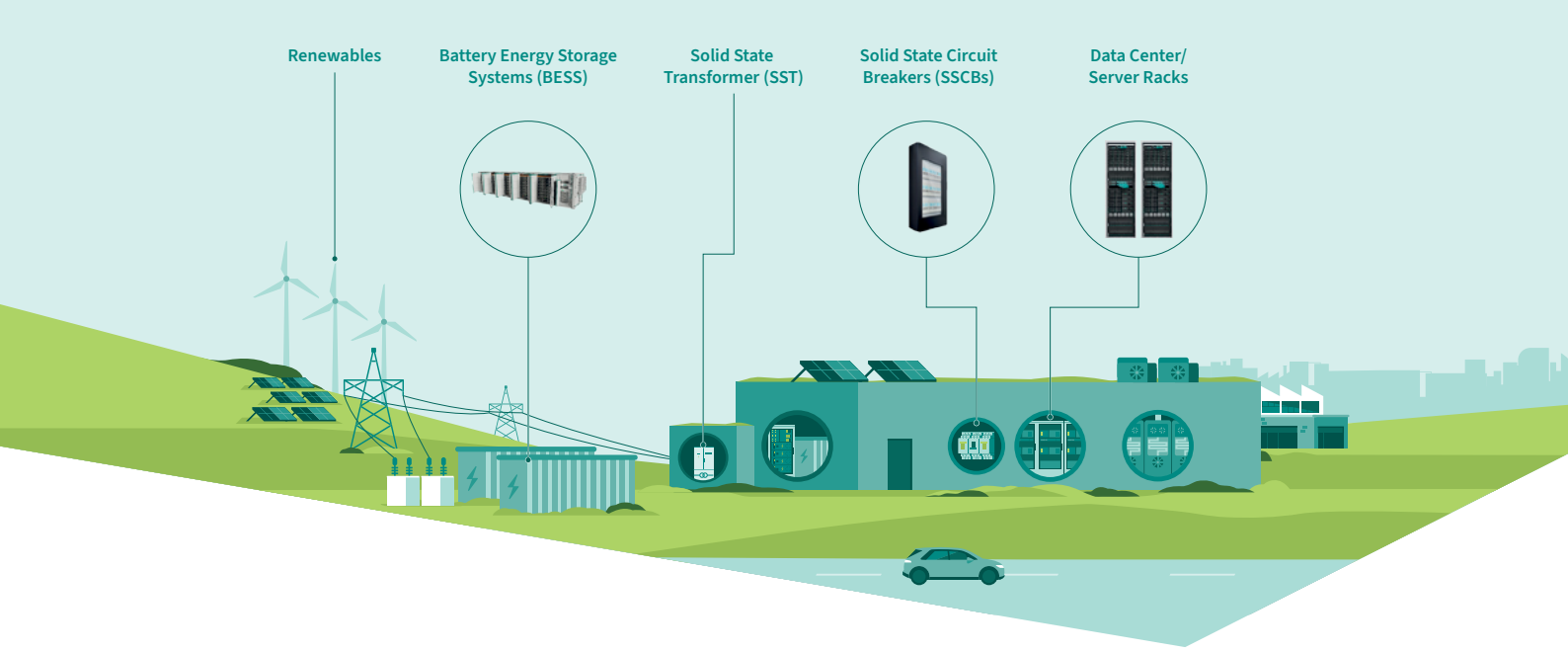

Powering the future: solutions for next-generation power grids

Connect with Infineon experts at PCIM Europe 2026 – Hall 7 / Booth 7-470

The power grid is undergoing fundamental change. What was once a one-way flow of electricity from central power plants to industry and consumers is rapidly evolving into a complex, decentralized energy ecosystem. Semiconductor solutions from Infineon support this transition and enable a scalable, reliable, and resilient power infrastructure.

Solid-state transformers

Solid-state transformers (SSTs) are redefining power conversion by replacing conventional transformers with advanced semiconductor solutions, delivering superior efficiency and performance. Infineon's CoolSiC™ MOSFET EasyPACK™ modules leverage the full potential of silicon carbide technology to maximize power density, reliability, and efficiency – making them the ideal solution for next-generation AI data centers and high-demand industrial power architectures.

www.infineon.com/SST

Solid-state circuit breakers

The transition to digitalized power distribution demands a new generation of protection devices, with solid-state circuit breakers (SSCBs) leading the way. Infineon's CoolSiC™ JFET technology rises to this challenge by combining the advantages of silicon carbide with innovative packaging and advanced chip design – delivering unmatched efficiency, robustness, and reliability for the most demanding next-generation power distribution.

www.infineon.com/sscb

We congratulate "Bodo's Power Systems" on its 20th anniversary and wish it many more successful years as the leading magazine in the power electronics industry.

Scan the QR Code to connect with us at PCIM Europe 2026!
www.infineon.com/pcim

Ruggedness Matters: MOSFETs Built on Mature Planar Technology

As the availability of planar MOSFETs continues to decline, many industrial and mission-critical systems continue to depend on devices with proven robustness and predictable behavior under stress. Littelfuse Polar MOSFETs address this need with a portfolio based on mature planar technology, offering high avalanche capability, strong safe operating area, and reliable switching performance.

By Sachin Shridhar Paradkar, Liutauras Storasta, Raymon Zhou, José Padilla; Littelfuse

Balancing Efficiency and Reliability in Power Electronics

Power electronics systems including industrial power supplies, process control equipment, and test platforms, require reliable operation under a wide range of electrical conditions. Transient events, including load interruptions, inductive load switching and input disturbances can generate voltage overshoots and current spikes. Repetitive thermal cycling adds mechanical and electrical stress, making device robustness as important as efficiency. At the component level, designers typically consider voltage capability, current rating, switching speed, and on-state resistance to achieve acceptable efficiency and thermal performance. However, practical operation rarely follows ideal assumptions.

Key reliability-driven requirements include:

- Strong tolerance to overvoltage events
- Wide safe operating area (SOA)
- Low thermal resistance
- Capability to withstand pulsed energy
- Stable operation during abnormal events

While modern semiconductor technologies such as superjunction silicon and wide-bandgap materials excel in efficiency, they may require tighter design control or additional protection in stress-intensive environments. In contrast, planar-based devices such as Polar MOSFETs provide a balance of switching performance and ruggedness, making them well suited for applications where robustness under diverse operating conditions is a key design constraint.

The Polar MOSFET Platform

The Polar MOSFET offering includes two primary device families: Polar and Polar3, each tailored to support a broad spectrum of voltage and current requirements. Both series offer standard MOSFET and HiPerFET™ devices with optimized body diodes for fast switching performance. Devices are available in industry-standard packages, isolated, and high-voltage package options designed for harsh environments. The planar-gate architecture provides balanced conduction, switching, and ruggedness performance.

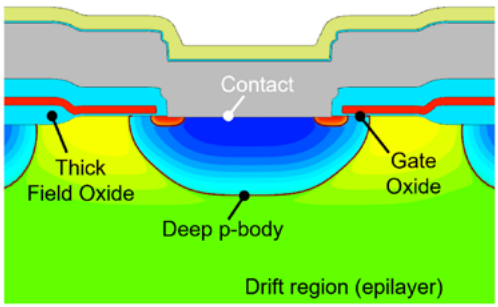

Figure 1: Polar MOSFET cell technology

Polar family

- Blocking Voltage range: 100 V to 1200 V
- Current capability: 0.2 A to 300 A
- On-state resistance down to 5.5 mΩ

Polar3 family

- Blocking Voltage capability extending up to 3000 V
- Current ratings up to 210 A
- On-state resistance from 14.5 mΩ upward

The core of the Polar MOSFET technology is a vertical DMOS cell architecture as illustrated in Figure 1. The active area is composed of optimised rugged MOS cells incorporating a deep p-body, which enhances robustness under avalanche stress conditions. A reduced gate-to-drain capacitance is achieved by introducing a thick field oxide layer between the cells. The device employs a robust, thick planar gate oxide, ensuring high long-term reliability.

High blocking capability is achieved through a sufficiently thick epitaxial layer grown on a highly conductive substrate. The epitaxial layer parameters, together with the transition region between the epitaxial layer and the substrate, are carefully optimised to balance conduction losses $R_{DS(on)}$, breakdown voltage, and avalanche ruggedness. The ring termination is designed with a high margin, ensuring longterm reliability under application-induced and environmental stresses.

A key advantage of planar MOSFET architectures is their predictable switching behavior and tolerance to real-world circuit conditions. This often allows designers to reduce implementation complexity compared with more sensitive device technologies. Polar MOSFETs simplify system integration by offering several advantages.

- High single-pulse avalanche capability
- Wide SOA at elevated voltages
- Standard gate-drive requirements (no negative gate bias)
- Reliable parallel operation
- Reduced dv/dt stress, contributing to cleaner switching
- HiPerFET diode variants for improved reverse-recovery behavior
- Simple thermal design

Polar Advantage

Managing Overvoltage Events Through Avalanche Capability

Regardless of topology, transient overvoltage events are unavoidable in practical systems. Even well-designed circuits exhibit voltage spikes during switching transitions, especially when inductive elements are present. Avalanche-rated MOSFETs address this challenge by allowing the device to safely dissipate excess energy

when the drain voltage temporarily exceeds its breakdown threshold. During this controlled avalanche condition, the device absorbs transient energy without catastrophic failure, provided it remains within specified limits. In such events, an avalanche-rated MOSFET provides controlled dissipation of excess energy, preventing immediate device failure. This capability improves fault tolerance, reduces the risk of device failure, and increases resilience to real-world disturbances, enhancing system uptime.

In continuously operating industrial or mission-critical systems, such robustness directly improves reliability and reduces downtime. Avalanche capability is therefore a critical factor in hard-switching converters, industrial control systems and pulse-power applications. Datasheet comparison shows that Polar MOSFETs offer higher avalanche energy levels than many alternatives across various voltage classes, providing additional margin in applications where transients are frequent.

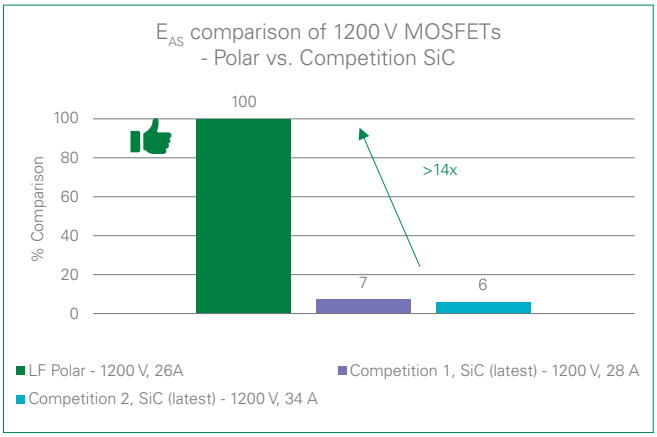

Figure 2: Comparison of measured single pulse avalanche energy for 1200 V MOSFETs from different technologies

Figure 2 illustrates the superior avalanche capability of Littelfuse Polar MOSFETs compared to other existing technologies. This comparison is based on single-pulse avalanche energy measurements, evaluated across 1200 V MOSFETs from different technologies with similar nominal current ratings.

Safe Operating Area as a Reliability Indicator

The safe operating area defines the allowable combinations of voltage, current, and time duration a MOSFET can tolerate without degradation. It provides a clear representation of the device's ability to survive high-power conditions - especially during temporary operation in the linear region.

Transient linear-mode operation may occur during:

- System start-up
- Load transitions
- Short-duration overloads
- Control-loop response events

Applications particularly dependent on wide SOA performance include:

- Linear amplifiers
- Push-pull converter stages
- Auxiliary supply modules
- Booster circuits

Pulse Duration / Nom. Current, Technology	Datasheet SOA values, 1200 V MOSFET		
	26 A LF Polar	28 A Competition1 Latest gen. SiC	34 A Competition2 Latest gen. SiC
1 ms	2 A	0.02 A	0.3 A
100 µs	20 A	0.16 A	1.8 A
10/25 µs	40 A	2 A	10 A
Comparison	**Polar is at least 4x better**		

Pulse Duration / Nom. Current, Technology	Measured SOA values, 1200 V MOSFET		
	26 A LF Polar	28 A Competition1 Latest gen. SiC	34 A Competition2 Latest gen. SiC
100 ms	0.3 A	0.08 A	0.08
10 ms	0.51 A	0.1 A	0.11
1 ms	3 A	0.2 A	0.25
Comparison	**Polar is at least 3x better**		

Figure 3: Comparison of datasheet and measured SOA parameters of 1200 V MOSFETs for pulsed operation

Coilcraft

AEC Q200 +125°C

HTX8045C Series
LLC Half-Bridge Transformers

- Low interwinding capacitance (as low as 0.55 pF) to minimize EMI and achieve high CMTI (Common Mode Transient Immunity)
- Optimized for isolated bias supplies for SiC and GaN gate drivers, such as the UCC25800-Q1 from Texas Instruments and the MPQ18913 from Monolithic Power Systems
- Ideal for automotive OBC and traction inverters in EV/HEV

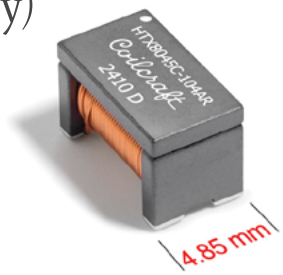

Request Free Samples @ coilcraft.com

Devices with extended SOA capability provide increased design margin and reduce the probability of failure under dynamic operating conditions. Comparative evaluations across common voltage classes indicate that Polar MOSFET devices maintain strong pulsed SOA capability, providing additional reliability headroom in demanding applications. Figure 3 compares the datasheet and measured SOA maximum current values during pulsed operation at the maximum voltage rating for 1200 V MOSFETs in similar packages. The comparison highlights that Littelfuse Polar MOSFETs offer greater safety margins than competing technologies.

Where Ruggedness Delivers the Most Value

Many industrial systems operate in environments where electrical disturbances, high power density, and long operational lifetimes are unavoidable. In some scenarios, device ruggedness often outweighs efficiency gains. Application areas that benefit from enhanced robustness include:

- Industrial power supplies
- Motor control and drive systems
- Process power equipment
- Test and measurement platforms
- Auxiliary and standby power systems
- High-voltage pulse systems

In these applications, the ability to tolerate occasional fault events without immediate failure can extend system life and reduce maintenance costs. Table 1 captures key applications Polar MOSFETs provide a clear advantage.

Conclusion

Polar MOSFET technology continues to provide a dependable foundation for power conversion systems operating under demanding conditions. Combining strong avalanche capability, wide SOA performance, and predictable thermal behavior, these devices offer a reliable alternative to newer technologies focused solely on efficiency metrics. For designers supporting both legacy platforms and modern industrial systems, Polar MOSFETs represent a practical solution - delivering proven reliability while supporting evolving application requirements.

Applications	Key Concern	Polar Advantage
Industrial and laboratory power supplies	Overvoltage, pulsed linear mode operation	Avalanche ruggedness, robust SOA
Test and measurement equipment	Sustain transient linear mode operation	Robust SOA
Medical and mission-critical power systems	Lifecycle, EMI, maturity, legacy designs	Availability, mature technology with proven decades in the field, clean noise free switching
Process and pulsed power such as plasma, laser and welding	Packaging, pulsed power, availability	Special packaging, superior pulsed power capability
Industrial servo drives and robotics	Overvoltage, pulsed linear mode, pulsed power handling	Avalanche ruggedness, robust SOA, superior pulsed power capability
Auxiliary power supplies in transmission and distribution, PV inverters and motor drives	Overvoltage, transient linear mode operation, ease of design	Avalanche ruggedness, robust SOA, simplified design
Power amplifiers for e.g. in audio and signal amplifiers	Transient linear mode operation, EMI	Robust SOA, clean noise free switching

Table 1: Typical applications where reliable operation is a critical requirement

References

Littelfuse offering of Polar MOSFETs (https://www.littelfuse.com/products/power-semiconductors-control-ics/mosfets-si-sic/n-channel-standard) and gate drivers (https://www.littelfuse.com/products/power-semiconductors-control-ics/gate-drivers/gate-driver-ics)

www.littelfuse.com.

LASTING QUALITY WITH DIFFUSION SOLDERING

PINK® Thermosysteme

Modular · Scalable · Future-Proof

SIN 50+

- Two joining technologies in one system: pressure sintering and diffusion soldering
- Flexible tool interface for 3D soft tool, 2D hard tool, and multi-punch tool
- Modular expandable: preheating, cooling, and automation on demand
- Process operation under protective gas or vacuum
- Fully and semi-automatic operation available

pcim
Nuremberg
9 – 11 June 2026
Visit us at booth 5-410

PINK GmbH Thermosysteme · Am Kessler 6 · 97877 Wertheim/Germany · info@pink.de · www.pink.de

APEX MICROTECHNOLOGY
PRECISION • POWER • ANALOG

NEW PRODUCT RELEASE!

MSA303

600V, 40A Silicon Carbide 3-Phase Integrated Power Module

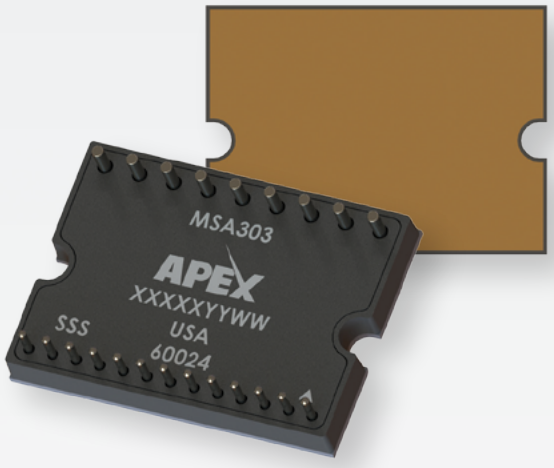

- Three-fully Independent Half-bridges
- Integrated Gate Driver
- Compact 30mm x 42mm Design
- Under-voltage Lock-out & Active Miller Clamping

Applications:

Motor Control, Variable Frequency Drives, DC/AC Converters, Power Inverters, Test Equipment

To learn more, visit: apexanalog.com

Improving Efficiency and Thermal Margin in a 204W Quarter-Brick Converter Using a 150V MOSFET

The quarter-brick DC/DC converter remains one of the most widely deployed isolated power modules in telecom infrastructure, networking equipment, industrial systems, and distributed 48V architectures. A typical implementation operating over an 18–75V input range and delivering 12V at 17A continues to serve as a workhorse intermediate bus solution in systems where footprint, thermal density, and long-term reliability are tightly constrained.

By Orion Kress-Sanfilippo, Systems and Applications Engineer, iDEAL Semiconductor

Despite the maturing of the quarter-brick format, incremental efficiency improvements on the order of 0.5–1% remain technically and economically consequential. At 200W power levels, a 1% efficiency improvement corresponds to approximately 2W reduction in dissipated heat. That reduction directly impacts thermal margin, airflow requirements, and long-term reliability. In densely populated telecom shelves or data-center racks, where dozens or hundreds of modules may be deployed, such improvements accumulate at the system level and can materially affect cooling infrastructure design and operating cost.

In recent years, increased rack-level power density in data centers and the expansion of 48V distribution architectures have intensified the need for higher efficiency within established converter footprints. Although higher-voltage distribution backbones are emerging in certain applications, the 36–75V input range remains dominant for intermediate bus conversion supplying downstream point-of-load regulators. Within this environment, designers are under pressure to improve efficiency without increasing module size or cost. As switching frequencies rise to reduce magnetics volume and improve transient response, the choice of primary-side MOSFET becomes increasingly influential.

To evaluate the impact of device selection on converter performance, testing was conducted on an off-the-shelf 204W quarter-brick power supply rated for 18–75V input, and 12V/17A output, operating at 270kHz in an active clamp forward topology (Figure 1). The default configuration utilized two 120V MOSFETs in parallel on the primary side. Comparative testing was performed by replacing the parallel pair with a single 150V MOSFET. Devices evaluated included the iS15M7R1S1C SuperQ™ MOSFET as well as two commercially available 150V devices representative of recent leading resistance competitors. A comparison of the evaluated devices is shown in Table 1. All testing measurements were taken at 48V input under no-airflow conditions to evaluate intrinsic electrical and thermal performance differences.

In an active clamp forward converter operating near 270kHz, primary switch losses are governed by the combined effects of conduction loss, switching overlap loss, and output capacitance discharge loss. While conduction loss has historically been the dominant loss in lower-frequency converters, at switching frequencies approaching or exceeding 250kHz, the relative contribution of switching and capacitive losses increases. Consequently, figures of merit beyond on-resistance must be considered.

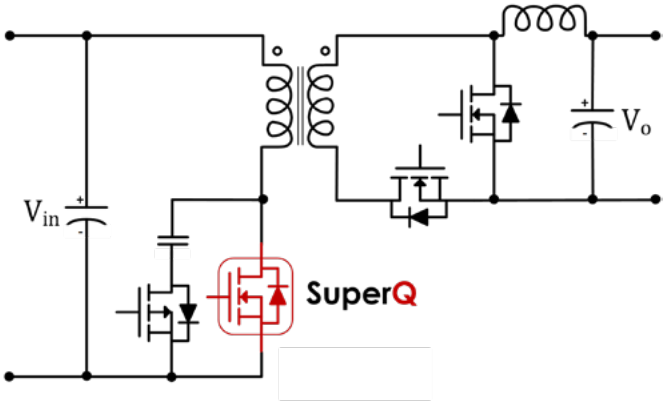

Figure 1: Active clamp forward converter schematic

Device parameters show that the SuperQ device combines low $R_{DS(on)}$ with significantly reduced switching charge (Q_{SW}) and lower output capacitance energy (E_{OSS}) compared to the evaluated alternatives. Although one competing 150V device exhibits slightly lower maximum $R_{DS(on)}$ under datasheet conditions, it does so at the expense of significantly higher Q_{SW} and E_{OSS}. In a 270kHz hard-switching environment, this tradeoff materially increases switching-related dissipation.

	SuperQ iS15M7R1S1C (x1)	Default Configuration - per FET (x2)	Comp Gen 5 (x1)	Comp Gen 6 (x1)
BV_{DSS} (V)	150V	120V	150V	150V
$R_{DS(ON),TYP}$ (mΩ)	5.4	9.6	6	5
$R_{DS(ON),MAX}$ (mΩ)	6.4	11.5	7.4	5.5
E_{OSS} (75V) (µJ)	1	1.3	3.4	4.1
Q_{SW} (nC)	4.9	6.8	14	15.9

Table 1: Devices tested in 204W Active-Clamp Forward Converter

Efficiency measurements taken at 48V input demonstrated that replacing the default dual-120V MOSFET configuration with a single 150V SuperQ device reduced total power loss by up to 2W and improved overall efficiency by more than 0.8%. For a 204W converter, this level of improvement is consistent with the calculated reductions in switching and conduction losses derived from measured Q_{SW}, E_{OSS}, and $R_{DS(on)}$ values. The measured data correlated closely with calculated loss estimates, indicating that the observed performance gains are attributable to intrinsic device characteristics rather than layout or measurement artifacts.

Thermal measurements further illustrate the practical significance of these electrical differences. Under 48V input and full 17A output load with no forced airflow, the default dual-device configuration reached a peak temperature of approximately 133°C after a five-minute soak. Under identical conditions, the single 150V SuperQ MOSFET reached approximately 120.5°C. In contrast, a representative 150V Gen6 competitor reached approximately 151.5°C (shown in Figure 2). The approximately 12°C reduction versus the default design and roughly 31°C reduction versus the Gen6 device are not incremental variations; they represent meaningful shifts in junction temperature. Reductions of this magnitude can substantially increase reliability margin or permit higher allowable ambient operating temperatures.

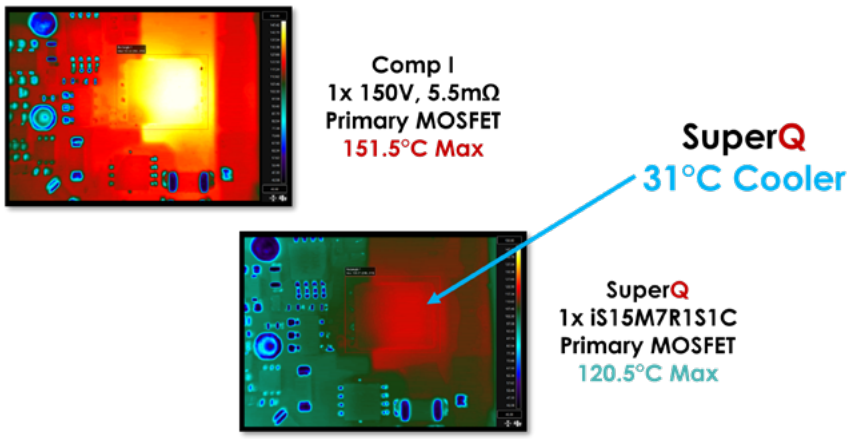

Figure 2: Thermal performance 48V_{IN}, 17A_{OUT}, No Air Flow, 5min soak

The thermal data also demonstrate that reducing device count does not necessarily increase stress when intrinsic device loss is sufficiently low. The default configuration required two 120V MOSFETs in parallel to satisfy conduction and thermal requirements. The 150V SuperQ device achieved lower loss and lower peak temperature using a single device. From a system design perspective, eliminating parallel devices simplifies layout, reduces gate drive current, and mitigates parasitic imbalance concerns. It can also reduce bill-of-materials cost and improve assembly yield in high-volume production. In a cost-sensitive quarter-brick module produced at high volume, component consolidation is a meaningful advantage.

From a broader architectural perspective, 48V distribution remains dominant in telecom and networking infrastructure and is expanding within data-center environments supporting high-performance computing and AI accelerators. Although 400V and 800V backplanes are emerging, in certain applications, intermediate bus converters operating within the 36-75V range remain central to power distribution. As system power density increases, designers continue to push switching frequency upward to reduce magnetics size and improve transient response. In this environment, minimizing switching charge and stored energy becomes as important as minimizing static resistance. Therefore, devices optimized solely for $R_{DS(on)}$ without simultaneous reduction in Q_{SW} and E_{OSS} may demonstrate limited net benefit in high-frequency isolated converters.

The data presented here indicate that simultaneous optimization of $R_{DS(on)}$, switching charge, and output capacitance energy can produce measurable improvements in both efficiency and thermal performance within an established quarter-brick platform. In the evaluated 204W active clamp forward converter operating at 270kHz, the 150V SuperQ MOSFET delivered up to 2W lower loss, an efficiency improvement of greater than 0.8%, and up to 31°C lower peak temperature compared to representative alternatives. These results demonstrate that even in mature converter formats, careful device optimization can meaningfully extend performance limits without requiring changes to topology, magnetics design, or control architecture.

As power density requirements continue to increase across telecom and data-center applications, incremental efficiency gains at the device level remain an important lever for system optimization. The quarter-brick converter, though long-standing in form factor, continues to benefit from advances in silicon power-device architecture. By addressing conduction, switching, and capacitive losses simultaneously, it is possible to extract meaningful efficiency and thermal improvements from an established topology while preserving the cost and manufacturability advantages of silicon technology.

www.idealsemi.com

pcim

International Exhibition and Conference
for Power Electronics, Intelligent Motion,
Renewable Energy and Energy Management
Nuremberg, 9 – 11 June 2026

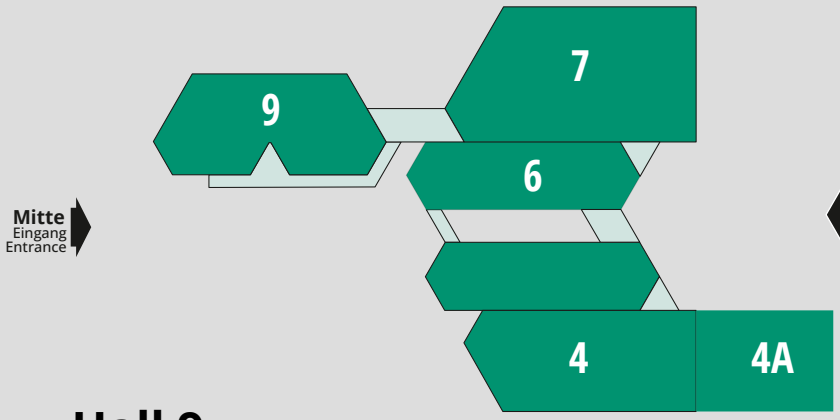

Hall 9

A.L.M.T. Corp. · soitec · ALPHA & OMEGA SEMICONDUCTOR · xfab · YOKOGAWA · BROADCOM connecting everything · CISSOID · MERSEN · ARCEL POWER ELECTRONICS · power integrations · Navitas · Littelfuse Expertise Applied | Answers Delivered · fine power YOUR INNOVATION HUB · nexperia · GVA POWER ELECTRONICS EXPERTS · starpower · ROGERS CORPORATION · Hitachi Energy · EPC EFFICIENT POWER CONVERSION · ROHM SEMICONDUCTOR · onsemi · TDK · LEM Life Energy Motion · PAYTON PLANAR · DOWA · Sanan · plexim electrical engineering software · VisIC TECHNOLOGIES · SSM SUSUMU Thin Film Specialist and Innovator

Bodo's Panel at the Technology Stage

Technology Stage | Hall 4, 139

1:25 – 2:25 PM (GMT+2)
10. June ´26

Riding the SiC Wave Efficiently Session 1

Bodo's WBG Panel

Technology Stage | Hall 4, 139

2:30 – 3:30 PM (GMT+2)
10. June ´26

Riding the SiC Wave Efficiently Session 2

Bodo's WBG Panel

Technology Stage | Hall 4, 139

11:45 – 12:45 AM (GMT+2)
11. June ´26

What´s up, What´s Next für GaN?

Bodo's WBG Panel

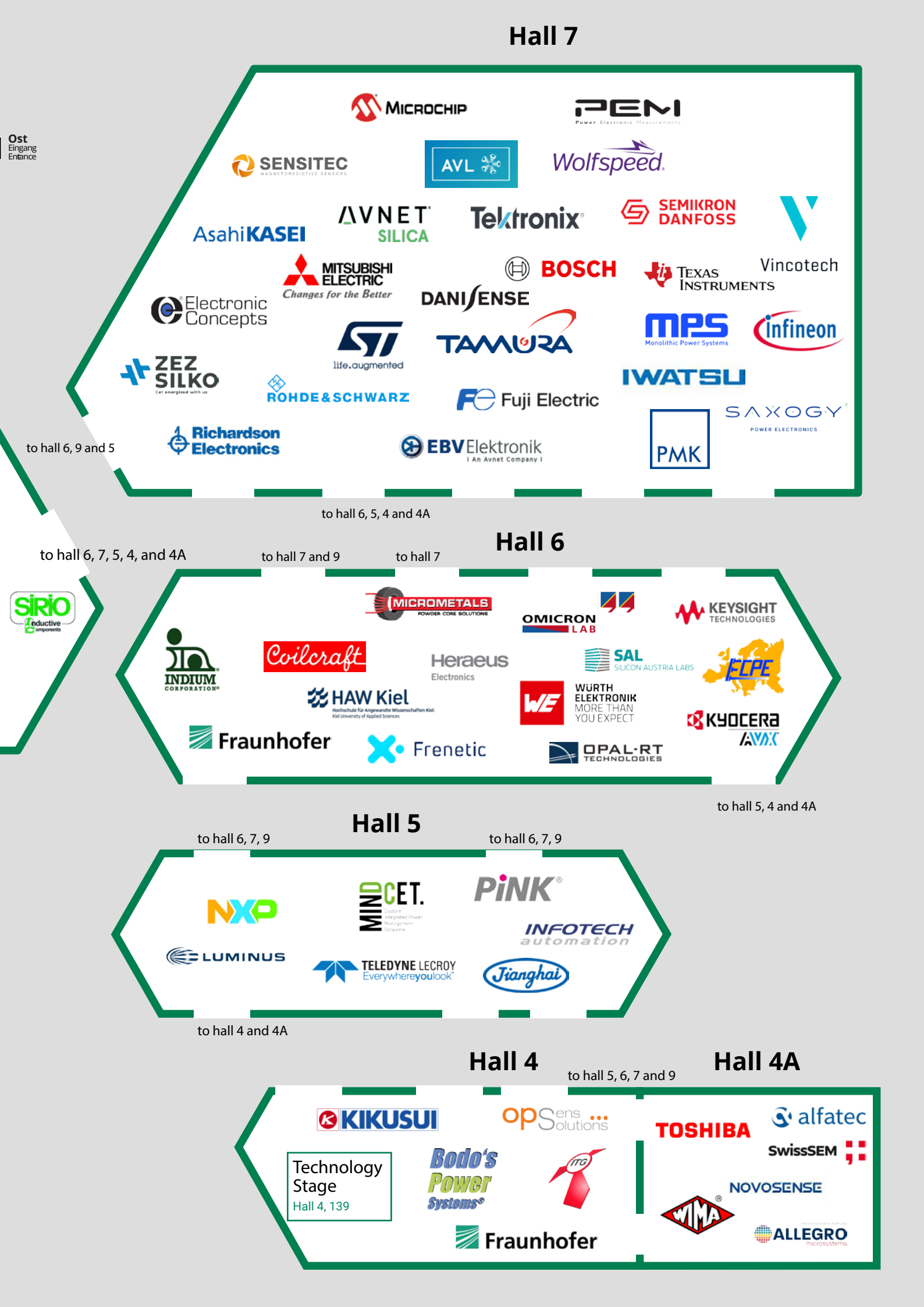
Hall 7
Ost
Eingang
Entance
MICROCHIP
PEM
Power Electronic Measurements
SENSITEC
AVL
Wolfspeed
AVNET
SILICA
Tektronix
SEMIKRON
DANFOSS
AsahiKASEI
MITSUBISHI ELECTRIC
Changes for the Better
BOSCH
TEXAS INSTRUMENTS
Vincotech
Electronic Concepts
DANISENSE
life.augmented
TAMURA
MPS
Monolithic Power Systems
infineon
ZEZ SILKO
IWATSU
ROHDE&SCHWARZ
Fuji Electric
SAXOGY
POWER ELECTRONICS
Richardson Electronics
EBV Elektronik
I An Avnet Company I
PMK
to hall 6, 9 and 5
to hall 6, 5, 4 and 4A
Hall 6
to hall 6, 7, 5, 4, and 4A
to hall 7 and 9
to hall 7
SIRIO
Inductive components
MICROMETALS
POWDER CORE SOLUTIONS
OMICRON LAB
KEYSIGHT TECHNOLOGIES
INDIUM CORPORATION
Coilcraft
Heraeus
Electronics
SAL
SILICON AUSTRIA LABS
ECPE
HAW Kiel
Hochschule für Angewandte Wissenschaften Kiel
Kiel University of Applied Sciences
WÜRTH ELEKTRONIK
MORE THAN YOU EXPECT
KYOCERA AVX
Fraunhofer
Frenetic
OPAL-RT TECHNOLOGIES
to hall 5, 4 and 4A
Hall 5
to hall 6, 7, 9
to hall 6, 7, 9
NXP
MINDCET
PiNK
INFOTECH automation
LUMINUS
TELEDYNE LECROY
Everywhereyoulook
Jianghai
to hall 4 and 4A
Hall 4
to hall 5, 6, 7 and 9
Hall 4A
KIKUSUI
opSens Solutions
TOSHIBA
alfatec
SwissSEM
Technology Stage
Hall 4, 139
Bodo's Power Systems
ITG
NOVOSENSE
WIMA
ALLEGRO
microsystems
Fraunhofer

More Power, More Tokens: How SSTs are Reshaping Data Center Infrastructure

The transition from AC distribution to the 800 V DC architecture is reshaping the data center power infrastructure, boosting token generation and revenue potential. Higher voltage SiC devices are simplifying SST designs and enabling 34.5 kV systems. Matrix converters are emerging as a promising alternative to the cascaded H-bridge architecture.

By Ehab Tarmoom, Applications Engineering Manager of Microchip Technology's High-Power Solutions Business Unit

Hyperscalers are turning to Solid-State Transformers (SSTs) to boost AI data center compute performance and maximize revenue. AI data centers are increasingly being described as factories that produce tokens during the inference process, where the token represents the compute output. An AI factory's throughput in the generation of tokens is limited by the available electrical power and is directly tied to its revenue potential.

Maximizing Grid-to-Chip Efficiency

Unlike storage, networking and edge workloads, the power demands of AI and modern High-Performance Computing (HPC) workloads continue to increase exponentially. As the GPU power consumption and the number of synchronized GPUs increase, compute rack power will continue to grow rapidly from tens of kilowatts to hundreds of kilowatts, and ultimately 1–2 megawatts. The compute output is constrained by the finite power that is available. Maximizing efficiency from the grid to the GPU not only reduces infrastructure and operating costs, but just as importantly, it maximizes compute power capacity, resulting in higher operating revenue.

Token production throughput is measured in Tokens Per Second (TPS) per MW, with a related metric of Tokens Per Watt (TPW), which measures efficiency at the token level. Both metrics tie token generation directly to power consumption. TPS per MW is used in planning the capacity of a facility, while TPW drives hardware- and system-level optimizations. The deployment of the 800 V AI data center architecture is planned to maximize the available power for token generation. The goal is to minimize the losses in the power distribution and conversion stages throughout the facility, from the utility grid feed to the sub-1 V GPU supply.

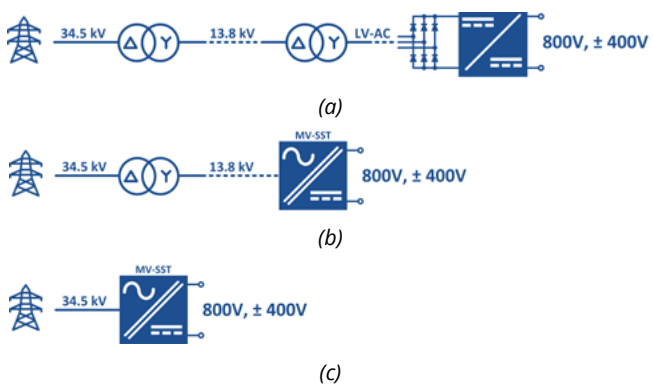

Figure 1: Phased deployments of grid-to-800 V architectures: (a) rectifier-based, (b) 13.8 kV SST and (c) 34.5 kV SST

The global AI data center build-out is driving a sharp demand for Low-Frequency Transformers (LFTs). Today, lead times are approaching 5 years[1], up from 18–24 months in recent years. LFT production cannot keep up with AI data center demand. Nearly half of U.S. data centers planned for this year have been delayed or canceled due to equipment shortages. Beyond the supply constraints, the LFT-based, system-level solution in Figure 1a suffers from low efficiency, low power density and inadequate power quality, and lacks the ability to support grid regulation.

The maximum voltage under Medium-Voltage (MV) AC classification varies by standards, with 35 kV under IEEE/ANSI and up to 72.5 kV under IEC standards. In the initial deployment of the 800 V distribution architecture, 34.5 kV utility power is fed into an LFT to step down the voltage to another MV-AC level, such as 13.8 kV, followed by a second LFT to produce Low-Voltage (LV) AC, such as 480 V. The LV-AC supplies a three-phase rectifier and DC/DC converter to output a regulated 800 V DC. Subsequent deployments will transition to an SST-based architecture.

Solid-State Transformer

In the context of an AI data center, a solid-state transformer is a power electronics system that converts MV-AC to LV-DC voltages, such as 800 V or ±400 V. The utility power and regulated output are galvanically isolated by means of a Medium-Frequency Transformer (MFT). SSTs can include bidirectional power flow capability for maintaining grid stability. Outside of data centers, such as in microgrids, an SST may be used to generate regulated AC outputs with higher or lower voltage at a different line frequency and may also be implemented as a multi-port system.

As AI data centers scale to hundreds of megawatts and beyond, volumetric power density of power equipment within the facility becomes an increasingly critical design constraint. AC power distribution architectures that provide a three-phase feed to a power rack local to the compute rack will be replaced with an 800 V or ±400 V DC distribution architecture. This frees up valuable floor space for compute racks.

Dry-type LFTs used in data center gray space have a typical power density of 200 kW/m^3, while outdoor-rated, oil-filled LFTs are higher at 450 kW/m^3, as the oil reservoir and cooling radiator provide effective thermal management. The power density of both 3-phase 6-pulse and 12-pulse rectifiers is typically 600 kW/m^3. The DC-DC converter has a typical power density of 400 kW/m^3. For the solution in Figure 1a, the total volume for a 3.5 MW system is 40 m^3 and the power density is 88 kW/m^3. Excluding the 34.5 kV LFT, the volume of the 13.8 kV LFT, rectifier and DC/DC converter is 32 m^3 and the power density is 109 kW/m^3. Further improvements in this architecture's power density are marginal.

Integrated Multiphase Inductor 20% Less Copper, 20% Less Losses, 30% smaller Size

5 kW - 500 kW with minimized coupling coefficient

Streamline your power management with our innovative integrated multiphase inductor, designed to replace traditional multiple inductors **in three-phase and single-phase systems**. This advanced solution reduces both size and weight, while minimizing magnetic coupling issues that disrupt inductance balance and complicate power control. Experience enhanced efficiency and performance with our compact design, featuring a common magnetic flux area for optimal operation. Upgrade to a smarter power solution today!

	Traditional Type	**Integrated Multiphase Type**
Volume	1,158 cm^3	**642 cm^3 (45%↓)**
Weight	3.5 kg	**2.2 kg (37%↓)**
Inductance balance*	±14%	**±0.1%**
Coupling coefficient	0.45	**0.15**
B_{pk}	98.7 mT	**88.7 mT**
Core Loss**	21 W	**12.7 W**
Coil Loss**	19.2 W	**15.7 W**

* @0A **@1 phase

Integrated inductors combine several inductors into a single unit without requiring changes to the circuit, achieving significant reductions in both volume (45%) and weight (37%). Additionally, by minimizing the magnetic coupling coefficient compared to traditional methods, they maintain inductor balance under DC bias (DCB), facilitating easier power control.

Ajka Transformatoren Kft
8400 Ajka, Liszt Ferenc u. 617, HU

Contact: Wolfgang Schmidt
+49 171 6423-937
wolfgang.schmidt@ajka-trafos.com

Chang Sung Corporation CSC

The power density of today's 13.8 kV SSTs is approximately 100 kW/m³. Unlike the LFT-rectifier-based solution, which has largely plateaued in power density scaling, the SST is an emerging technology with future power density targets of 1 MW/m³ as projected by industry leaders.

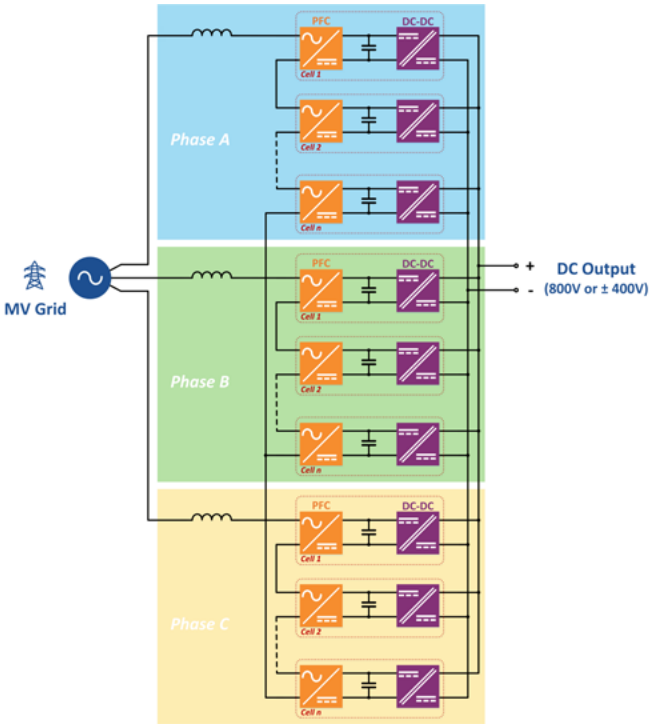

Figure 2: MVAC-fed cascaded H-bridge SST

The migration from three-phase AC distribution to 800 V DC distribution alone offers efficiency improvements of 5 % or more, with further gains as the architecture transitions from rectifier-based to SST-based deployments. The rectifier-based 800 V DC architecture in Figure 1a is estimated to achieve a grid-to-800 V efficiency of approximately 95 %. The 13.8 kV SST-based architecture in Figure 1b is expected to reach 97–98 %, while the 34.5 kV SST in Figure 1c is expected to reach 98–99 %.

SST Architecture

The Cascaded H-Bridge (CHB) in Figure 2 is the predominant architecture used in SST designs. The CHBs in each of the three phases are composed of cells connected in an Input-Series Output-Parallel (ISOP) configuration. The front-end series connection uses devices with blocking voltage ratings less than the applied phase voltage. The CHB cells are sized such that the sum of their individual voltage ratings exceeds the peak phase voltage with margin. In an SST design with N+2 redundancy, a 13.8 kV SST may have 14 cascaded cells per phase, each using 1200 V SiC MOSFETs to block the 8 kV

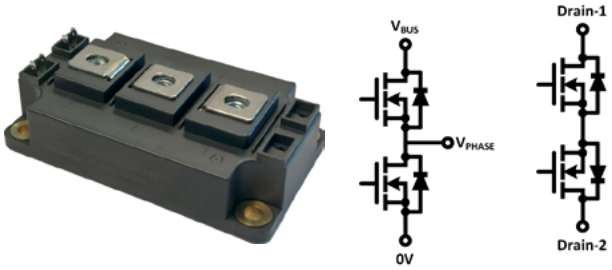

(a) *(b)* *(c)*

Figure 3: (a) Microchip 3.3 kV HV-D3 SiC Power Module, (b) half-bridge configuration and (c) common-source configuration

phase voltage. The secondary side of the cells connects in parallel to provide the high-current, 800 V regulated output. An N+2 SST with 14 cells per phase, 42 in total, each rated at 40 kW, may have a 1.4 MW power rating with maximum continuous output current of 1800 A.

For additional voltage headroom and a system with fewer cascaded cells, the trend has been to use SiC MOSFETs with higher voltage ratings, such as 1700 V-rated devices. This reduces the per-phase cell count to ten.

A promising alternative to the CHB is the matrix converter. Matrix converters have been extensively researched in academia, and advances in SiC technology are now enabling their adoption in high-power SST applications where power density and efficiency are critical. While there are several challenges in developing a robust matrix converter, one of the key benefits enabling higher reliability is the absence of energy storage elements, such as DC link capacitors or inductors.

The switch design of a matrix converter differs from that of a cascaded H-bridge. The CHB uses one or more (unidirectional) MOSFETs per switch position, connected in parallel for higher current capability. In a matrix converter, the switch must operate as a four-quadrant switch. That is, it must block voltage of both polarities and conduct current in both directions. This is achieved by connecting SiC MOSFETs in an anti-series configuration: common-drain or common-source. In low-voltage and low-power applications, 700 V or 1200 V MOSFETs connected in a common-drain configuration may be co-packaged in a discrete, surface-mount package. This configuration requires isolated gate drivers for each of the two MOSFETs. With the SST's high blocking voltage and its creepage and clearance distance requirements, discrete, surface-mount packages are typically not an ideal solution.

Microchip HV-D3 mSiC® Module

The Microchip HV-D3 family of 3.3 kV SiC power modules offers solutions for both CHB and matrix converter-based SST architectures. The HV-D3 in Figure 3 is available in a half-bridge configuration with two unidirectional series-connected switches and in a common-source configuration forming a single bidirectional switch. An advantage of the common-source configuration over the common-drain is that only one isolated gate driver is needed per bidirectional switch, further reducing system complexity. This is because the MOSFETs' gate and source terminals are part of the same isolation zone.

The HV-D3 module conforms to the industry-standard 62 mm footprint but with higher voltage isolation. In MV-SST applications, the power module must withstand high voltage transients while maintaining safe isolation. While 4 kV isolation voltage is the industry-standard for this package type, the HV-D3 is rated for 6 kV isolation voltage and classified as Material Group 1 with a Comparative Tracking Index (CTI) of ≥600V. The terminal-to-terminal and terminal-to-baseplate creepage distances are 23 mm and 28.3 mm, respectively.

The 3.3 kV HV-D3 SiC power module design addresses practical challenges in developing high-voltage converters, including SSTs. Its performance characteristics and topology options enable designers of CHB- or matrix converter-based SSTs to meet challenging MV application requirements.

[1] The US Data Center Boom Is Hitting a Transformer Crunch - Bloomberg

www.microchip.com

Dry-Type Film Capacitors for High-Frequency Power Applications

Modern semiconductor materials such as SiC or GaN operate at significantly higher switching frequencies than traditional silicon transistors. This results in substantially increased demands on capacitors in power applications such as converters, voltage regulators, and similar systems. Next-generation dry-type film capacitors with low-ESL designs are capable of meeting these challenges. The key factor is the interaction between component and system design.

By Joe Bond, CTO, and Peter Best-Lydon, Application Engineer, both Electronic Concepts

Dry plastic dielectric (film) capacitors represent a key technology in modern power electronic systems. Their high reliability, low losses, and stable capacitance over temperature and frequency make them ideally suited for applications with stringent efficiency and lifetime requirements. In contrast to commonly used electrolytic capacitors, they do not require liquid media or complex sealing, enabling compact and flexible designs.

Metallized film capacitors, in particular, offer a decisive advantage in terms of long-term stability due to their self-healing properties. Typical applications include snubber circuits, DC link circuits, EMC filters, and output filters of inverters. With the advancement of modern power semiconductors, the focus is increasingly shifting from pure capacitance provision to highly optimized, application-specific components.

Technological Background

The use of wide bandgap semiconductors such as SiC and GaN leads to significantly increased switching frequencies. At the same time, this broadens the spectrum of harmonics and electromagnetic interference. As a result, the requirements for passive components, especially capacitors, become more stringent.

While in many power conversion topologies higher frequencies reduce the required capacitance, the demands on parasitic parameters increase. Low equivalent series inductance (ESL), low losses (ESR), and high self-resonant frequency become dominant design criteria. Conventional designs with solid lead wires are increasingly reaching their physical limits.

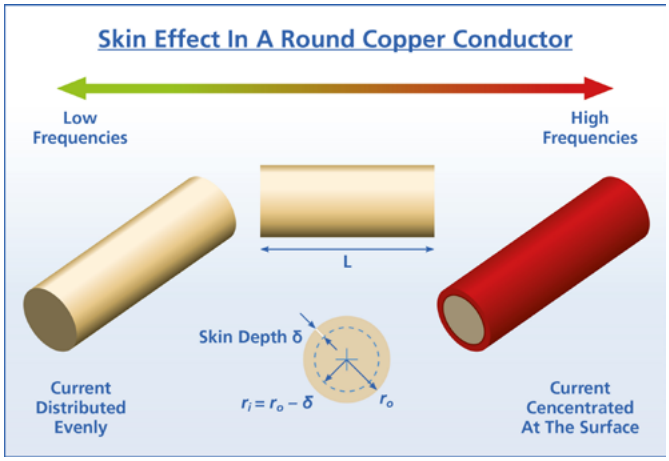

Figure 1: Skin Effect in a Round Copper Conductor. Picture by Electronic Concepts

High-Frequency Effects

Skin Effect and Penetration Depth

A key phenomenon in high-frequency applications is the skin effect, where current flow concentrates on the surface of a conductor. The characteristic penetration depth δ decreases with increasing frequency, reducing the effectively usable cross-sectional area.

The distribution of penetration depth along the conductor perimeter is significant for both round and flat conductors, as illustrated in Figure 1 and 2.

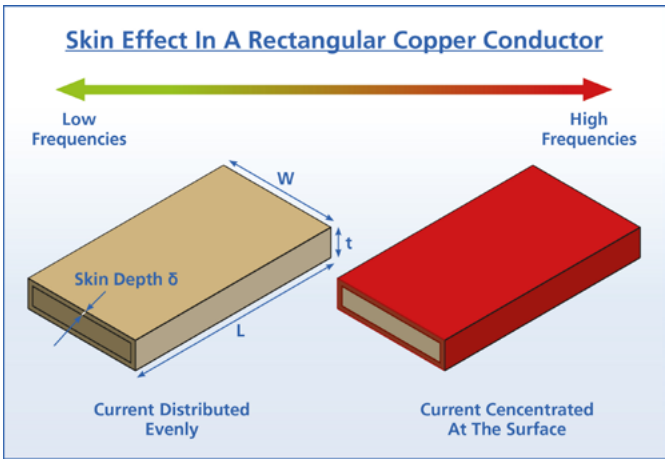

Figure 2: Skin Effect in a Rectangular Copper Conductor. Picture by Electronic Concepts

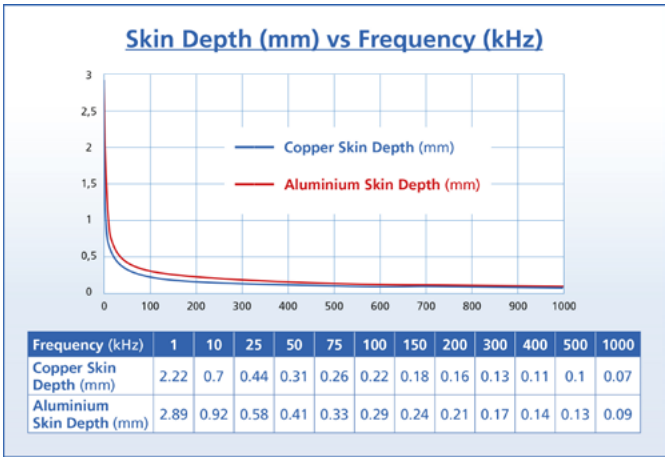

Frequency (kHz)	1	10	25	50	75	100	150	200	300	400	500	1000
Copper Skin Depth (mm)	2.22	0.7	0.44	0.31	0.26	0.22	0.18	0.16	0.13	0.11	0.1	0.07
Aluminium Skin Depth (mm)	2.89	0.92	0.58	0.41	0.33	0.29	0.24	0.21	0.17	0.14	0.13	0.09

Figure 3: Comparison of Skin Depth (mm) vs Frequency (kHz) in Copper and Aluminium Conductors. Picture by Electronic Concepts.

This leads to an increase in AC resistance, resulting in higher losses and thermal stress. The optimal conductor design results when the DC and AC resistance of the conductor are equal at the required frequency. The conductor material, such as copper or aluminium, also affects penetration depth, as shown in Figure 3.

For copper, the penetration depth is approximately 2.2 mm at 1 kHz, decreasing to below 0.1 mm in the MHz range. The skin depth must be greater than the radius of a round conductor or half the thickness of a flat conductor to maintain low resistance at high frequencies. The threshold or crossover maximum frequency occurs when the skin depth equals the radius or half thickness.

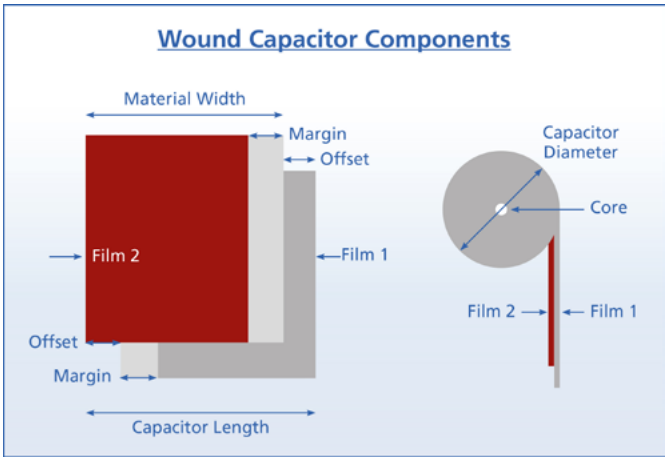

Figure 4: Components of a Wound Capacitor (Colouring is for Illustrative Purposes). Picture by Electronic Concepts

Above this threshold frequency, the conductor will get hotter as the conducting cross section is insufficient and the resistance increases. The resonant frequency of the capacitor must be less than the threshold frequency. As the ESL of the capacitor decreases, the resonant frequency increases.

Typical measures include the use of flat conductors, multiple terminals, or special geometries such as tubular or foil conductors. These approaches ensure that the effective conductor cross-section remains sufficient even at high frequencies, while limiting thermal effects.

Interaction Between ESL and Resonant Frequency

The parasitic inductance of a capacitor significantly determines its self-resonant frequency. Reducing ESL shifts this frequency to higher values and extends the usable bandwidth. At the same time, losses caused by the skin effect must be controlled to avoid thermal overload.

System and Circuit Strategies

At the system level, various approaches exist to reduce parasitic effects. In lower-power applications, multiple standard capacitors are often connected in parallel on printed circuit boards. By arranging opposing current paths, magnetic fields can partially cancel each other, reducing effective inductance.

However, this approach increases component count and incurs additional costs for PCB area and assembly. In high-power applications, specially developed low-ESL capacitors are often more economical, as the required properties are already integrated into their design.

Power Density Meets Rugged Reliability

The AOTL037V60DE2 delivers exceptional body diode performance, superior avalanche capability and extended short-circuit withstand time. Boost efficiency, maximize power density and enhance reliability across power supplies, converters and inverter applications.

- Exceptional body diode ruggedness
- Superior avalanche capability
- Extended short-circuit withstand time
- Robust surge and inrush current immunity

ALPHA & OMEGA SEMICONDUCTOR
Powering a Greener Future™

pcim Booth #9-539
Nuremberg, 9 – 11 June 2026

www.aosmd.com

Design of Film Capacitors

Winding Structure and Material Utilization

Film capacitors are based on wound dielectric structures, whose geometry is critical for electrical and thermal properties. The basic structure of such a winding, including margin and offset regions, is shown in Figure 4.

Inactive areas such as margins and offsets reduce effective surface utilization but are necessary for design reasons. Reducing the film width lowers volumetric efficiency but improves current-carrying capability and reduces ESR as well as ESL. These trade-offs require application-specific optimization.

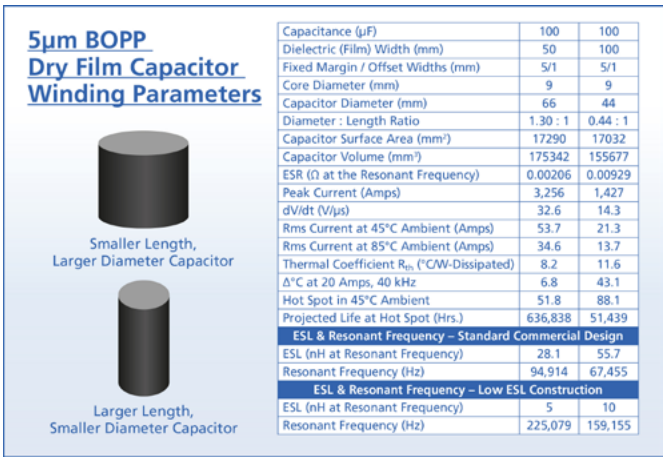

Capacitance (µF)	100	100
Dielectric (Film) Width (mm)	50	100
Fixed Margin / Offset Widths (mm)	5/1	5/1
Core Diameter (mm)	9	9
Capacitor Diameter (mm)	66	44
Diameter : Length Ratio	1.30 : 1	0.44 : 1
Capacitor Surface Area (mm²)	17290	17032
Capacitor Volume (mm³)	175342	155677
ESR (Ω at the Resonant Frequency)	0.00206	0.00929
Peak Current (Amps)	3,256	1,427
dV/dt (V/µs)	32.6	14.3
Rms Current at 45°C Ambient (Amps)	53.7	21.3
Rms Current at 85°C Ambient (Amps)	34.6	13.7
Thermal Coefficient R_{th} (°C/W-Dissipated)	8.2	11.6
Δ°C at 20 Amps, 40 kHz	6.8	43.1
Hot Spot in 45°C Ambient	51.8	88.1
Projected Life at Hot Spot (Hrs.)	636,838	51,439
ESL & Resonant Frequency – Standard Commercial Design		
ESL (nH at Resonant Frequency)	28.1	55.7
Resonant Frequency (Hz)	94,914	67,455
ESL & Resonant Frequency – Low ESL Construction		
ESL (nH at Resonant Frequency)	5	10
Resonant Frequency (Hz)	225,079	159,155

Figure 5: Winding Parameters of the 5µm BOPP Dry Film Capacitor. Picture by Electronic Concepts

Geometry and Thermal Performance

The ratio of winding diameter to length significantly affects performance. Compact, thick designs offer advantages in current-carrying capability and heat dissipation, while elongated geometries allow better material utilization. Such a comparison can be seen in Figure 5.

Experimental comparisons show that reducing dielectric width can yield significant improvements. The comparison shows when the material width is halved, the resonant frequency increases 42% from approximately 67 kHz to 95 kHz. The power advantages of half the material width are also apparent. The ESR drops 78% from 9.29 mΩ to 2.06 mΩ, and the peak and RMS current capacity more than doubles. The lower ESR and thermal coefficient results in much less internal heating and over a magnitude increase in life projection. The plastic dielectrics used are organic and follow the 10°C rule, whereby every 10°C decrease in temperature doubles the life.

Design Approaches for Modern High-Performance Capacitors

Advanced capacitor solutions employ targeted design measures to minimize parasitic effects. These include concentric winding structures, integrated bus structures, and large-area terminals.

Internal current reversal enables coaxial current paths, allowing effective inductance compensation. This forms a true coaxial winding effectively cancelling the inductance of the completed unit. Double or triple concentric wound capacitors are possible on open cores ranging from 9-38mm diameter. Electronic Concepts provides additional cancellation techniques for the terminals exiting the package to realize ESL down to 5nH as provided in the LH3 product series and optionally offered in UL3, UX3, and MP3 DC link series shown in Figure 6, along with other capacitors that Electronic Concepts offer.

Such designs achieve ESL values in the range of a few nanohenries and are therefore optimized for high-frequency applications. A key advantage of these integrated approaches is their independence from external layout measures, ensuring reproducible electrical characteristics.

Figure 6: A Selection of Electronic Concept's Film Capacitor Range. Picture by Electronic Concepts

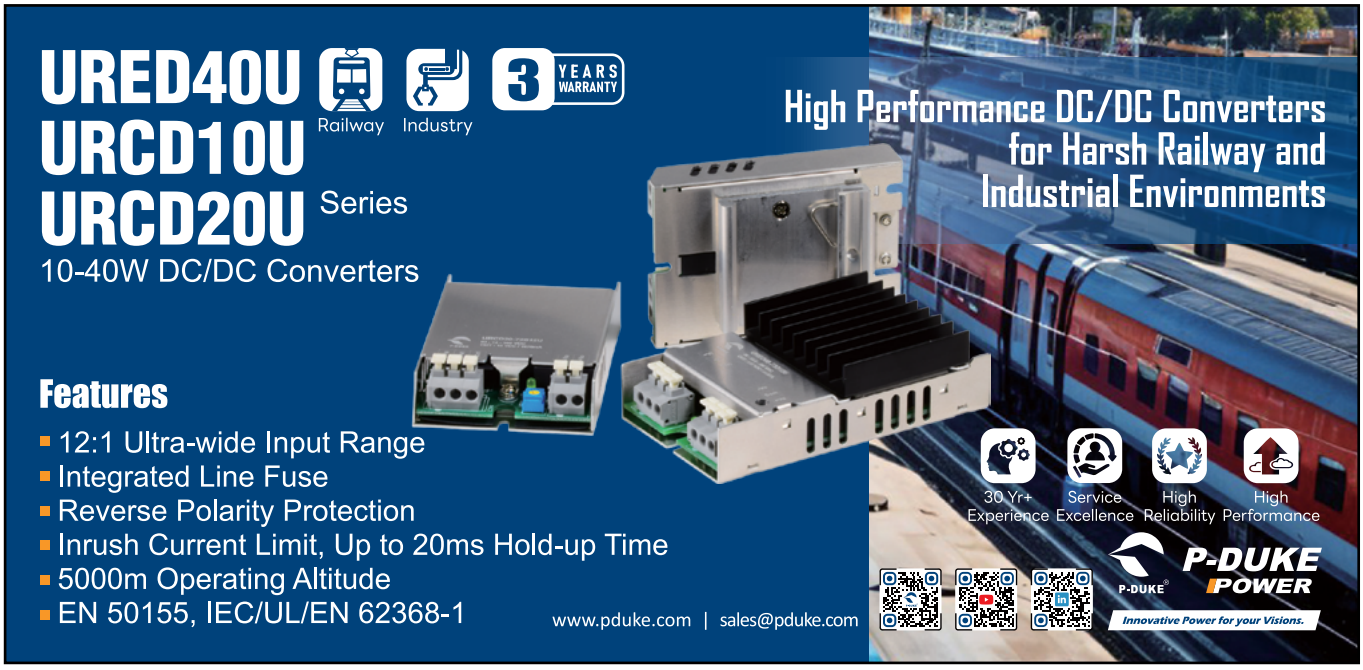

Interpretation of Capacitor Specifications

When evaluating datasheets, it is important to distinguish between component-level and system-level parameters. Frequently specified low ESL values often refer to optimized installation conditions rather than the standalone component.

Without appropriate PCB layout, the effective inductance can be significantly higher. Therefore, a deep understanding of the interaction between component and system environment is essential to avoid misinterpretation and mismatches.

Conclusion

The rising switching frequencies of modern power semiconductors significantly intensify the requirements for capacitors. In addition to traditional parameters, parasitic effects such as ESL and ESR are becoming increasingly important.

An optimal solution requires a holistic approach, considering both system design and component design. While circuit-level measures may be sufficient in some cases, integrated low-ESL capacitors offer clear advantages, particularly in high-power applications.

Modern film capacitors combine innovative materials, optimized geometries, and advanced manufacturing technologies to meet these growing demands. Their application-specific design is a key factor for the efficiency, reliability, and cost-effectiveness of future power electronic systems.

Glossary

- 10°C Rule A rule of thumb stating that a reduction in operating temperature by 10°C approximately doubles the lifetime of polymer dielectric materials.
- AS9100 A quality management standard for the aerospace industry, equivalent to EN 9100.
- Dielectric The insulating material between the electrodes of a capacitor, determining voltage withstand capability and high-frequency behavior.
- ESL (Equivalent Series Inductance) The parasitic inductance associated with a capacitor. Lower ESL enables better high-frequency performance.
- ESR (Equivalent Series Resistance) The effective resistive component of a capacitor, representing internal losses.
- Film Capacitor A capacitor using polymer film as dielectric. Metallized film capacitors provide self-healing capability after dielectric breakdown.
- Skin Effect The tendency of alternating current to concentrate near the surface of a conductor, increasing resistance with frequency.
- Snubber A circuit used to suppress voltage transients and damp oscillations.
- Wide Bandgap Semiconductors Semiconductors such as SiC and GaN with larger bandgaps, enabling higher efficiency, higher switching frequencies, and improved thermal performance of the respective circuit.

CADDOCK

High Performance Resistors

Power Film Resistors

Type MP800, MP900, and MP9000 Series
Heat Sink Mountable
Non-Inductive Designs
Resistance Range: From 0.005Ω to 100 KΩ
Power 15 watts up to 100 watts at +25°C case temp.

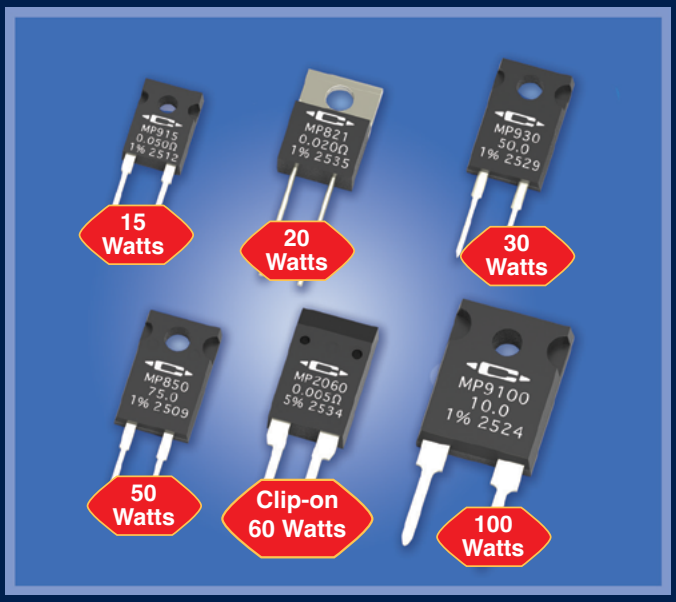

Type MS and Type MV Series
Axial lead - High Power
Non-Inductive Designs
Resistance Range: From 0.10Ω to 30 MegΩ
Power Rating: 0.5 Watt up to 22 Watts

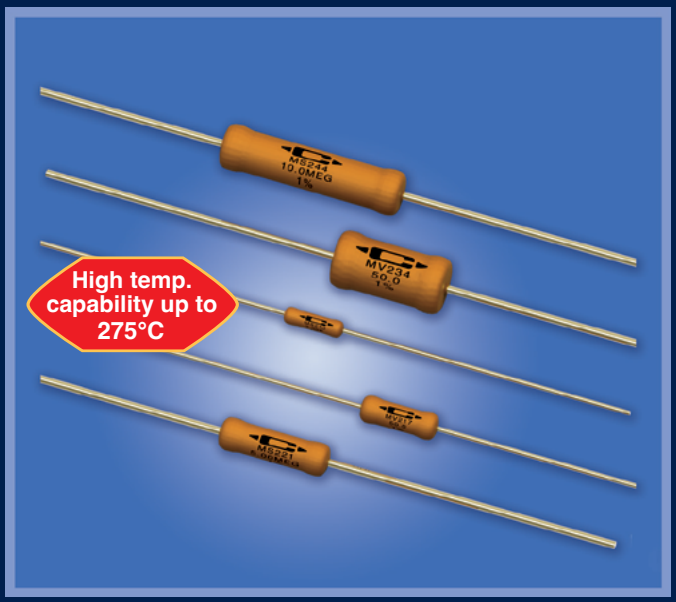

CADDOCK

For Distributors by country: see caddock.com/contact/dist.html
Applications Engineering, Roseburg, Oregon, USA
phone: 541-496-0700 • email: sales@caddock.com
website: www.caddock.com

© 2025 Caddock Electronics, Inc. L-500.1125

Third Generation SiC MOSFETs for Highly Efficient Electric Vehicle Drivetrains: Improving Robustness and Performance

The third generation of Bosch's SiC MOSFETs stands out with its advanced trench design, yielding significantly optimized efficiency in electrified vehicle drivetrains.

The new trench cell architecture effectively addresses the challenges posed by operation in the traction inverter. Improvements to the trade-offs between conduction losses, switching losses, reliability, and robustness have optimized the power transistor for high efficiency and a long lifetime.

By Jens Baringhaus, Samuel Araujo, Manuel Horvath, and Stephan Schwaiger, Robert Bosch GmbH

Advancing the dual-channel SiC trench gate MOSFET

Silicon carbide (SiC) trench MOSFETs are undisputedly the leading technology for automotive drivetrain inverters, which require high performance and robustness. As the demand for greater efficiency, power density, and reliability in electric vehicles continues to grow, Bosch is advancing the trench architecture to meet these needs.

The Gen2 dual-channel design (see figure 1) remains the foundation of this innovation. Its deep p-type shielding regions ensure optimal use of the trench architecture by utilizing both sides of the trench for on-state current conduction. This increases channel density, decreases resistance, and maximizes the active area for current flow, which is crucial for minimizing energy losses. The deep p-type shielding implantations protect the gate complex in the trench and provide a common JFET region for both channels, limiting saturation current in the event of a short circuit. This intrinsic short-circuit protection is a vital safety feature that prevents thermal runaway and catastrophic failure under fault conditions.

Bosch has further advanced this concept with Gen3. By adding an extra shield implant to the trench itself (see figure 1), the device is fully protected against off-state electric fields. During the off-state, the electric field experienced by the gate oxide is extremely low. Therefore, the off-state operation has no impact on the gate oxide's lifetime. This improves the long-term reliability of the historically sensitive gate oxide.

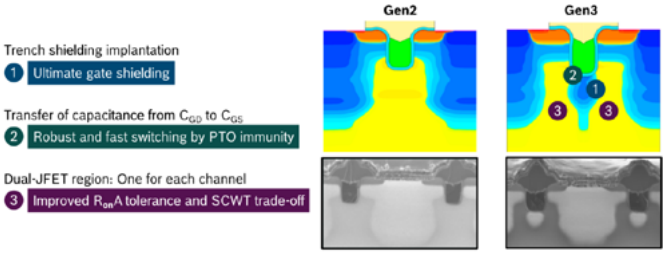

Figure 1: Advancing the dual-channel SiC trench gate MOSFET architecture from Gen2 to Gen3.

Gen3 SiC MOSFETs: superior performance, robustness, and heat dissipation

The novel cell design improves static as well as dynamic performance, robustness, and heat dissipation (see figure 2). A 20 percent reduction in specific on-resistance ($R_{on}A$) significantly decreases the required chip area, resulting in more cost-effective converter designs with Gen3 devices (figure 2, left). This directly translates to smaller and lighter power modules for electric vehicles (EVs). Shifting part of the gate-drain capacitance (CGD) to the gate-source capacitance (CGS) reduces the gate-drain charge (QGD), achieving faster voltage commutation. Switching losses are reduced by about 10 percent during typical traction inverter operation, enhancing partial load efficiency and significantly improving the overall system efficiency.

These performance improvements are achieved without compromising robustness. In fact, Gen3 enhances robustness against both short-circuits and parasitic turn-ons. This improvement is partially enabled by the newly implemented two-zone JFET region below the trench, which allows for more efficient current distribution during short-circuit events. In addition, decreasing the QGD lowers the Miller ratio. A lower Miller ratio effectively damps gate voltage oscillations at the gate of the passive switch, thereby reducing the risk of parasitic turn-on. This allows for higher switching frequencies without compromising reliability. Consequently, switching speed can be safely increased. The short-circuit withstand time (SCWT) of Gen3 devices is about 10 percent higher than that of Gen2 trench MOSFETs (see figure 2, right).

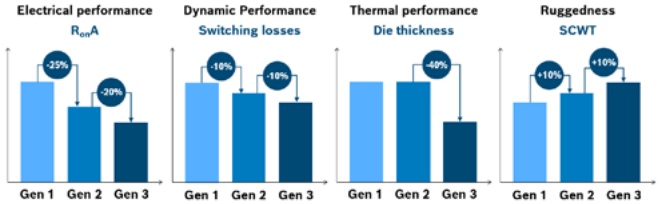

Figure 2: Gen3 outperforms Gen2 in terms of key performance metrics.

Advert

Finally, limiting the die thickness to 100 µm (figure 2, middle) has a positive impact on thermal properties, leading to superior heat dissipation and enabling higher power densities.

A new cell architecture: efficient under demanding conditions

The new cell architecture was key to enhancing both robustness and performance. The narrower JFET regions and the one-to-one correspondence between channels and JFET regions greatly improved the trade-off between specific overall $R_{on}A$ and short-circuit withstand time. This balance is crucial, since improving one often degrades the other. Although a narrower JFET naturally requires more processing, especially for lithographic alignment of the individual p-type regions, Gen3 elegantly circumvents this issue. Using a self-aligned implantation in the formed gate trench perfectly aligns the trench with its underlying protection implant, keeping the alignment tolerance at the same level as Gen2. In other words: No new lithography layer is required to create additional protection implantation, and the existing hard mask of the trench etching process is reused, making mass production feasible and cost-effective.

The larger design window is reflected in figure 3 (left), displaying the trade-off relationship between specific $R_{on}A$ and saturation current (I_{sat}) during a short-circuit event. The entire trade-off curve is shifted in parallel, which yields a wider design space for robust and high-performing devices. The device behavior during a short-circuit type 1 event (SC1, figure 3, right) reflects the lower current density during the short-circuit condition, providing additional time for the gate driver to detect the fault and shut off the transistor. As a result, peak temperature as well as dissipated energy are significantly reduced, providing high intrinsic short-circuit robustness.

For traction inverter operation in particular, a soft diode is important to reduce the current commutation slope for mitigating voltage peaks and high voltage commutation slopes during reverse recovery (V_{rr}). A "hard" recovery can result in damaging voltage spikes and increased electromagnetic interference (EMI). Gen3 body diodes are specifically designed to provide soft recovery behavior across the entire temperature range of -40 °C to 200 °C and a very high robustness against parasitic turn-on, especially at high temperatures as shown in figure 4 (left). The body diode exhibits a very soft recovery behavior with controlled current decay (dI/dt), indicating gradual and well-controlled current transitions during reverse recovery. Only minimal voltage ringing is observed in the V_{DS} waveform, indicating clean and fast switching behavior. Figure 4 (right) also illustrates high temperature stability by showing the maximum reverse recovery voltage ($V_{DS,max}$) as a function of junction temperature (T_j). Even at 200 °C, $V_{DS,max}$ remains well below 1,100 V – more than 400 V below the device's breakdown voltage. This provides ample safety headroom, ensuring extremely reliable and safe operation under the most demanding switching conditions.

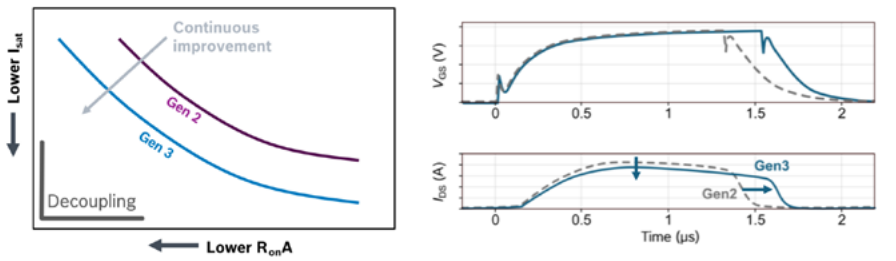

Figure 3: Compared with Gen2, the Gen3 SiC MOSFET device behavior shows a superior trade-off between specific on-resistance ($R_{on}A$) and saturation current (I_{sat}) during a short-circuit event. The transient gate-source voltage (V_{GS}) and drain current (I_{DS}) reflect a lower current density during the short-circuit event, as well as an extended time window for short-circuit detection and shutdown.

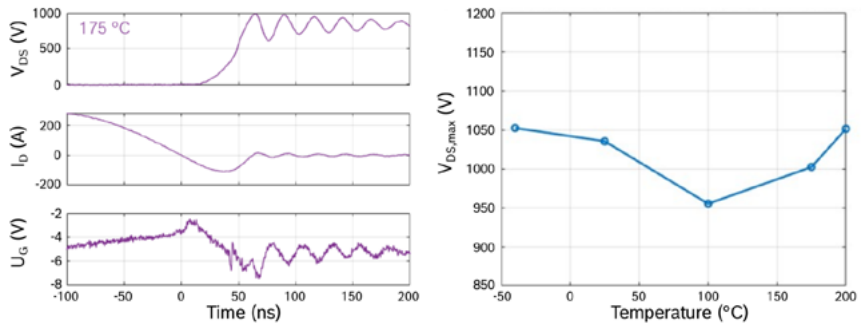

Figure 4: The reverse recovery behavior of the Gen3 SiC MOSFET body diode shows soft recovery with low voltage ringing. Transient drain-source voltage (V_{DS}) and drain current (I_D) versus time illustrate controlled current transition. Maximum reverse recovery voltage ($V_{DS,max}$) versus junction temperature demonstrates stable operation across the temperature range.

Conclusion

Bosch's third generation SiC MOSFETs represent a significant leap forward in power semiconductor technology for electric vehicle drivetrains. With its dual-channel trench architecture, enhanced by novel self-aligned shield implantations and refined JFET regions, these devices offer unmatched efficiency, robustness, and reliability. Demonstrated improvements include a 20 percent reduction in specific on-resistance, a 10 percent decrease in switching losses, significantly enhanced short-circuit withstand capability, improved parasitic turn-on robustness, and a soft body diode that operates across a wide temperature range. These improvements collectively address the stringent demands of modern automotive applications. By optimizing the $R_{on}A$-SCWT trade-off and ensuring stable and safe operation under challenging conditions, Bosch's Gen3 SiC MOSFETs maximize the performance and lifetime of EV inverters and contribute to the widespread adoption of high-performance electric vehicles. This continuous innovation underscores the critical role of advanced SiC technology in shaping the future of sustainable mobility.

www.bosch.com

Test Equipment for the next Generation of Power Semiconductors

Driven by the continuous optimization of modern power semiconductors towards higher blocking voltages and load currents while simultaneously minimizing switching and conduction losses, the requirements for test equipment increase accordingly. To qualify future high performance semiconductor devices reliably and safely, precise and robust measurement and testing solutions are essential.

By M. Sc. Philipp Berkemeier, Dipl. Ing. Konrad Domes, SAXOGY POWER ELECTRONICS GmbH

For more than 20 years, SAXOGY POWER ELECTRONICS GmbH, based in Chemnitz, Germany, has been developing customized solutions in the fields of safety test benches, and electronics for power electronic applications.

Stimulated by market-driven innovations in high-power semiconductor technology, development of the first electrical generators began two years ago. These generators enable comprehensive characterization of gate properties, blocking capability, and on-state performance of power semiconductor devices using modern and robust measurement technology. A wide range of generators is available for installation in 19-inch systems as can be seen in Figure 1.

Figure 1: SAXOGY´s electrical generators for semiconductor testing

The generators are designed for use both in production environments and development laboratories. They include application-specific safety and measurement features, allowing all test-relevant data to be integrated into higher-level data management and control systems.

Measuring gate characteristics

To evaluate electrical parameters related to the gate structure, SAXOGY offers two different generator systems, differentiated by whether voltage-controlled or current-controlled semiconductor are being tested.

For voltage-controlled devices, the Static Gate Unit (SGU) is typically used. This 1-U rack-mounted system is focused on highest measurement precision, particularly for currents down to the picoampere range. The SGU combines precision analog sources with highly sensitive measurement technology to determine threshold voltages, gate leakage currents, and to apply adjustable gate stress pulses up to 80 V to the gate oxide.

The measurement system for the strongly temperature-dependent threshold voltage provides a resolution of 1 mV over a measurement range up to 16 V. For gate leakage current measurements at voltages up to 80 V, currents in the lowest measurement range down to 200 nA can be resolved with a resolution of 200 pA. Measurement accuracy is better than 1 % of the measured value.

For current-controlled devices, the Static Trigger Unit (STU) is used to characterize the triggering behavior of thyristors. A variable gate current source of up to 3 A is available, with adjustable current slope, as this parameter directly influences the turn-on behavior of thyristors.

The STU determines latching current and holding current of modern thyristors and supplies load currents of up to 10 A. In addition, trigger current and trigger voltage can be measured precisely, and the minimum required anode-cathode voltage V_{ZAK} for triggering the thyristor can be determined. Time-optimized measurement methods are applied to reliably obtain high-quality data within defined production cycle times.

Semiconductor Forward Characterization

When characterizing modern power semiconductors in the forward direction, the on-state voltage drop under applied load current is a key parameter determining conduction losses. This requires both a high-current source and a precise voltage measurement system to reliably capture the strongly temperature-dependent forward voltage.

The Static Forward Unit (SFU) employs a switched current source capable of delivering pulsed currents from 50 A up to 5000 A. The forward voltage at the device under test is measured repeatedly with a resolution of 1,6 mV. Measurement accuracy for both current and voltage is better than 1% of the measured value.

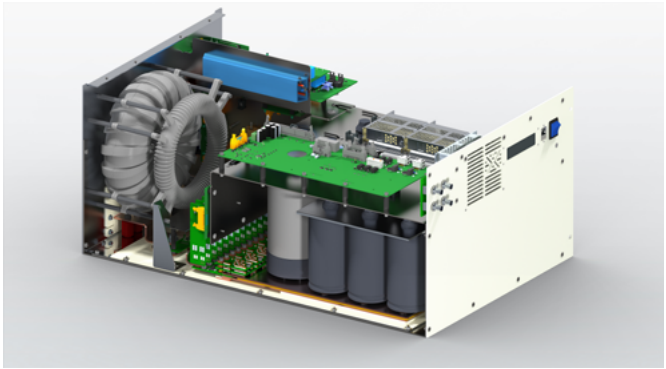

Figure 2: SAXOGY´s Static Forward Generator

The current waveform can be configured as trapezoidal or sinusoidal. The system operates from a single-phase mains supply and uses a capacitor-fed output stage, enabling pulse durations of up to 10 ms. Figure 2 shows a cross-section of the SFU.

The SFU also includes integrated gate drive functionality, allowing testing of voltage-, current-, or light-triggered devices. Gate voltages of up to 25 V and gate currents up to 5 A can be applied.

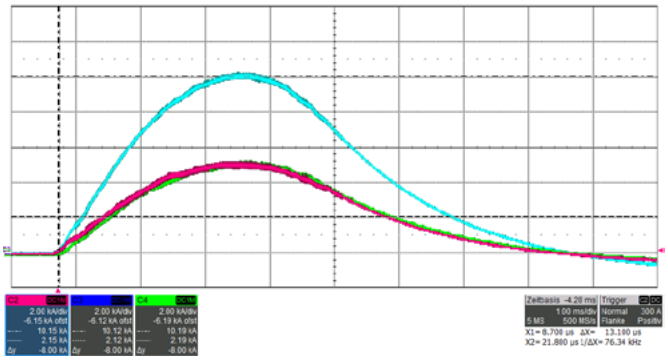

Figure 3: 10 kA current pulse by two SFU in parallel

For higher current requirements, multiple SFU systems can be synchronized and connected in parallel, currently enabling load currents of up to 10,000 A using two units as in Figure 3.

Reverse Blocking Tests

Validation of a device's blocking capability represents one of the final test steps in semiconductor production. For this purpose, a current-limited high-voltage source is required to safely limit fault currents and protect both the device and test equipment in case of breakdown.

SAXOGY offers two generator types for blocking tests, both capable of generating blocking voltages up to 10 kV and providing an integrated gate voltage source from 0 to –20 V.

The Static Reverse Unit (SRU) generates trapezoidal voltage pulses up to 10,000 V and measures the blocking current with a resolution of 10 µA in the most sensitive range. The maximum allowable current can be limited to up to 300 mA, while pulse durations can be set between 200 ms and 10,000 ms.

The AC Reverse Unit (ACRU) is designed to test blocking behavior of power semiconductors mainly used in grid-related applications. Therefore, a highvoltage source is used to generate 50 Hz sinusoidal half-waves up to 10 kVp und accurately measure the resulting blocking currents. Rising and falling voltage pulse sequences of sinusoidal half-waves can be generated, enabling the recording of characteristic curves for blocking voltage versus blocking current.

The minimum adjustable blocking voltage starts at 500 V with an accuracy better than 2% of the measured value. Over the full range from 500 V to 10 kV, voltage measurement accuracy is better than 0.5%. Current limiting can be set between 100 µA and 2 A with an accuracy better than 1% of the set value, while blocking current measurement accuracy is better than 0.5% across the range from 10 µA to 2 A.

A further feature of the ACRU is an integrated low voltage source enabling biasing of devices under test up to 40 V. This is particularly useful for precharging the output capacity of the semiconductor which is strongly voltage dependent and could be quite high at low voltage.

The highvoltage outputs of the blocking generators are earth-referenced and therefore potentially hazardous. For this reason, the voltage generators are equipped with a special designed disconnector unit. This approach enables the reliable detection of a disconnected high-voltage pole by verifying a redundant safety signal that is fed back into a programmable logic controller.

pcim Visit us: Nuremberg, June 09 – 11, 2026 Hall 9, Booth 446

ROGERS CORPORATION

ROGERS, MORE THAN ENGINEERING.

The Rogers Corporation in Eschenbach (Upper Palatinate) has been developing and manufacturing curamik® ceramic substrates (AMB & DBC) for power-electronic and optoelectronic applications since 1983. In doing so, it focuses on high power density, efficient thermal management and maximum reliability.

curamik® substrates consist of pure copper which is bonded to ceramic materials such as Al_2O_3, AIN or Si_3N_4 using AMB (Active Metal Brazing) or DBC (Direct Bond Copper). These technologies enable high power densities, an excellent level of heat dissipation and a long service life.

curamik® ENABLING POWER EFFICIENCY

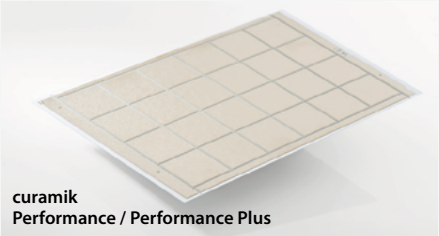

curamik
Performance / Performance Plus

curamik® Performance & Performance Plus (Si_3N_4) AMB
Maximum durability and lifespan for high-power applications.

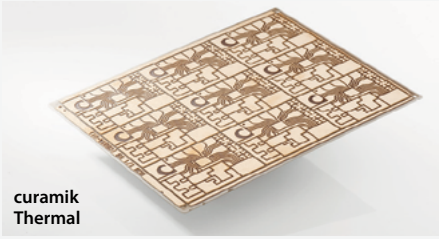

curamik
Thermal

curamik® Thermal (AIN) DBC
Ideal for high-voltage applications with efficient thermal management.

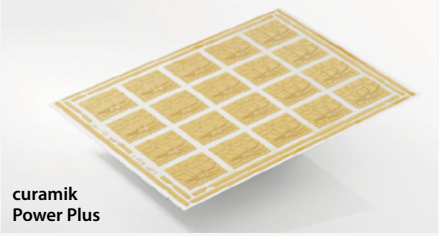

curamik
Power Plus

curamik® Power Plus (HPS) DBC
Increased reliability due to zirconium-doped ceramics.

curamik
Power

curamik® Power (Al_2O_3) DBC
Time-proven standard solution with an attractive price performance ratio.

Rogers Germany GmbH · Am Stadtwald 2 · 92676 Eschenbach · Phone +49 9645 92220 www.rogerscorp.com

dv/dt Generator for Thyristor Testing

An additional high voltage generator is the dv/dt generator, designed for testing thyristors to characterize their triggering or non-triggering behavior under adjustable voltage slew rates. Critical dv/dt, for example caused by dynamic transients at the device terminals, can lead to unintended turn on of the thyristor structure.

Figure 4: Fully integrated SAXOGY testbench for semiconductor in a production line

The dv/dt generator determines the critical voltage slew rate by generating voltage amplitudes from 500 V -10 kV with customizable rise times. Typically voltage slopes for this kind of tests starts at 50 V/µs up to 10 kV/µs. In the event of triggering the thyristor, the generator limits the current to 10 A and terminates the test automatically.

Development of All-in-One Test Systems

In addition to its portfolio of electrical generators, SAXOGY supports the integration of test equipment into existing production lines and existing systems. Furthermore, fully customized test systems are developed in close cooperation with customers as showed in Figure 4.

Years of experience in electronics development and test engineering enable SAXOGY to act as a competent partner in the application and testing of power semiconductor devices. This expertise includes semi- and fully automated handling of devices under test, as well as precise temperature control and reliable contacting of components with contact forces of up to 150 kN, all implemented with maximum safety.

www.saxogy.de

TOSHIBA

High Power SiC MOSFET Modules

Package highlights

- High reliability by using silver sintering technology
- Equipped with current sensing terminal & built in thermistor
- High channel temperature (Tch, max=175°C)
- Low stray inductance
- Low thermal resistance

Featured products

- 3300V 800A - MG800FXF2YMS3
- 3300V 500A - IX500FXF2YMS4
- 2200V 1500A - IX1500YD2YMS4

Internal circuit options

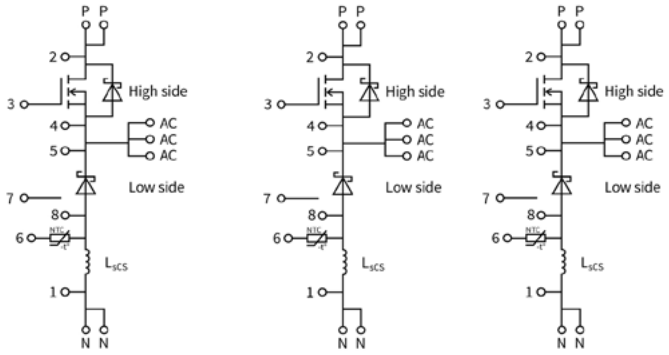

Half bridge | Chopper low | Chopper high

Valid for MG800FXF2YMS3 only

Package highlights

- High mounting compatibility with Si IGBT module
- Lower loss characteristics than Si IGBT module
- High channel temperature (Tch, max=150°C)
- Low stray inductance
- Low thermal resistance

Featured products

- 1200V 400A - MG400Q2YMS3
  600A - MG600Q2YMS3
- 1700V 250A - MG250V2YMS3
  400A - MG400V2YMS3
- 2200V 250A - MG250YD2YMS3

Internal circuit options

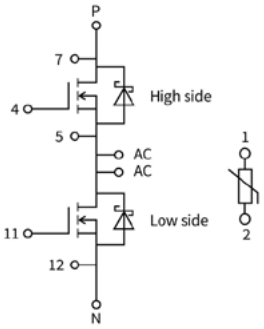

Half bridge

toshiba.semicon-storage.com

Excellence in Power
Visit us at PCIM 2026 -Hall 4A-227

A three-phase three-level flying Capacitor DC/AC Converter based on GaN FETs with integrated Gate Drivers

This article examines the deployment of gallium nitride (GaN) field-effect transistors (FETs) featuring integrated gate drivers in a three-phase three-level DC/AC converter designed to handle ≤30kW. Adopting a flying capacitor topology enables the use of 650V-rated GaN devices in applications with a high DC link voltage. This topology, combined with the FET's integrated gate drivers, enables both high-speed switching (despite the spatial separation between control circuits and switching devices inherent in multilevel configurations) and efficiency gains. DC/AC conversion efficiency measurements at various operating points under grid-connected conditions validate real system performance.

By Riccardo Ruffo, Systems Engineer for Energy Infrastructure, Texas Instruments

Power-conversion systems in renewable energy face increasing demands for both high efficiency and compact design. This requirement has established FETs based on GaN technology as a preferable solution for single-phase applications operating at $400V_{DC}$ link voltages [1], [2]. GaN devices offer advantages over traditional silicon semiconductors because their faster switching speeds reduce switching losses. The challenge emerges when transitioning to 800V systems. As system voltages increase, this voltage stress becomes a critical constraint that makes it hard to adopt GaN technology in higher-voltage applications, despite its superior switching characteristics. Multilevel converter topologies provide a solution by distributing voltage stress across multiple switching devices through the strategic addition of active and passive components [3].

Among the multilevel topologies documented in literature, the flying capacitor configuration emerges as the most cost-effective solution [3]. This topology achieves an optimal balance between FET voltage stress reduction and implementation complexity, making it particularly suitable for applications requiring both performance and economic viability. Furthermore, the flying capacitor topology's results are agnostic to the power factor, thus making it suitable for all inverter or power factor correction (PFC) applications.

In this paper, I will experimentally assess the performance of the three-level flying capacitor topology with a specific focus on implementation using Texas Instruments (TI) GaN FETs that have an integrated gate driver in the slim transistor-outline leadless top-side (STOLT) package.

Topology consideration

Figure 1 is a schematic representation of a three-phase three-level flying capacitor converter. From left to right, the system comprises a DC current source, three flying capacitor switching cells, switching inductors, an electromagnetic interference filter, and a connection to the three-phase grid by means of a point of common coupling. The AC phases are labeled L_1, L_2 and L_3, with positive currents exiting the converter. The DC side features positive and negative rails for a current generator operating as source or load.

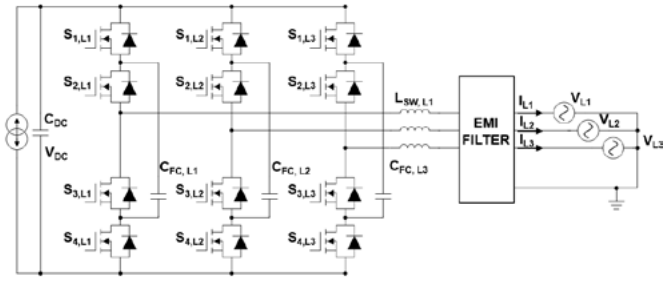

Figure 1: A schematic representation of a three-phase DC/AC converter based on three-level flying capacitor switching cells.

The single switching cell comprises:

- Four power FETs rated for half the DC link voltage (S_1, S_2, S_3 and S_4).
- The flying capacitor (C_{FC}). This capacitor is rated for half the DC link voltage, and its value is inversely proportional to the switching frequency [4].
- The DC link capacitor responsible for filtering out the ripple current (C_{DC}).
- A switch-node inductor with one-fourth the required inductance of two-level applications [4].

This DC/AC converter requires compliance with the following condition (Equation 1):

$$V_{DC} > \sqrt{2}V_{AC} \qquad (1)$$

where V_{AC} represents the root-mean-square (RMS) line-to-line voltage.

Operating principles of a flying capacitor switching cell

In the flying capacitor topology, a microcontroller (MCU) needs to control the flying capacitor voltage at a value half the DC link voltage. This specification avoids any possible overvoltage across the FETs. The MCU imposes the duty cycle and dead time so that the FETs switch at a nominal switching frequency (f_{SW}).

Switch pairs S_1 and S_4 and S_2 and S_3 are switching complementary to each other. Two pairs of dead times are required per switching cell. If these switch pairs are not complementary to each other, C_{DC} may short.

Switch pairs S_1 and S_4 and S_2 and S_3 are 180 degrees phase-shifted to each other. The phase shift doubles f_{SW} on the switching node.

Switch pairs at first approximation have the same duty cycle, expressed by Equation 2:

$$D = \frac{V_{SW}}{V_{DC}} \qquad (2)$$

where VSW is the voltage with negative DC rails as a ground reference.

Figure 2 shows the pulse-width modulation (PWM) signals and switch-node voltage when 920V on the switch node is present with 1,000V_{DC}. In this condition, the duty cycles are 92% (S_1 and S_2). The switch-node voltage is switching within two levels – 500V and 1,000V – because the duty cycles are >50%.

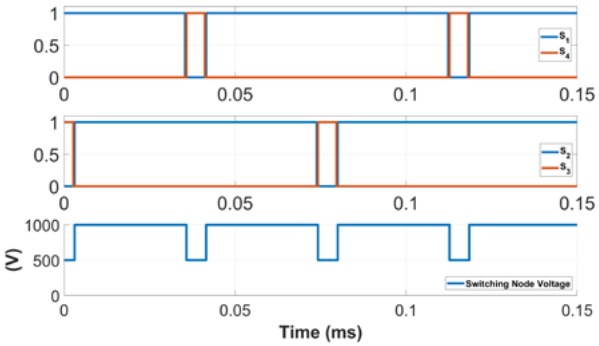

Figure 2: Simulation results – MCU PWM signals and switch-node voltage at 1,000V_{DC}, 920V and a 92% duty cycle.

Flying capacitor layout considerations

Maximizing f_{SW} is crucial for reducing flying capacitor capacitance [4]. Power devices such as GaN FETs enable both high f_{SW} and high efficiency, but there are design challenges. Higher switching frequencies inherently result in an elevated current slew rate, which when combined with parasitic loop inductance creates substantial device overvoltage that can lead to catastrophic device failure. In multilevel converters, the spatial separation between control circuits and switching devices compounds the problem by increasing the parasitic loop inductance and compromising FET gate control.

Figure 3 is a schematic representation of parasitic loop inductances within a three-level flying capacitor switching leg. The switching cell features two distinct commutation loops that significantly impact overall performance. The inner commutation loop, indicated by blue arrows, encompasses the parasitic inductances of switches S_2 and S_3 and the inner capacitor (C_{INNER}). This loop offers substantial optimization potential through strategic component placement, where positioning elements in proximity effectively minimizes the parasitic inductance.

In contrast, the outer commutation loop depicted by the red circle comprises switches S_1 and S_4, the outer capacitor (C_{OUTER}), and C_{INNER}, forming the external switching path. Since the inner loop has already been optimized for minimum inductance, achieving simultaneous optimization of the outer loop presents considerable design challenges. Strategically positioning an additional capacitor (C_{ADD}) in electrical parallel with switches S_2 and S_3 reduces the overall parasitic effects to their minimum achievable values [5].

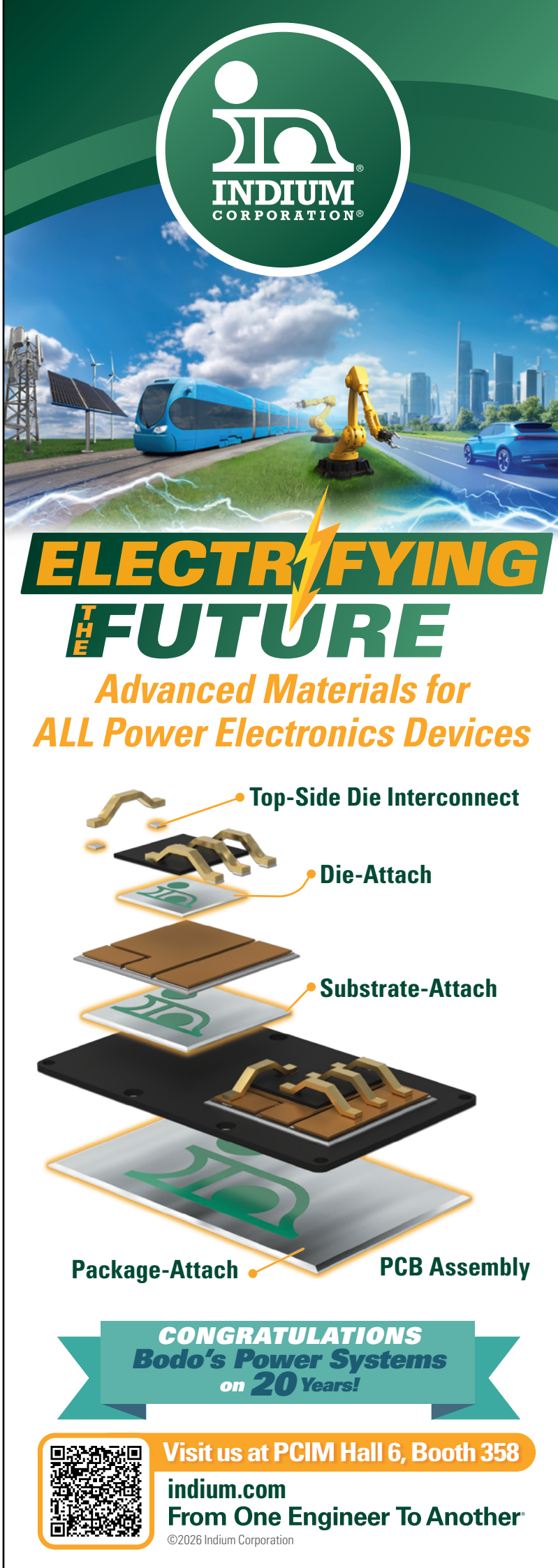

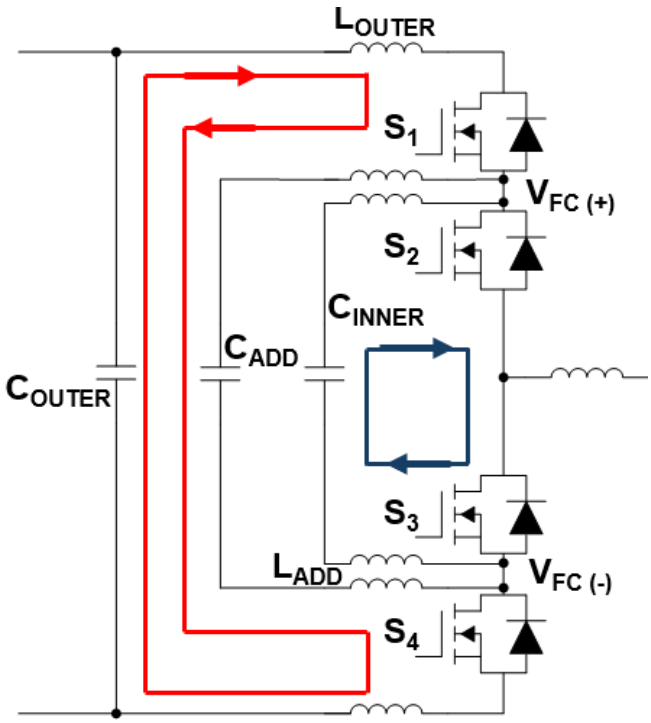

Figure 3: Commutation loops of a three-level flying capacitor switching cell.

Figure 4 demonstrates a practical implementation of this optimization strategy using GaN devices in the STOLT package. Figure 4a reveals the presence of three ceramic capacitors. The addition of C_{ADD} results in significant improvement of the switching loop performance characteristics. However, as evident from Figure 4b, incorporating additional components increases overall board dimensions and introduces complexities in gate-driver signal management.

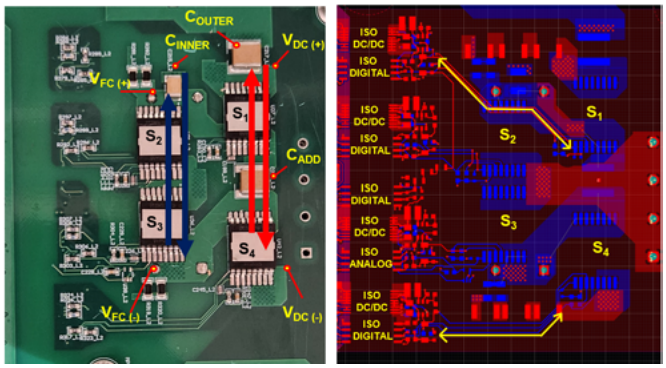

Figure 4: Bottom view of a flying capacitor switching leg plus printed circuit board layout view (top and bottom layers).

While this signal management complexity frequently necessitates derating the switching speed – resulting in increased total losses that offset the advantages gained from higher f_{SW} – it is possible to mitigate losses by implementing transistors with integrated gate drivers, such as the TI LMG3670R010. This gate driver's integrated architecture enables GaN transistor switching performance by leveraging an internally optimized gate-driver design, eliminating many of the layout-dependent parasitic effects that compromise discrete implementations.

While integrated gate drivers address switching-related parasitics, auxiliary components can become performance bottlenecks. Components such as isolated DC/DC converters for gate-driver power supplies, voltage sensors for flying capacitor voltage sensing, and digital isolators for control signals must feature superior common-mode transient immunity to maintain signal integrity. Components such as TI's UCC35131, AMC0311D and ISO7721 exemplify the specifications required to preserve the high-frequency switching advantages of integrated GaN solutions.

Experimental results

The TI *15kW to 30kW Bidirectional, Three-Phase Plus Neutral Flying Capacitor Based on GaN Reference Design* (https://www.ti.com/tool/TIDA-010957) can evaluate the performance of a three-phase flying capacitor DC/AC converter [6]. This design is capable of delivering 30kW using GaN devices in the STOLT package with an on-resistance value of 10mΩ. The converter is operating at 65kHz by having a controlled switching speed of 70V/ns.

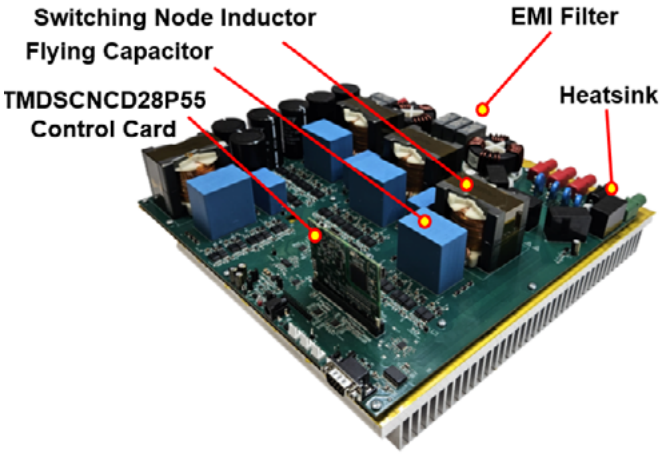

Figure 5: Lateral view of the hardware prototype board of the 15kW-to-30kW bidirectional reference design, where LMG3670R010 connects directly to the heat sink.

Power vs. efficiency measurements

This experiment kept the DC bus voltage constant and controlled at $800V_{DC}$. AC connected first at $480V_{RMS}$ and later at a $400V_{RMS}$ power grid.

Figure 6 shows the current and voltages of one phase of the DC/AC converter operating at full power. The converter is operating as a PFC. The switch-node voltage shows three distinctive levels when considering the electrical frequency grid period. This is because half of the period requires a duty cycle <50%, while the other half of the period requires a duty cycle >50%. Having three voltage levels plus doubling the equivalent f_{SW} enables the grid current to have low ripple current.

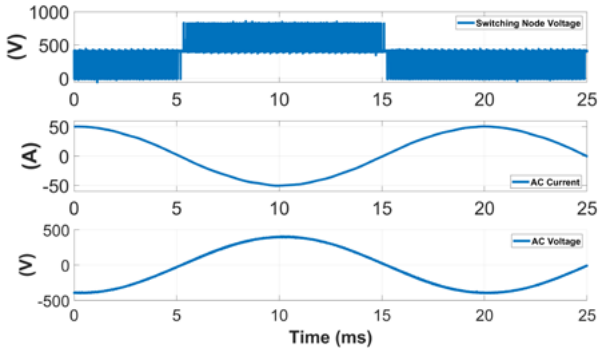

Figure 6: Experimental waveforms of the reference design operating at 30kW with a grid connection at $480V_{RMS}$.

Additional tests at different power factors but the same apparent power value indicated no significant worsening in ripple current or total losses.

Subsequently, varying the DC/AC converter power from 2.5kW to 30kW enabled measurement of the corresponding efficiencies at each operating point. Figure 7 depicts efficiency vs. power curves for two different grid voltage levels. At first observation, it is evident that both efficiency and power performance at $480V_{RMS}$ are superior compared to $400V_{RMS}$ operation.

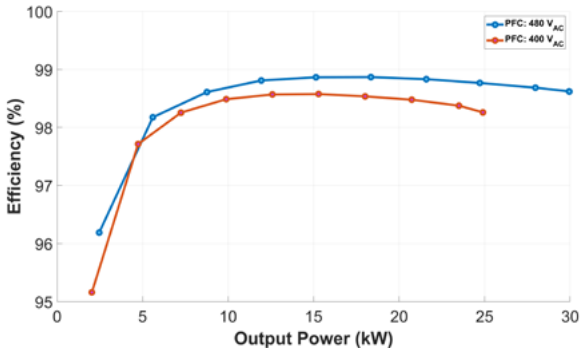

Figure 7: Efficiency vs. power at $800V_{DC}$ and two different line-to-line grid voltages.

Operating at $480V_{RMS}$ at the maximum power output of 30kW resulted in a peak efficiency measurement of 98.7%. While there were lower efficiencies during $400V_{RMS}$ operation, these results remain impressive. The performance difference occurs because for equivalent RMS current levels, the losses remain similar while the power-transfer capability is higher at the elevated voltage, resulting in improved overall efficiency at $480V_{RMS}$ operation.

Conclusion

Flying capacitor topologies are preferable when trying to decrease converter size and increase efficiency. Adopting GaN transistors can significantly increase f_{SW}, making this topology even more appealing. Using TI GaN FETs with integrated gate drivers optimizes power layout, achieving a switching speed of 70V/ns with no significant voltage overshoot.

A three-phase power board rated 30kW was tested in this work. This topology can operate in inverter, PFC and reactive power compensation, with peak efficiency close to 99% when operating the converter at $480V_{RMS}$.

References

1. R. Ruffo and V. Ghosh. “Assessing Performance of a 10-kW String Inverter Based on GaN FETs.” How2Power, January 2025.
2. R. Ruffo and V. Ghosh. “Design considerations of a 10kW single-phase string inverter based on TI GaN FETs.” (https://www.ti.com/lit/ta/ssztd75/ssztd75.pdf) Texas Instruments technical article, literature No. SSZTD75, March 2025.
3. R. Ruffo, K. Le, and H. Parzhuber. “Comparison of AC/DC Power-Conversion Topologies for Three-Phase Industrial Systems.” (https://www.ti.com/lit/ml/slup417/slup417.pdf) Power Supply Design Seminar SEM2600, literature No. SLUP417, 2024.
4. R. Ruffo and B. Ling. “Design Consideration of 3-Level Flying Capacitor Converters for Three-Phase AC/DC Applications.” (https://www.ti.com/lit/an/sdaa195/sdaa195.pdf) Texas Instruments application note, literature No. SDAA195, January 2026.
5. T. Modeer, C.B. Barth, N. Pallo, W.H. Chung, T. Foulkes, and R.C.N. Pilawa-Podgurski. “Design of a GaN-based, 9-level flying capacitor multilevel inverter with low inductance layout.” 2017 IEEE Applied Power Electronics Conference and Exposition (APEC), Tampa, Florida, 2017, pp. 2582-2589. DOI: 10.1109/APEC.2017.7931062
6. R. Ruffo and B. Ling. “15kW to 30kW Bidirectional, Three-Phase Plus Neutral Flying Capacitor Based on GaN Reference Design.” (https://www.ti.com/lit/ug/tidufg9a/tidufg9a.pdf) Texas Instruments reference design guide, literature No. TIDUFG9A, December 2025.

www.ti.com

Advantages of integrated half-bridge GaN Devices in Home Appliance Motor Drive Applications

As the energy star requirements for home appliances become more stringent, motor drive systems need to be more efficient. Thanks to CoolGaN™'s Figure of Merit (FoM), both switching and conduction losses are significantly reduced. This advanced semiconductor technology not only improves efficiency but also offers significant system advantages, such as better thermal performance compared to traditional solutions, in certain applications like inverter-based washing machines and dryers, can eliminate the need for heatsinks.

By Zhemin (Jimmy) Zhang, Lead Principal Engineer, Infineon Technologies

In small applications such as modern hair-styling appliances, motors operate at ultra-high speeds (>100 kRPM), requiring high-frequency inverters. Here, achieving a high-efficiency performance at high switching frequencies (>50 kHz) is a real challenge that can be addressed using GaN power devices.

Beyond the intrinsic benefits of using GaN power devices, system integration plays a key role in advancing motor inverter efficiency and cost-effectiveness. By integrating critical components such as gate drivers, bootstrap switches, and current-sensing circuits alongside robust protection mechanisms, substantial reductions in the system components can be achieved. This integration not only drives cost savings at the system level but also simplifies assembly processes, paving the way for more compact, reliable, and economical inverter systems.

Integrated GaN half-bridge device

Figure 1 (a) illustrates CoolGaN™ Drive HB 650 V G5, an integrated GaN device in half-bridge (HB) configuration, in a small QFN 6×8 package, and how it is typically configured in a circuit. This device requires only a few external components for operation, enabling a compact design. As seen in Figure 1 (b), this device integrates two 650 V GaN transistors with dedicated gate drivers and a lossless current sensing circuit. Moreover, several protection features, including overcurrent protection (OCP), short-circuit protection (SCP), overtemperature protection (OTP), and undervoltage lockout (UVLO) protection, are integrated into the device. Additionally, the voltage slew rate at both turn-on and turn-off transitions for low- and high-side GaN transistors is adjustable via the external resistors RDDL and RDDH, respectively. This feature is critical to achieve the desired EMC levels.

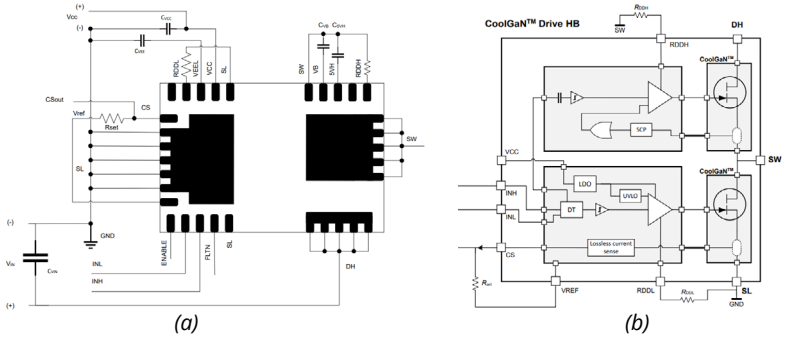

(a) (b)

Figure 1: Integrated GaN HB device in QFN 6×8 package. (a) Application schematic. (b) Simplified diagram.

Due to the integrated current-sensing circuit, there is no need for lossy current shunts or their amplifier circuits. Integrating HB power switches with gate drivers, current-sensing circuits, and protections into a single package enables a compact, efficient solution for low- to medium-power motor drive applications.

Experimental evaluation

1) High speed motors (125 kRPM) for hair dryers

Performance of CoolGaN Drive HB 650 V G5 is evaluated in a hair dryer application by implementing a 3-phase inverter using three GaN HB devices. Figure 2 shows a picture of the test setup, including the implemented board and the BLDC motor used for testing. The selected motor has two poles rated for 115 W and rated for a speed of 125 kRPM. The implemented system is tested in a closed-loop control using the sensor-less field-oriented control (FOC) method. In this system, the phase currents are measured using integrated bidirectional current-sensing circuits, instead of traditional current shunts.

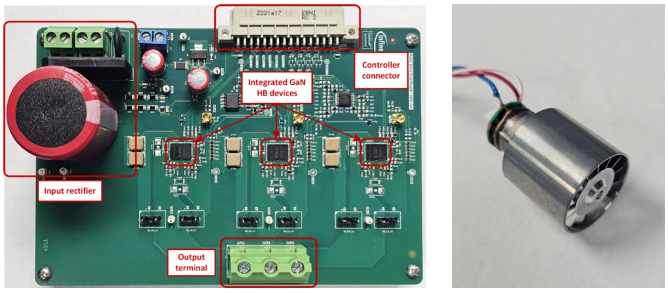

(a) (b)

Figure 2: Picture of the test setup. (a) Implemented 3-phase inverter. (b) Tested motor.

Figure 3 shows the experimental waveforms obtained from testing the closed-loop system at the rated speed. In this figure, key waveforms of one of the inverter legs, including low-side input P_{WM} signal V_{INL}, switch-node voltage V_{SW}, phase current I_{PH}, and sensed current signal V_{CS}, are illustrated in line- and switching-time scales. As seen in Figure 3 (a), the electrical frequency of the phase current is 2.083 kHz, which is equivalent to a mechanical speed of 125 kRPM. As shown in Figure 3 (b), the switching frequency is 80 kHz.

Additionally, it is observed that the current sense signal V_{CS} completely follows the corresponding phase current whenever V_{INL} is high. The case temperature of the GaN devices are below 55°C with no heatsink when driving the motor at its full speed.

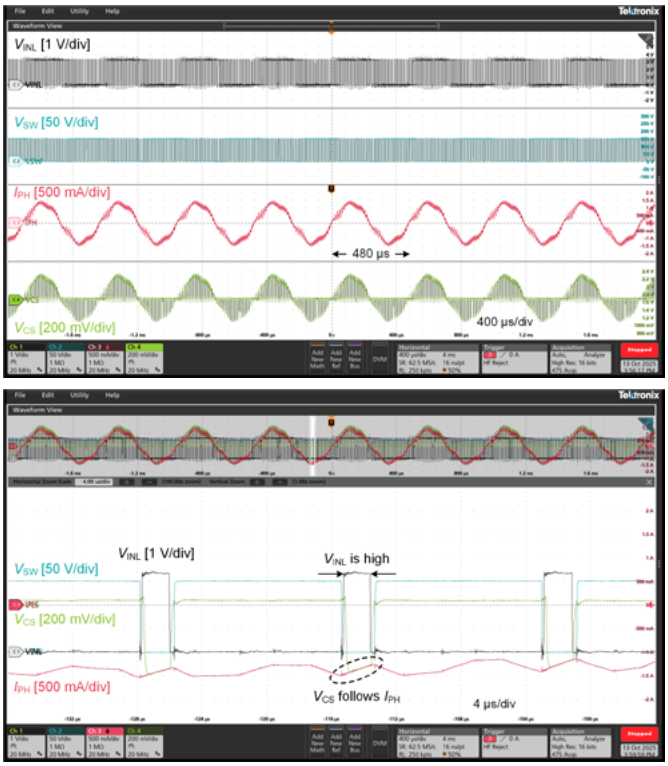

Figure 3: Experimental waveforms. (a) Line-scale waveforms. (b) Switching-scale waveforms.

2) Drum motors in washing machines

The motor drive boards with IGBT integrated power module (IPM) and CoolGaN™ Drive HB 650 V G5 in Q-DPAK package are built and compared in washing machines. Table 1 summarizes the evaluation board setup, key components, and the thermal environment. Because of the lower gate charge, the high-side bootstrap capacitor can also be reduced. For the integrated GaN HB board, the heat is only dissipated by the PCB itself, and an aluminum heat sink is required for the IGBT IPM. The CoolGaN™ Drive HB only has a 39°C temperature rise, while the IGBT IPM's temperature increases by 76°C at 800 W power.

	CoolGaN™ Drive HB 650 V G5	IGBT IPM
Device	3x GaN 650 V/55 mΩ (Full pack)	IGBT 600 V/10 A (Full pack)
Heatsink	No (Heat dissipation by PCB pattern)	Yes (Heatsink (120 × 120 × 25 mm^3), natural convection)
Case temperature	64°C	101°C
Temperature rise	39°C	76°C
Inverter efficiency	99.3%	97%
Total losses	5.6 W	24 W

Table 1: Comparison between integrated GaN HB and IGBT IPM at 800 W input power

Advert

We develop innovative methods to identify and resolve EMC issues early in the design phase. With our worldwide industrial partners we successfully established Electromagnetic Interference simulation methods to:

- **Reduce costs & speed up the entire design process**
- **Minimize number of EMC issues**

We support your product development to fulfill necessary EMC standards – with modelling, simulation and measurement.

COMPLY.
IMPROVE.
ANALYZE.
SIMULATE.

Discover our EMC services:

SAL SILICON AUSTRIA LABS
www.silicon-austria-labs.com

Conclusion

The two application studies that were compared, collectively illustrate the broad applicability and scalability of integrated GaN half-bridge technology in motor drives for home appliances. GaN technology provides many benefits and as an integrated solution, delivers significant system-level benefits applicable to both application domains cited above:

a) Space savings: No heatsink and nearly 40% reduction in case temperature. Power losses reduce by nearly 80%, resulting in increased output power and power density
b) Cost savings: Reduction in discrete components (gate driver ICs, current sense resistors, protection circuits, etc.) results in a lower BOM cost and reduces the required PCB area
c) Simplified assembly: Fewer components and reduced PCB complexity streamline manufacturing processes, particularly important for high-volume production
d) Improved reliability: Integration eliminates inter-device parasitics and reduces the risk of heatsink-related mechanical failures resulting in longer system lifetime
e) Design scalability: The wide portfolio of integrated GaN half-bridge platforms can be adapted across a range of power levels in motor drives for home appliances, from compact 100 W hair dryers to 1 kW washing machine drives, demonstrating strong platform reusability.

The CoolGaN™ Drive HB 650 V G5 is coming soon. Stay informed and learn more about integrated GaN devices here.

www.infineon.com

7th Gen Fast Recovery Diode Enabling Full Performance of Modern IGBTs

With the rise of 7th generation IGBTs, power electronics designers are facing a new reality: switching speed is no longer limited by the transistor itself but increasingly by the fast recovery diode. As IGBT technologies push toward steeper di/dt, lower gate resistance and reduced switching losses, the diode becomes the decisive component that defines operating limits.

By Alexander Zapf, Product Manager, Semikron Danfoss

Why the Fast Recovery Diode Can Become a Performance Limiter

In hard switched converter topologies, the turn on of the IGBT is inseparably linked to the reverse recovery behaviour of the fast recovery diode. Any abrupt interruption of reverse current results in voltage overshoot, higher electromagnetic interference (EMI), and increased stress on the anti-parallel IGBT chip.

With earlier IGBT generations, conservative gate driving often masked diode limitations. In contrast, modern 7th generation trench IGBTs are capable of extremely fast current commutation, making them highly sensitive to diode behaviour, particularly at low forward currents and high junction temperatures.

Soft recovery diodes like the Controlled Axial Lifetime (CAL) diodes from Semikron Danfoss are a perfect option to limit voltage overshoot and enable higher switching speeds without the need for excessive gate resistance or snubbing circuits.

The CAL Concept: Controlled Axial Charge Carrier Distribution

The CAL diode concept is designed to limit voltage overshoot via a clever device structure utilizing semiconductor physics. Instead of solely on bulk lifetime killing, CAL diodes use an axially tailored lifetime profile (Figure 1). Charge carrier lifetime τ is intentionally reduced close to the p-n junction to minimize the reverse recovery charge Q_{rr} and recovery peak current I_{RRM}. The base lifetime in the n^- region is higher and is complemented by a tailored buffer zone at the n^-/n^+ interface.

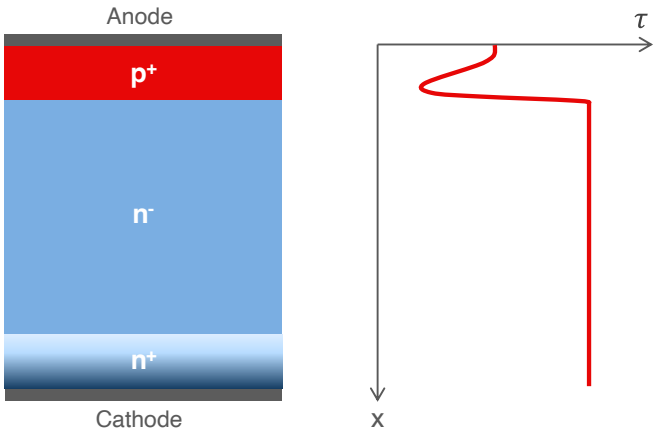

Figure 1: CAL diode structure and charge carrier lifetime

During reverse recovery, this lifetime profile promotes a controlled overlap between the rising voltage and a residual tail current. As sufficient charge carriers remain in the n^- region, the reverse current decays smoothly instead of abruptly. This prevents snap-off behaviour, reduces current transients, and consequently limits voltage overshoot caused by circuit inductances.

Overvoltage Behaviour

One of the defining characteristics of the newest 7th–generation CAL diode is its low dynamic overvoltage, enabled by an exceptionally soft reverse recovery behaviour. The CAL7 maintains its softness across the entire operating range. For the system designer, this translates into greater freedom in gate driver tuning. Reduced reverse recovery stress allows higher turn-on di/dt, which reduces IGBT switching losses. At the same time, the soft recovery behaviour mitigates voltage overshoot and high-frequency oscillations, helping to control EMI.

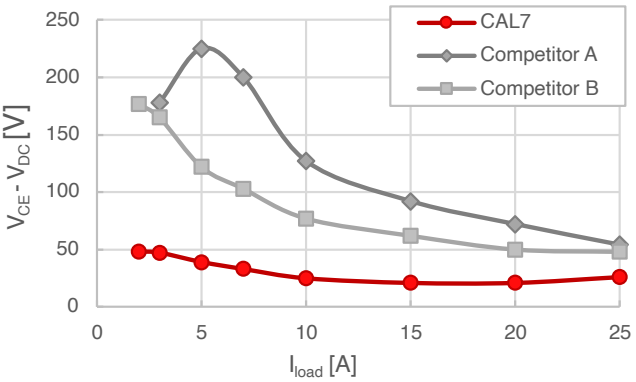

Figure 2: Overvoltage vs. load current – Benchmark

Benchmark measurements (Figure 2) show that CAL7 generates significantly lower switching overvoltage $V_{CE} - V_{DC}$ than competitor fast recovery diodes under identical commutation conditions: R_{Gon} = 1Ω, di/dt = 4kA/µs, V_{DC} = 900V, T_j = 150°C.

Thin wafer enables Higher Current Density and Power cycling durability

CAL7 is the first CAL diode generation from Semikron Danfoss manufactured using thin wafer silicon technology. This innovation brings two decisive advantages. First, the reduced silicon thickness enables a lower forward voltage and a significant increase in current density, more than 25% compared to CAL4. This allows higher current ratings within the same chip footprint, supporting a higher power density at module level.

Second, thin wafer technology reduces thermomechanical stress during operation. Lower silicon stiffness results in reduced strain on solder joints and bond wire connections during temperature swings, leading to markedly improved power cycling capability. Tests indicate lifetime improvements of 30% compared to previous generations.

Cosmic Ray Robustness

As blocking voltages increase, cosmic ray induced failures can become a non negligible reliability concern, especially in high power, high voltage converters operated at altitude or over long lifetimes.

Fast recovery diodes often exhibit lower tolerance to cosmic radiation than IGBTs, making them the weak link in module robustness. CAL technology has historically addressed this issue and CAL7 continues this tradition.

Although the move to thinner silicon slightly reduces absolute margins compared to CAL4, CAL7 still delivers best-in-class cosmic ray failure rates, outperforming competitor fast recovery diodes by orders of magnitude (Figure 3). At application-relevant voltages, CAL7 exhibits extremely low FIT rates, ensuring highly reliable operation with negligible impact from cosmic ray induced failures.

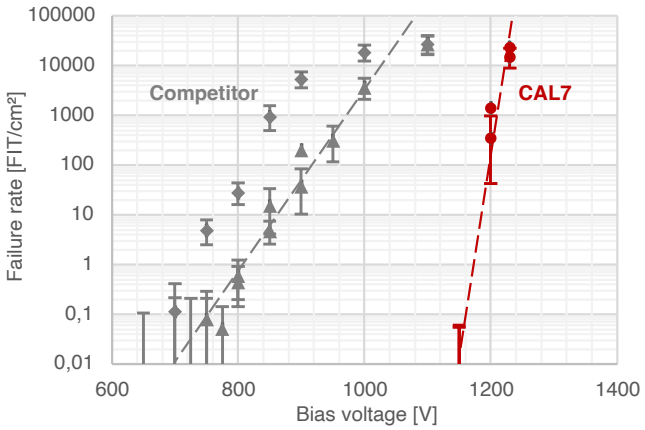

Figure 3: Cosmic ray FIT rate vs. Bias voltage

Cornerstone of New Medium Power Module Platforms

CAL7 diode technology is a key building block in Semikron Danfoss' next generation of power modules. Compared to earlier CAL generations, it achieves significantly lower forward voltage improving overall efficiency without sacrificing softness.

CAL7 has been optimized for a typical switching frequency range up to 10 kHz relevant for most industrial applications. Like previous generations it exhibits a positive temperature coefficient of forward voltage, facilitating safe paralleling of devices and stable current sharing.

The CAL7 diode generation will first be integrated into Semikron Danfoss' new medium power module platforms

- SEMITRANS 3+, extending the platform to a market-leading 1000A / 1200V variant in a 62mm form-factor
- SEMiX 3p+, enabling new 1200V high-power variants up to 900A
- SEMITRANS 20, roll-out of 1200V platform with ratings ranging from 1200A to 1800A

Power Loss Comparison

In the following section a UPS application example for a three level TNPC topology of SEMITRANS 3+ 800A 1200V with 7th generation IGBT is provided and compared in terms of power losses for CAL7 vs. CAL4 diode variants. The calculation was performed via Semikron Danfoss' customer simulation tool SemiSel with the following application parameters: V_{DC} = 740V, I_{out} = 300A, f_{sw} = 6kHz.

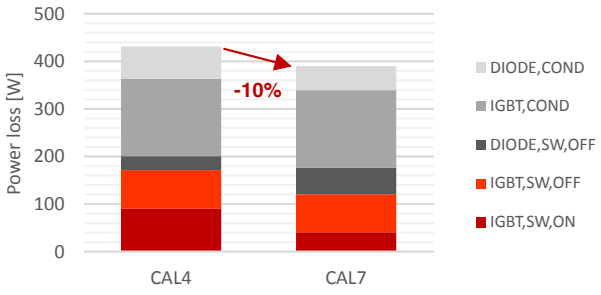

Figure 4: Power factor +1 loss comparison

Advert

In inverter operation (Figure 4) the IGBT switch-on losses can be reduced significantly by 55% with the CAL7 module variant due the faster IGBT current rise enabled by lower gate resistance. This results in an overall loss reduction of around 10% improving the inverter efficiency by 0.1%.

In active front-end operation (Figure 5) the overall losses can be reduced by 16% with CAL7 module variant due to its significantly lower forward voltage and the ability to reduce IGBT switch-on losses.

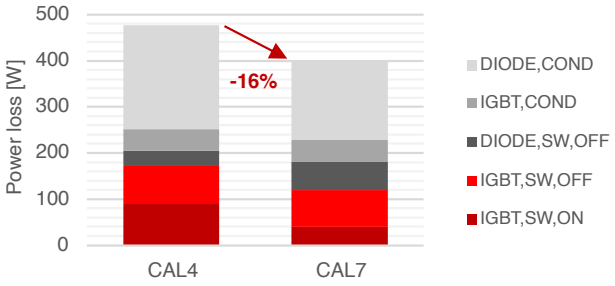

Figure 5: Power factor -1 loss comparison

In both operative modes the overall loss reduction of the CAL7 module variant lowers the requirements towards the cooling setup or enables up to 10% higher output power within an existing cooling setup.

Conclusion: Softness as Competitive Advantage

As power electronics enters an era defined by high power density, fast IGBT switching enabled by soft diode behaviour has become a decisive differentiator. With CAL7, Semikron Danfoss delivers a fast recovery diode that sets benchmarks where it matters: best-in-class low overvoltage through exceptional softness and industry leading cosmic ray robustness bundled with high current density.

www.semikron-danfoss.com

A novel Current Sensing Technology utilizing III-V compound Hall Elements as an Alternative to Shunt Resistors and isolated Σ-Δ Modulators

This article discusses a novel current sensing technology to address the challenges of shunt resistors and isolated modulators used in applications such as AC servo driver and robots. It also examines magnetic current sensors, focusing on devices utilizing Si Hall elements, xMR elements, and III-V compound semiconductor Hall elements, comparing the characteristics and assessing their suitability for these applications.

By Miho Onuma, Technical expert of Current Sensors, Asahi Kasei Microdevices Corporation;
Takenobu Nakamura, Technical expert of Current Sensors, Asahi Kasei Microdevices Corporation;
Takahisa Shikama, Strategy & Business Leader of Magnetic Sensor Products, Asahi Kasei Microdevices Corporation;
Takaya Higa, Field Application Engineer, Asahi Kasei Microdevices Europe GmbH

Introduction

Driven by the growing demand for automation in the manufacturing industry, the use of industrial robots in factories has been rapidly expanding in recent years. This trend is largely attributed to structural challenges such as labor shortages and the increasing need for high-mix, low-volume production. At the same time, advances in AI technology have enabled robots to perform delicate tasks that previously required human intervention, as well as physically demanding operations, thereby accelerating the adoption of robotic solutions to address these challenges. Industrial robots widely employ high-performance motors based on servo motor systems. Motor drives and robot controllers are essential for controlling these motors and robotic systems. However, these components occupy a certain footprint within factories, making further miniaturization of controllers essential to improve production density. In addition, as energy-saving requirements in factories continue to increase, there is a strong demand for improved energy efficiency in each of the electronic components that constitute servo motor systems and robot controllers.

One of the key functions of servo drives and robot controllers is precise torque control and fault detection through high-resolution current sensing. Currently, shunt resistors are widely used for this purpose. To achieve high-resolution control, Σ-Δ modulator is commonly employed following the shunt resistor. Furthermore, since the current sensing section operates at high voltages exceeding several hundred volts, electrical isolation between the primary and secondary sides is required. In conventional systems using shunt resistors, significant heat generation in the shunt resistor and the large number of components - such as bootstrap circuit and Σ-Δ modules - present challenges in achieving miniaturization and energy efficiency. Therefore, there is a growing need to replace this approach with a novel current sensing technology that can address these issues.

Current Sensors as an alternative to shunt resistors

One of the most suitable solutions to these challenges is a magnetic current sensor that integrates a primary conductor carrying the current and Σ-Δ modulator. Figure 1 illustrates the comparison of system configurations using shunt resistors and magnetic current sensors in the inverter circuit of a three-phase servo drive. For control in servo drive, it is common to perform current sensing on two or all three phases of the three-phase system.

Magnetic current sensors provide galvanic isolation and can operate with only a single power supply on the secondary side, enabling replacement of all high-voltage-side peripheral components required in shunt resistor solutions with a single device. In addition, magnetic current sensors can suppress heat generation, which is a key issue when measuring large currents with shunt resistors. As a result, they enable both miniaturization and improved energy efficiency and are attracting attention as an alternative to shunt resistor solutions.

The performance of magnetic current sensors depends on the type of magnetic sensing element used. However, conventional

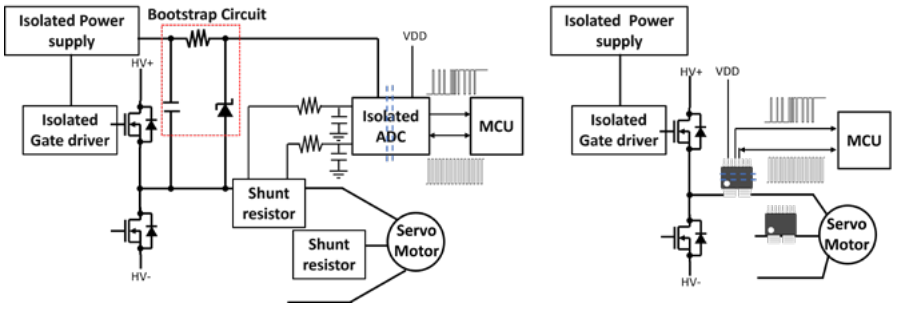

(a) Shunt resistor + isolated Σ-Δ modulator *(b) Magnetic current sensor*

Figure 1: Comparison of system configurations using shunt resistor solutions and magnetic current sensor

Advert

magnetic sensors have faced challenges in achieving the current resolution required for servo drives and robotic applications. In the following, several candidate magnetic sensing technologies for current sensors are introduced, and their suitability for current sensing in servo and robotic applications is discussed.

The challenges with Si Hall element and xMR elements

Si Hall elements are widely used in magnetic current sensors. However, their sensitivity is inherently limited by material properties, making it difficult to achieve high current resolution. One approach to improving the current resolution is to increase the current density in the primary conductor; however, this introduces a trade-off, as increased conductor resistance leads to higher heat generation. As a result, it is difficult to simultaneously achieve the high current resolution and low heat generation required for servo drives and robotic applications. To address this, a common approach is to use a magnetic core to amplify the magnetic field applied to the Hall element, thereby improving resolution. However, the use of a magnetic core increases the overall size, and the magnetic hysteresis of the core material also degrades accuracy, which remains a challenge.

xMR elements generally provide higher sensitivity than Si Hall elements, making them a promising solution for achieving the current resolution required in servo drives and robotic applications. However, xMR elements typically exhibit a trade-off between input magnetic field range and sensitivity, which poses challenges for improving current resolution in high-current applications. In addition, accuracy degradation due to magnetic hysteresis has been observed, and challenges remain in applying these sensors to industrial equipment that demands high-resolution and high-accuracy current sensing at large currents.

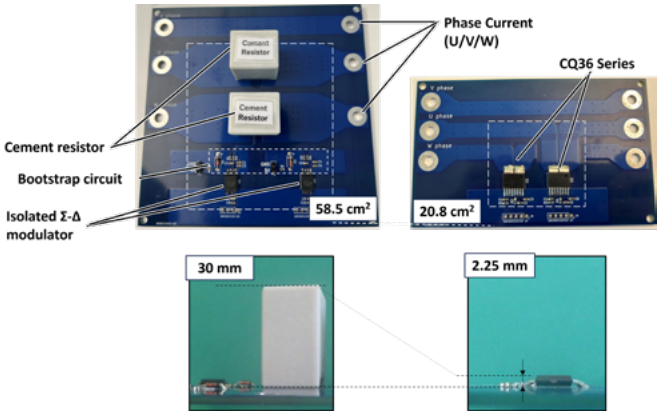

(a) Shunt resistor + isolated Σ-Δ modulator, *(b) Magnetic current sensor (CQ36 series*

Figure 2: CQ36-enabled shunt system miniaturization

III-V compound semiconductors hold the key

III-V compound semiconductor Hall elements are known to offer significantly higher sensitivity than Si Hall elements. This high sensitivity enables high current resolution without being limited by the input magnetic field, allowing large currents to be measured with both high resolution and high accuracy. It also permits the current density in the primary conductor can be reduced while maintaining high resolution, which in turn allows the conductor resistance to be minimized and low heat generation to be achieved. As a result, this approach is attracting attention as a solution that can achieve the current resolution required in servo drives and robotic applications while addressing the challenges associated with shunt resistors.

A representative example is the CQ36 series developed by Asahi Kasei Microdevices (AKM), which achieves an effective number of bits (ENOB) of 14 or higher - comparable to isolated Σ-Δ modulator - using a sinc3 filter with an oversampling rate (OSR) of 256. It offers selectable interfaces, including 10 MHz or 20 MHz clock frequency, and internal(output) or external(input) clock. The sensor also features a very low current conductor resistance of 0.27 mΩ. The lineup covers a wide range from small- to large-capacity AC servos, supporting currents from ±10.5 A_{peak} to ±168 A_{peak}. With a creepage and clearance distance of 8mm, bootstrap circuits are not required, as the sensor operates using only the secondary-side supply.

Figure 2 illustrates the size reduction achieved by replacing shunt resistors (cement resistors) and isolated Σ-Δ modulator with CQ36 series in the inverter circuit of a three-phase servo drive. The results show that the footprint can be reduced by more than 60%, and the height by over 90%.

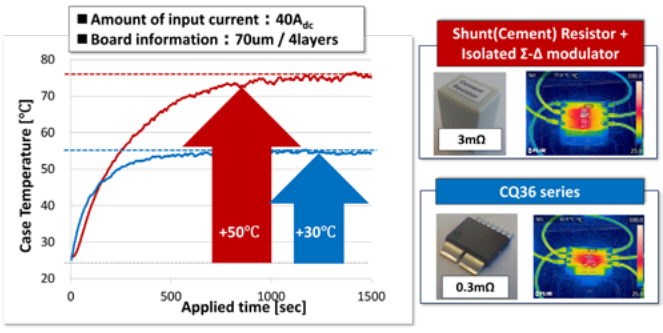

Figure 3: Heat reduction effect of the CQ36 series

Figure 3 shows the results of thermal measurements using the board shown in Figure 2. While a cement resistor (2.7 mΩ) exhibits a temperature rise of approximately +50 °C when 40 A DC is applied, the CQ36 series shows a temperature increase of only around +30 °C.

Conclusion

A current sensor based on III-V compound semiconductor Hall elements can replace conventional shunt resistors and isolated Σ-Δ modulators. This enables miniaturization and energy savings in servo and robotic systems.

www.akm.com

Transforming Energy Storage: The Role of Bidirectional Charging in BESS

This article explores the role of Bidirectional functionality in enhancing Battery Energy Storage Systems performance, reducing energy infrastructure costs, and helping to maximise renewable energy utilisation, reducing reliance on fossil fuels.

By Harvey Wilson, Senior Manager Industrial Vertical Markets EMEA, Avnet Silica

Global efforts to reduce emissions are driving the transition to electrical energy as a cleaner alternative to fossil fuels. Electricity now plays an increasingly important role in our daily lives, powering everything from electric vehicles (EVs) to transportation systems. With the growing use of heat pumps, electricity is also making inroads in domestic heating. At the same time, grid operators are increasingly integrating renewable sources, such as wind and solar, into their energy mix. Unlike the coal and gas power stations, which can produce energy 24/7, these renewable energy sources are intermittent in nature – if the sun doesn't shine and the wind doesn't blow, these systems cannot generate energy.

These circumstances and trends are fuelling strong growth in the market for Battery Energy Storage Systems (BESS). Traditionally, the preserve of large-scale grid developments, the scale, flexibility, and cost of BESS are being transformed by innovations in battery and power electronics technologies. These advancements are creating opportunity and demand for an ever-growing range of applications.

Power conversion is a core function of a BESS, and Bidirectional Charging (BDC) systems represent a significant innovation in the field of power electronics. Traditional BESS power conversion systems were unidirectional, requiring separate circuits for charging (AC/DC) and discharging (DC/AC) the battery. BDC systems, however, allow electricity to flow in both directions, offering numerous benefits to the BESS developer.

What is a BESS?

The fundamental purpose of a BESS is to store electrical energy, making it available when needed, irrespective of when it was generated. Consisting of a collection of battery units, associated power electronics, control systems, and safety equipment, BESS can be characterised by their storage capacity in kWh (the amount of energy that the battery can store) and power capability in kW, (the rate at which the battery can deliver or receive power).

The scale of BESS varies widely, depending on the end application, which can be classified into Front-of-the-Meter (FTM) and Behind-the-Meter (BTM), Table 1.

Front-of-the-Meter	Behind-the-Meter
Transmission and distribution	Transport
Power Stations	Commercial
Substations	Residential
Utility-scale generation and storage	Industrial
	Microgrid

Table 1: BESS applications can be categorised into Front-of-the-Meter and Behind-the-Meter

Front-of-the-Meter (FTM)

Front-of-the-Meter (FTM) – or grid-scale – BESS supply power to electricity grids or off-site locations, and are deployed mainly by utility companies, grid operators, and renewable energy developers. FTM BESS are used in the energy industry for a variety of purposes, such as balancing the supply and demand of energy in the grid, providing ancillary services, and, increasingly, enabling the integration of renewable energy sources like wind, solar, and tidal. Grid-scale BESS can store over 1,000 kWh of energy and can occupy large tracts of land; they are increasingly viewed as crucial components of a country's energy supply. Fidra Energy's Thorpe Marsh project, for example, the largest BESS project in the UK at 1,400 MW (3,100 MWh), is being developed on 55 acres of land and will ultimately have enough capacity to supply 800,000 homes during peak demand times.

Behind-the-Meter (BTM)

Behind-the-Meter (BTM) BESS provide power to on-site locations, such as residential homes or businesses, with applications including EV charging infrastructure, telecommunications networks, data centres, and residential energy storage. Capacities of commercial BTM systems range from 20 kWh to 1,000 kWh, while residential BESS are typically within the 5 kWh to 20 kWh range. The physical sizes of BTM systems range from a domestic refrigerator up to multiple shipping containers.

As this fast-growing market attracts increasing levels of investment and incentives, innovations in BESS technologies are leading to the development of flexible, scalable, and highly portable systems, creating new opportunities and enabling new applications.

Increasing energy densities drive BESS innovation

The BESS sector has undergone rapid evolution over the last 15 years, with energy densities (a key characteristic of a BESS) increasing dramatically. Higher energy densities enable more energy to be stored in a given footprint, which brings multiple advantages. Land acquisition and construction costs are reduced, and transportation of higher capacity BESS becomes easier and more cost-effective.

Figure 1: Containerised battery systems (Source: Avnet Silica)

The utility-scale stationary storage installations of the early 2010s, often housed in large buildings, are giving way to containerised BESS (Figure 1), particularly in BTM systems, where applications range from mining and construction to EV charging infrastructure.

Containerised BESS are designed to be shipped out to remote areas, such as mining or construction sites, where they are used to power equipment before being returned from the field for re-charging. Higher energy densities allow the mobile BESS to deliver power for longer intervals, reducing downtime and transportation costs. BESS can also be installed at EV charging stations to smooth the impact on local grid connections at peak charging times. With space often limited around charging stations, in urban areas, for example, the physical size of the BESS is important. To understand this evolution in energy density, it is useful to consider how a BESS works briefly.

A look inside the BESS

The key subsystems within a BESS consist of the Battery Modules, the Battery Management System (BMS), the Energy Management System (EMS) and the Power Conversion System (PCS, Figure 2).

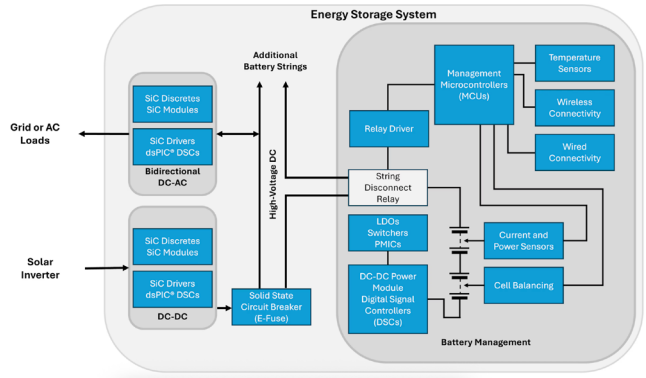

Figure 2: Battery management system breakdown (Source: Microchip Technology)

While all of these sub-systems work in collaboration to deliver the overall efficiency and energy density of the BESS, developments in two specific areas have contributed significantly to increased energy densities.

Advancements in battery chemistry

As the primary energy storage units, the battery cells are at the heart of the BESS, and recent advancements in battery chemistry have focused on enhancing energy density, charging speeds, and safety. Solid-state batteries, including lithium-sulphur, and lithium-air batteries, which offer higher energy densities and improved safety over liquid electrolytes, are emerging as alternatives to conventional lithium-ion technology.

The evolution of power electronics

The Power Conversion System (PCS) plays a crucial role in converting the supplied power to a form that can charge the batteries and also in converting the stored energy back into a suitable output form for the grid or other loads, such as machines or EV charging stations. Power electronics devices perform these conversions, and the field of power electronics has evolved significantly since the early 2010s. Power conversion solutions use a combination of switched semiconductors and passive components arranged in various topologies paired with control devices which turn the semiconductors on and off to achieve the desired outputs.

Silicon (Si) MOSFETs and IGBT devices were used in power conversion for many years, due to their low conduction and switching losses. In the relentless drive for increased efficiencies and power densities, the switching speed limits of these silicon devices were eventually reached, and designers have increasingly turned to wide bandgap technologies, such as Silicon Carbide (SiC).

Alongside these developments in semiconductor technologies, advancements in topology design and control strategies have delivered more flexible and innovative power conversion solutions. One specific development in power electronics, Bidirectional Charging (BDC), has had a transformational impact on BESS.

Bidirectional Charging – transforming BESS

Traditional power management solutions could only transmit power in one direction, either from the AC grid to the DC battery or vice versa. This limitation obliged BESS developers to include two separate power conversion circuits in the design, which added to the overall cost, complexity, and size of the BESS.

BDC solutions, however, use a single circuit for both AC-DC and DC-AC conversion, offering multiple benefits to BESS developers, including reduced space, weight, power, and cost (SWaP-C), as well as lower complexity. BDC systems are thus simpler to implement, with lower Bill-of-Material (BoM) costs, and can easily be scaled up by paralleling multiple circuits. Popular BDC topologies include buck-boost converters (Figure 3) and dual active bridge (DAB) converters (Figure 4).

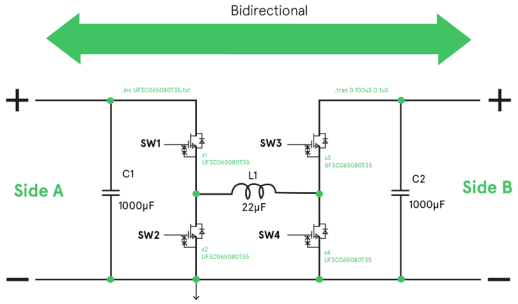

Figure 3: The buck-boost converter (Source: Avnet Silica)

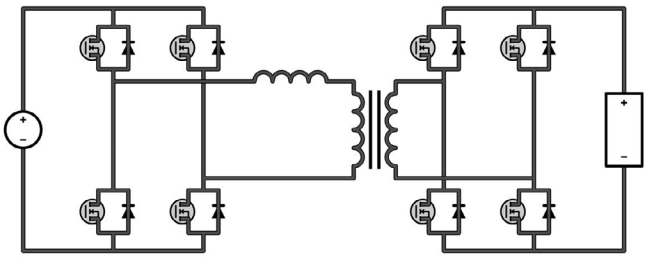

Figure 4: The dual-active bridge converter (Source: MathWorks)

Buck-boost converters are commonly chosen for bidirectional DC/DC conversion due to their simple design and ease of control, while DAB converters are popular where isolation is required. Other notable BDC topologies include the CLLC converter, the Phase-Shifted Full Bridge (PSFB) Converter, and the Totem-Pole PFC.

Bidirectional charging also requires sophisticated control algorithms to manage the charging and discharging cycles; modern solutions use advanced control strategies like Linear Active Disturbance Rejection Control (LADRC).

Conclusion

BESS play an increasingly important role in our society as we integrate renewable energy and EVs batteries into the energy ecosystem and support a growing range of BTM applications. The evolution of power conversion topologies has been instrumental in fulfilling the growing demand for more flexible and efficient energy storage solutions, with BDC offering significant space, weight, and cost benefits to BESS developers.

Ongoing research efforts into the efficiency of bidirectional converter topologies and control strategies will continue to enhance the overall reliability and lifespan of BESS and connected devices.

www.avnet-silica.com

Bodo's Power Systems® · bodospower.com

Three-Phase CoolSiC Inverter Evaluation Kit with Double Sided Cooling: Architecture, Thermal Design, and Test Methodology

This article provides an overview of a flexible evaluation platform for three-phase inverters that use silicon carbide power semiconductors in double-sided cooling (DSC) modules. It focuses on the fundamental design principles, as well as the thermal and electrical aspects of system integration and typical commissioning, measurement, and analysis procedures. The goal is to facilitate early, application-oriented research and establish a solid foundation for evaluating various application scenarios. The article is intended for engineers seeking a foundation for systematic testing and application-oriented evaluations.

By Hakan Akabay, Edmund Schmidt, and Christoph Pannemann, all Infineon Technologies

Introduction to the DSC Evaluation Kit

The DSC-SiC Inverter Evaluation Kit (see Figure 1) is designed to analyze the technical properties and performance characteristics of the HybridPACK DSC CoolSiC G2 Module. It supports power outputs of up to 150 kW. Rather than requiring a fully custombuilt setup, the kit provides a functional three-phase inverter that can be quickly commissioned to provide early insights into the behavior of the SiC module under realistic operating conditions.

The focus areas are switching behavior, dynamic effects within the SiC power stage, loss performance at defined operating points, and the effectiveness of double-sided cooling. The goal is to provide a comprehensive assessment of the module's capabilities and potential applications to serve as a basis for product development and implementation.

Figure 1: Inverter Evaluation Kit for HybridPACK™ DSC CoolSiC™

This kit is an evaluation platform, not a production ready product. Protection and operating limits can be adjusted via software to enable boundary tests and targeted scenarios. Therefore, it is the user's responsibility to ensure a safe, controlled test environment with appropriate high-voltage safety measures and a reliable cooling system.

The inverter is implemented as a three-phase B6 topology. The core power module is the Hybrid-PACK DSC-S (FF06MR12A04MA2) featuring 1200 V SiC MOSFETs and an integrated NTC temperature sensor. The gate driver boards use a high-voltage gate driver optimized for SiC (EiceDriver). A logic board based on the AURIX platform handles operation, status management, and communication. A DC-link capacitor (TDK, 135 µF, 850 V) is integrated on the supply side. For laboratory testing, a high-voltage source, a load (e.g., an inductive load or an electric machine), and a cooling system with volume and temperature control is also required.

The kit is compatible with all DSC-S-SiC variants because the modules share a common footprint, which enhances their versatility and adaptability across applications. With dimensions of 370 mm × 135 mm × 190 mm, the kit has a compact form factor suitable for various test environments.

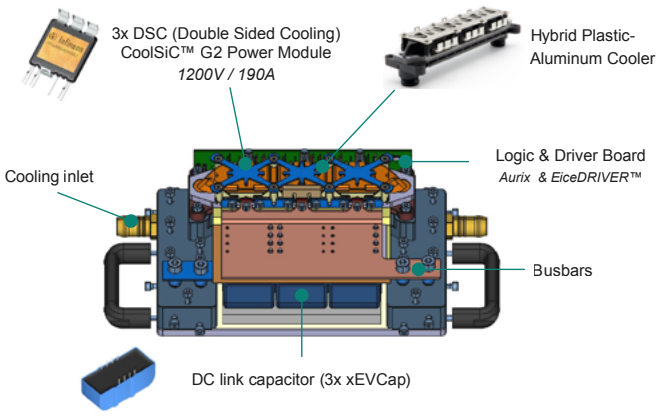

Figure 2: Main components of the Evaluation Kit

Optimized thermal and electrical design of the doublesided-cooled sic module

The DSC package (see Figure 3a) is designed for double-sided heat dissipation. Compared to single-sided cooled modules, its architecture provides an additional thermal path, which leads to a significant reduction in junction-to-fluid thermal resistance Rth,jf. Estimates indicate a reduction of up to 40% relative to single-sided concepts (see Figure 3b). In a typical DSC heat stack, heat dissipation is asymmetrical, with a greater proportion of heat dissipated through the bottom than the top.

Since cooling is indirect, there is a thermal interface layer between the module and the cooler (see Figure 3c). Therefore, Rth,jf is determined by the module itself, the quality of the contact interface, the clamping mechanics, and the thermal interface material (TIM).

Thus, measured thermal perfor-mance should be interpreted as a system-level characteristic considering the entire assembly, including the module, TIM, clamping mechanism, cooler, and operating conditions.

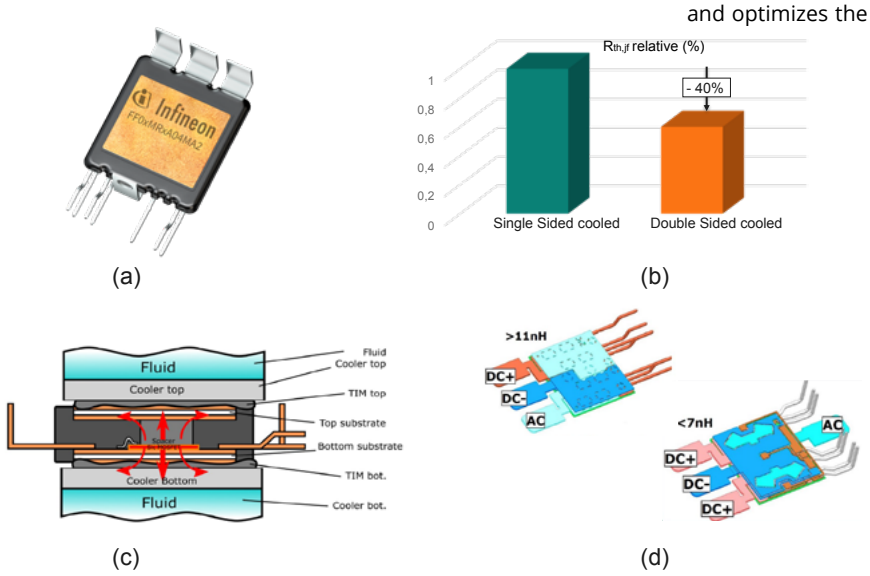

Figure 3: a) Double-sided cooled module (DSC); b) Thermal resistance junction-to-fluid (Rthjf) comparison: SSC vs DSC Thermal stack of DSC; c) Thermal stack; d) Electrical layout [3]

DSC-S-SiC modules are scalable and suitable for applications ranging from 750 V to 1200 V. This allows them to adapt to specific requirements and diverse operating scenarios. For SiC MOSFETs, parasitic inductance in the commutation path is critical because it can cause overshooting and additional switching stress. It also impacts electromagnetic compatibility (EMC) and component reliability. The DSC package mitigates these issues with a highly symmetrical design that distributes parasitic inductances and resistances evenly and optimizes the commutation loop. The target stray inductance is specified to be less than 7 nH (see Figure 3d). This low inductance enables controlled switching under realistic conditions and simplifies tuning of gatedriver parameters to achieve the desired dv/dt limits [1,2].

High-performance hybrid cooler: architecture and reliable thermomechanical integration

The kit features a hybrid cooling system from Erwin Quarder Systemtechnik GmbH (see Figure 3) that combines an aluminum heat transfer surface with plastic components that distribute fluid and facilitate mechanical integration. This design uses MPDB® technology to creates a helium-tight and mechanically robust joint between the aluminum and plastic components without the use of adhesives or additional sealing materials. During manufacturing, the aluminum surface is pre-structured so that the plastic can penetrate its nano-microstructures during the joing process and form a sealed connection as it cools and solidifies.

MAXIMIZE EFFICIENCY
on High Power
starpower
pcim
June 09-11, 2026
Nuremberg
Hall 9, Booth 442
FEATURES:
• StarPower Si-IGBT and SiC-Mosfet Technology
• Low Stray Inductance of 9 nH
• High CTI Value Package with High Creepage and Clearance Distance
StarPower Europe AG
info@starpowereurope.com
www.starpowereurope.com
DRIVEN BY QUALITY

Three DSC half-bridge modules are positioned within a support frame and clamped between the top and bottom cooler sections with approximately 800 N of force per module. Fluid distribution on the top side is configured as serial flow, while the bottom side is arranged in parallel. The total volume flow splits at a ratio of about 20% to the top and 80% to the bottom, aligning with the typical heat dissipation characteristics of the DSC package.

To compensate for temperature gradients in the top-side flow, which is cooled serially, the flow rate in the bottom-side parallel path increases slightly from the first to the last module position. This ensures a more uniform temperature distribution across all three modules.

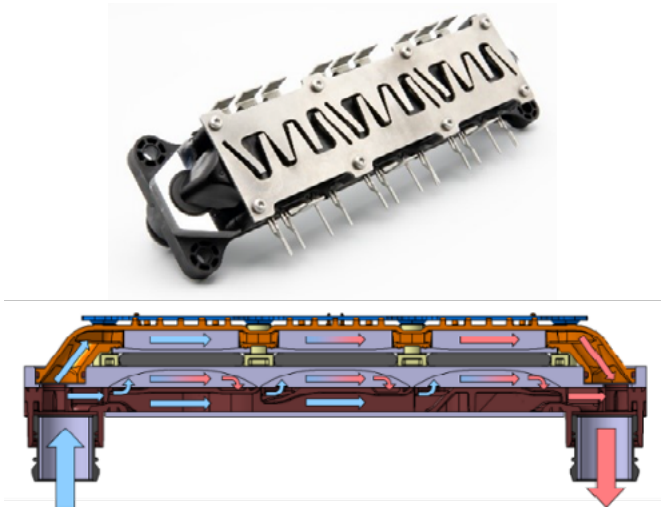

Figure 4: Quarder DSC MPDB® HybridCooler & Cooling Path

In the indirectly cooled DSC setup, the quality of contact between the module and the cooler is paramount. The cooling system addresses this issue by ensuring the contact surfaces have low surface roughness and high planarity. It also incorporates flexible elements in the top cooler and metallic springs above to compensate for tolerances and thermo-mechanical effects. Additionally, a thin thermal interface material closes micro air gaps and reduces contact thermal resistance [3,4].

Evaluation kit testing capabilities nd applicationoriented measurement methodology

The evaluation kit provides a range of interaction and analysis options. Communication can be established via a USB serial interface or a CAN bus. For testing under high voltage and load conditions, the CAN bus is strongly recommended due to its stability and robustness (e.g. via a PEAK PCAN-USB interface).

The OneEye software from Infineon manages operation and analysis, offering user-friendly configuration of operating modes and parameters. It provides comprehensive visualisation and recording capabilities for measured data and includes a pre-configured CAN message catalogue, facilitating the reading of status and measurement data, or the injection of setpoints via external CAN tools.

A typical workflow begins in configuration mode, where parameters such as pulse width modulation (PWM) frequency, dead time, shutdown limits and sensor scaling can be customised and saved as non-volatile data. Once configured, the system transitions to run mode, where open-loop setpoints such as amplitude, speed or output frequency can be defined.

Measurements are continuously monitored via status pages. Advanced analysis is supported by a data logger and a software-based scope function that captures signals synchronised to the PWM pattern.

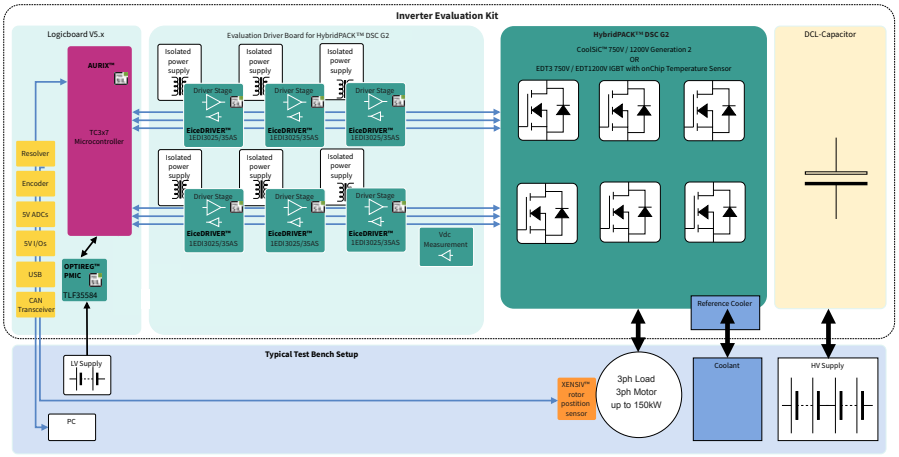

Figure 5: Structure of the DSC HybridKIT™

A laboratory setup with an inductive load is recommended for structured electrical characterisation. In this configuration, the three-phase pulse width modulation (PWM) inverter generates defined currents, which are measured by integrated sensors. An oscilloscope can capture switching transitions, enabling the analysis of switching performance and energy losses based on parameters such as the gate-driver settings, the DC-link voltage, the switching frequency and the package inductance.

To take a more application-oriented approach, the evaluation kit can be integrated into an electric motor test bench. Unlike with passive loads, the inverter powers an electric machine in this configuration, enabling dynamic states such as acceleration, steady-state operation and regenerative braking to be simulated. These tests provide valuable data on system efficiency, the interaction between the inverter and motor, and thermal performance under dynamic load conditions.

Conclusion

In summary, the new DSC Evaluation Kit provides a robust foundation for application-oriented characterization of three-phase SiC inverters with double-sided cooling. The kit's combination of a symmetrical, low-inductance power stage; an optimized, double-sided thermal path; and a customizable measurement and control environment enables the reproducible investigation of switching behavior, losses, and thermal performance under realistic conditions.

From the users's perspective, the platform is available as a fully integrated, ready-to-use system. This includes a high-performance hybrid plastic-aluminium cooler from Quarder for double-sided cooling. Commissioning only requires standard laboratory equipment: a programmable high-voltage DC source, an inductive load or motor test bench, and a conventional cooling loop with volume and temperature control. Thanks to the integrated protection, parameterisation and data acquisition (CAN/USB, OneEye), there is no need for custom mechanics, PCBs or firmware to begin carrying out safe, controlled boundary and application-oriented tests. This lowers the entry barrier, shortens time-to-first-data, and mitigates the risks associated with early design decisions.

These integration and testing principles can be transferred to other module families and power classes. The common DSC-S footprint supports variants across 750–1200 V, enabling the early evaluation of efficiency, power density, and reliability across diverse operating points.

References

1. A. P. Pai, M. Ebli, T. Simmet, A. Lis and M. Beninger-Bina, "Characteristics of a SiC MOSFET-
2. based Double Side Cooled High Performance Power Module for Automotive Traction Inverter Applications", IEEE/AIAA Transportation Electrification Conference and Electric Aircraft Technologies Symposium, 2022.
3. A. P. Pai, A.Widhalm, M.Eibli, M.Kurz, M.Foresta, M. Osorio, "SiC MOSFET-Based High Performance Double Side Cooled Module and Compact Cooler for High Power-Density Automotive Inverter Applications", IWIPP, 2021.
4. C. Schweikert, S. Bruns and D. Meichsner, "Performance Enhancements and Easy Integration of Double Side Cooled Automotive SiC Power Modules - Enabled by a Sophisticated Cooler System", PCIM Europe, 2023.
5. D. Meichsner, A. Thomas, B. Rosam, C. Schweikert, M. Leitner, "Performance and Feature Benchmarking of SiC Trench Technologies and Cooling Systems for DSC Modules in Traction Inverters", PCIM Europe, 2023

www.infineon.com

Lab Skills For Switch-Mode Power Supply Evaluation – Part 1: Measuring Voltage Ripple and Switching Node

This article discusses how to carefully select passive probes for measurement, how to optimize measurement methods, and introduces alternative measurement techniques to further aid in diagnosing converter operations. Reference setups are shown to illustrate how typical data sheet figures are captured such as voltage ripple and switching waveforms.

By Wesley Ballar, Senior Product Applications Engineer, and Jake Ciolfi, Field Applications Engineer, both Analog Devices

When evaluating a switch-mode power supply (SMPS), there are many key parameters to assess and many factors to consider when observing a particular measurement. Making these measurements accurately is necessary to ensure design decisions are not led astray by faulty data, and proper oscilloscope probe selection is the first step.

Oscilloscope Probe Selection

An oscilloscope is a powerful tool that engineers use to evaluate the performance of SMPS. However, it cannot be overstated how important proper measurement technique is to oscilloscope capture accuracy. The first step is selecting the right oscilloscope probe for the measurement being taken.

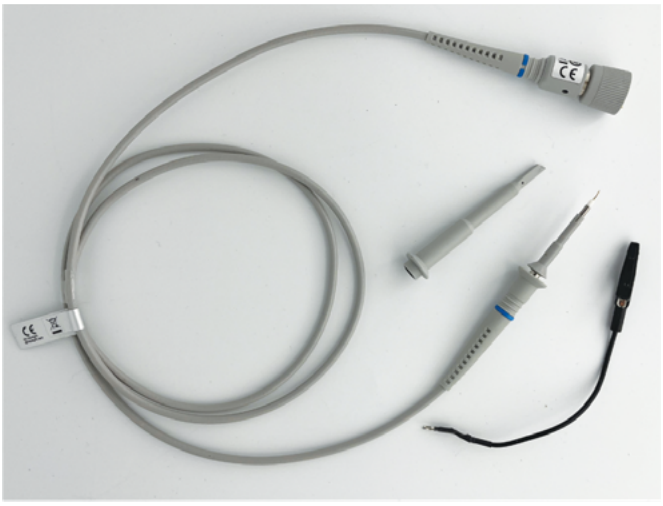

(a)

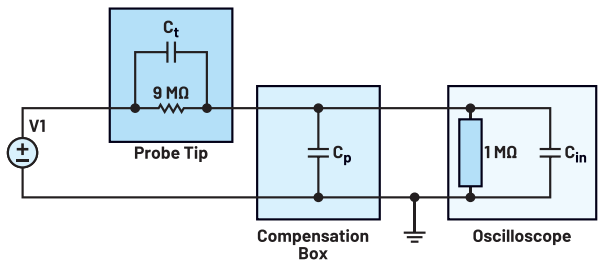

(b)

Figure 1: (a) Keysight N2873A 10× probe and (b) its simplified circuit.

Passive probes are versatile and useful for accurate signal measurements, and they contain no active circuitry and do not require external power. While less disruptive measurements for extremely sensitive circuits can be achieved with active probes, they are also more complex and expensive. This section will explore oscilloscope measurements using passive 10× probes, passive 1× probes, and coaxial cables, with a brief discussion on how to determine which of the three is appropriate for certain measurements.

Oscilloscope Probes: 10×

The 10× probe is the general-purpose standard probe for most modern oscilloscopes. They are designated 10× because they have a 10:1 attenuation ratio and reduce the signal being measured by a factor of ten. The oscilloscope's display adjusts for this attenuation to display the correct voltage measurement, but this should be verified by the user because oscilloscopes may vary. The probe has a large internal impedance, which, along with the oscilloscope impedance, divides the voltage signal by 10, as shown in Figure 1. This high impedance reduces loading on the oscilloscope and allows the probe to measure high voltages typically in the hundreds of volts. The typical bandwidth for 10× probes reaches hundreds of megahertz. The Keysight N2873A 10× probe, for example, is rated for 400 V DC voltage and up to 500 MHz.[1]

Care must also be taken to check the voltage derating curve vs. the frequency of the probe. A voltage derating curve shows the maximum voltage the probe can measure while the signal has a certain frequency. As frequency increases, the maximum voltage that the probe can pass will decrease. The curve in Figure 2 shows an example of N2873A.

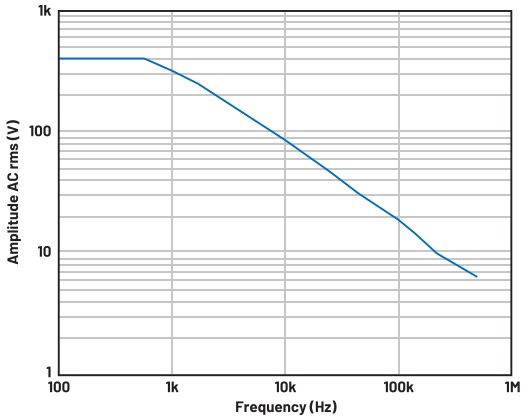

Figure 2: An N2873A 10× probe voltage vs. frequency derating plot from its data sheet by Keysight.

(a)

(b)

Figure 3: How to tune 10× probe compensation with a screwdriver tool.

To ensure measurement accuracy in the kilohertz frequency range, many 10× probes have a built-in adjustable compensation screw, as shown in Figure 3. This probe adjustment allows users to match the probe capacitance with the oscilloscope's input capacitance, $Ct/(C_{in} + C_p) = 1\ M\Omega/9\ M\Omega$. Once adjusted, the voltage measurement will have the correct frequency response, ensuring that fast edges are measured correctly without overshoot or undershoot distortion. The probe should be calibrated each time it is connected to a new oscilloscope input to account for slight differences in the analog front ends, even when switching between different channels of the same oscilloscope. To calibrate the probe, connect it to the oscilloscope's on-board square wave generator and adjust the probe's compensation screw until the observed voltage signal appears square with little to no overshoot or rounding, as shown in Figure 4.

The 10× probes are especially suited for measuring switch-node voltage in SMPSs, and can also be used to measure VIN, VOUT, and high frequency signal-level waveforms. The 10× probe is recommended for these measurements because of its ability to pass higher frequencies and voltages.

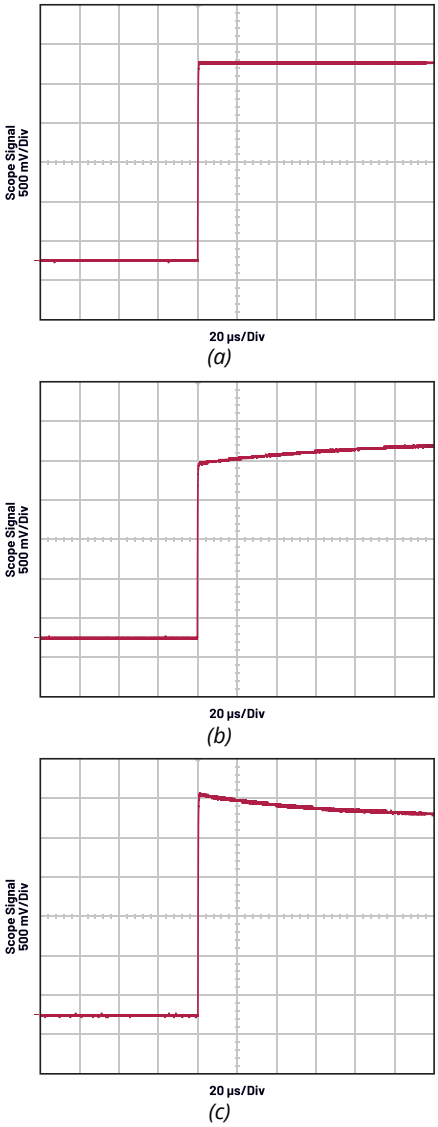

Figure 4: (a) Sharp square, (b) overdamped, and (c) underdamped oscilloscope calibration measurement captures.

Oscilloscope Probes: 1×

Another common passive probe is the 1× probe, as shown in Figure 5. These probes have a 1:1 attenuation ratio and do not attenuate the voltage signal. These probes have a much lower impedance compared to the 10× probe and do not require user calibration. The oscilloscope does not adjust its scale for the measurement, allowing the screen capture to have a finer resolution—typically down to 1 mV/div.

These probes have a voltage range in the tens of volts. The bandwidth for these probes is typically rated to the tens of megahertz. A Fluke PM9001 1× probe, for example, has an impedance of less than 1 kΩ, a maximum voltage of 30 V, and a bandwidth of 15 MHz.[2] A 1× probe is recommended for low voltage and low frequency measurement. When measuring voltages in SMPSs, this probe is recommended for small signal tests such as input or output voltage ripples as long as the frequency of these ripples is in the low megahertz.

(a)

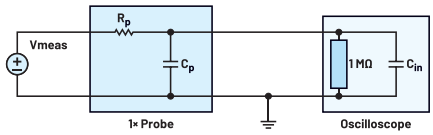

(b)

Figure 5: (a) A 1× probe (Fluke PM9001) and (b) its simplified circuit.

Coaxial Cables

The 10× and 1× probes connect to the oscilloscope through cables with coaxial construction. Coaxial cables have a center conductor that is used to transmit a signal and an outer metal braided mesh layer to shield the cable and the signal from electromagnetic interference (EMI). The coaxial cable itself can also be used as a voltage probe with proper terminations, as shown in Figure 6. These cables typically have a 50 Ω characteristic impedance, so the oscilloscope input impedance must be set to 50 Ω.

When the 50 Ω impedance setting is applied in the oscilloscope, the maximum voltage that the scope can support is then limited, typically to 5 V. This limit protects the oscilloscope from excess load. Although coaxial cable measurements are limited to a low voltage range, they pass a much higher bandwidth. A Pomona 2249-C-12 BNC-BNC cable has a bandwidth of 4 GHz, higher than that of many oscilloscope probes.[3]

In order for coaxial cables to be used for SMPS measurements, the printed circuit board (PCB) itself must be equipped with the appropriate matching connector. This means that the board must be designed in advance to incorporate the connector or have enough space to insert one. There are several styles of coaxial cables varying by gauge and connector type that are suitable for demo board measurements.

Many ADI µModule® demo boards utilize the 10 mm diameter BNC connectors. The female BNC-BNC is commonly used for oscilloscope measurements because of its sturdy, reliable construction, and wide availability. These coaxial cables are typically used to measure VOUT ripple in a dynamic load circuit on the output of an SMPS. Subminiature Version B (SMB) and Uf.l connectors are two types of connectors used especially for high frequency measurements.

These two examples are also good for PCBs where space is a critical concern because of their small footprint.

Probe Selection Summary

The 10× probe is recommended for capturing high voltage and some high frequency measurements. The 1× probe is recommended for small voltage and low frequency measurements. Coaxial cables are useful for low voltage and high frequency measurements but require a connector at the test point on the PCB. These differences are summarized in Table 1.

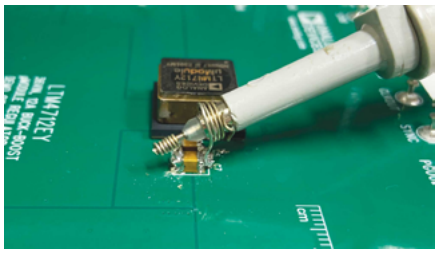

Figure 7: Probe measurement connection with scope pigtails.

	10× Probe (Keysight N2873A)	1× Probe (Fluke PM9001)	Coaxial Cable (Pomona 2249-C-12)
Voltage Range	400 V	30 V	5 V (oscilloscope limited)
Bandwidth	500 MHz	15 MHz	4 GHz
Allows Calibration	Yes	No	No
Requires PCB Connector	No	No	Yes
Recommended Usage	High frequency, high voltage	Low frequency signal, small signal voltage	High frequency signal, small voltage

Table 1: 10×, 1×, and BNC Coaxial Cable Usage Summary

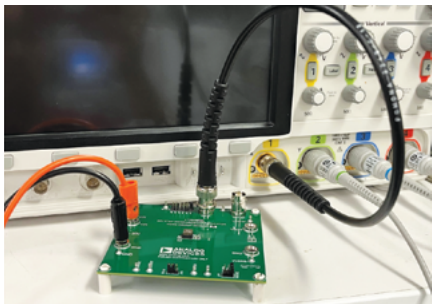

Figure 6: A coaxial cable with a BNC connector.

Measuring Voltage Ripple

Output voltage ripple is a primary specification for power supplies and is a major parameter used to compare different designs. When measuring a ripple that is tens of millivolts or smaller, the location on the board and the method of measurement can significantly influence the results. Coaxial cables can be used to measure the input or output ripple if the voltage is less than 5 V, and if the proper connectors are available on the evaluation board. Otherwise, a 10× probe and a 1× probe are both good options. However, the standard ground clip of these probes would form a long measurement loop that will reduce the accuracy of measurement by increasing the probe's impedance. Pigtail leads are recommended to take this measurement and should make solid contact with the probe tip and ground ring as shown in Figure 7. The difference between test results with a standard probe ground connection and pigtail leads can be seen in Figure 8. Standard bus wire can be used to construct pigtails by wrapping them into a tightly looped coil. Be sure to avoid creating the scope pigtail on the probe itself because this could damage the probe.

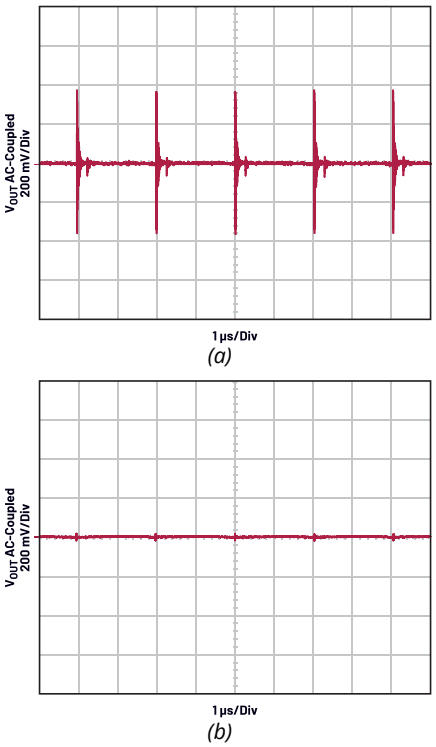

Figure 8: V_{OUT} ripple (a) with normal probe ground clip vs. (b) with scope probe pigtails.

Output voltage ripple is typically measured across the device's output voltage sensing point. In µModule demo boards, the optimized minimal ripple is captured on a ceramic capacitor underneath the board, directly beneath the SMPS output. By measuring on a ceramic capacitor, the ripple from the capacitor's equivalent series resistance (ESR) is less than when measured across a bulk capacitor. By measuring on the bottom of the board, opposite the converter, the board itself provides shielding from EMI noise. In other applications, users may be interested in measuring output voltage ripple at a point far from the converter such as where load is applied. The shape of the output voltage ripple will differ here vs. next to the converter because of parasitic effects from the PCB and the amount of capacitance at this measurement point.

Input voltage ripple should be measured across the input voltage capacitor closest to the IC, as this directly measures the input voltage seen by the IC. Oscilloscope probe pigtails should be used in this measurement for the same reasons described above.

Measuring Switch-Node Waveforms

Proper measurement of the switch node is critical because improper measurement techniques can yield incorrect waveforms, most commonly by introducing false ringing, which can derail debug efforts. To prevent this, use short pigtail leads to ground the oscilloscope probe. Often there will not be an easily accessible ground next to the switch node. To remedy this, scrape off a small patch of solder mask from the ground plane next to the switch node and install a pigtail on the newly exposed ground to use for the measurement. Take care not to short the switch node to ground while doing this. The difference between switch-node waveforms with a standard probe ground connection and with pigtail leads can be seen in Figure 9.

In some µModule parts, the switch node is integrated into the part to reduce the solution's area and is not directly accessible, such as for the LTM8050, a single-channel, 2 A step-down converter. For these parts, the switching node waveform shape can still be viewed by placing a floating scope probe above the µModule package. This will take a coupled measurement of the waveform shape that can be used to view the switching frequency and check for cycle to cycle stability. This coupled waveform will not give an accurate voltage magnitude measurement.

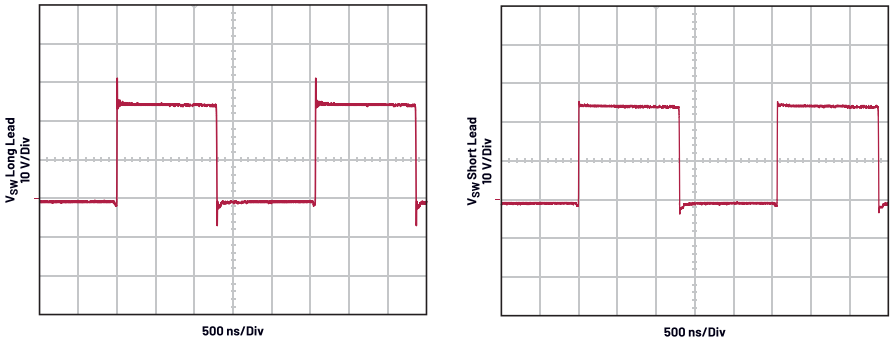

(a) (b)

Figure 9: A switch-node waveform measured (a) with standard scope probe ground lead and (b) with pigtail connections.

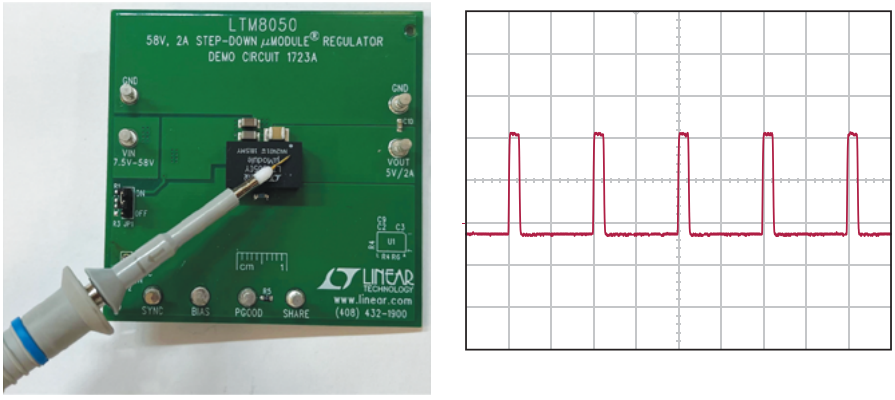

(a) (b)

Figure 10: Example of getting SW node waveform from µModule package by floating the probe over the package, taking a coupled measurement.

The best probe to measure the switch node is typically a 10× probe, as the signal is typically higher frequency or amplitude than a 1× probe will be able to measure.

Conclusion

SMPSs are the go-to power circuit for most applications requiring voltage increases or significant voltage decreases, and for good reason—they offer the optimal combination of noise performance, efficiency, and solution size for many situations. There is a plethora of decisions to be made when designing a SMPS circuit, and accurate measurements of key parameters are needed to inform these decisions and ensure you are making the right choice.

References

1 Keysight N2873A 10× Oscilloscope Probe.
2 Fluke PM9001 1× Oscilloscope Probe.
3 Pomona Electronics BNC Cable.
"Switch Mode Power Supply Basics." Analog Devices, Inc., September 2007.
Aldrick Limjoco. "Understanding Switching Regulator Output Artifacts Expedites Power Supply Design." Analog Dialogue, Vol. 48, No. 8, August 2014.
Aldrick Limjoco. "Measuring Output Ripple and Switching Transients in Switching Regulators." Analog Devices, Inc., January 2013.

www.analog.com

WÜRTH ELEKTRONIK
MORE THAN YOU EXPECT

SIMPLE
BUT
EFFICIENT!

Check the WE-PD standard, robust and performance power inductor options.

www.we-online.com/pd

© sos/iStock

WE meet @ PCIM Europe
Hall 6 - 306

The Premier Global Event in Power Electronics

SAVE *the* DATE

March 7-11, 2027

New Orleans, LA

Ernest N. Morial Convention Center

APEC 2027

IAS IEEE INDUSTRY APPLICATIONS SOCIETY — Linking Research to Practice

IEEE — Advancing Technology for Humanity

pels — IEEE POWER ELECTRONICS SOCIETY — Powering a Sustainable Future

PSMA

1-Cell Li-ion Battery Protection IC for use with Low-Side MOSFETs

Nisshinbo Micro Devices released the NB7130 single-cell Li-ion battery protection ICs in a WLCSP-8-ZA1 package for applications including hearing aids and wearable devices, smartphones, and handheld data terminals.

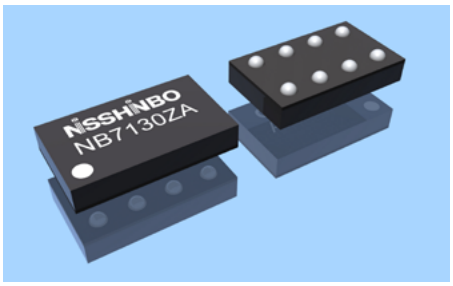

The NB7130 is equipped with all standard safety features, such as overcharge/over-discharge voltage, charge/discharge overcurrent and short circuit detection. The additional safety measures are mainly focussed on the detection range and improved accuracy level of these measurements, which is particularly important for small devices worn on the human body to prevent unintentional injuries when the Li-ion battery may fail. It provides overcharge and over-discharge detection (OVP & UVP), overcurrent detection (OCP) and a low current sense voltage. Using a small (R_{sens}) current-sense resistor causes lower heat generation at high currents. Charging a deeply discharged battery from 0 V can cause an internal short circuit; therefore, the inhibition threshold voltage can be set in a 0.001 V step rate from a safety perspective. A T_{IN} pin is available to connect a thermal sensor to monitor the temperature of the battery cell. An additional STB input offers a Forced Standby Function to set the product into a standby mode. The supply current in normal mode is 3.00 µA / Max. 6.00 µA and max 0.04 µA in standby mode.

www.nisshinbo-microdevices.co.jp

Third-Generation 1500 W wide-range AC/DC Power Modules

TDK Corporation introduced the TDK-Lambda 1500 W rated PFE1500FB AC/DC power modules. This third-generation series accepts a wide 85 to 305 V_{AC} input range, providing the ability to operate on a 277 V_{AC} nominal input to power industrial, lighting, and building automation equipment. The module's metal baseplate allows operation where convection or forced air cooling is not feasible, with the ability to be mounted in a sealed outdoor enclosure or where liquid-cooling is preferred. The five-sided case also provides easier thermal management and lower radiated EMI. The PFE1500FB features a PMBus interface with read/write capability, enabling remote monitoring and programming. This includes output voltage, overvoltage, overcurrent, and undervoltage adjustment. Modules can be connected in parallel for higher output current using the droop mode current share, which can also be programmed using the PMBus. Other signals and functions include remote on/off, a power good signal and a 9.5 - 14 V, 200 mA auxiliary voltage.

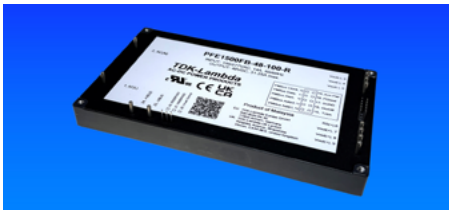

The output voltage adjustment range is 38.4 - 57.6 with typical efficiencies of 92 % at 230 V_{AC} input. The no-load power consumption is 2 W with the output voltage enable toggled to "off". Overall dimensions for the power module are 157.2 mm x 89.9 mm x 15.2 mm (L x W x H) and the "weight" is 540 g. Safety certifications include IEC/UL/CSA/EN62368-1 and carry the CE and UKCA marking for the Low Voltage, EMC and RoHS Directives. The units also comply with EN55032-A with external filtering, meeting the IEC 61000-4 immunity standards. The power supply has 3000 V_{AC} input to output, 2500 V_{AC} input to ground, and 1500 VDC output to ground isolation.

www.tdk.com

AEC-Q Qualified 1200 V SiC Schottky Rectifiers

Taiwan Semiconductor introduces 1200 V SiC Schottky diodes with 1 A and 2 A models in SOD-128 packages. Applications benefiting from these diodes include auxiliary power supplies, bias rectification, bootstrapping circuits, gate driver bias supply, snubbers, bleeder clamp paths, PFC boost diode in low-power designs, and secondary rectification in high-frequency flybacks. All products in the SiC Schottky series are available with PPAP certification.

www.taiwansemi.com

WIMA®

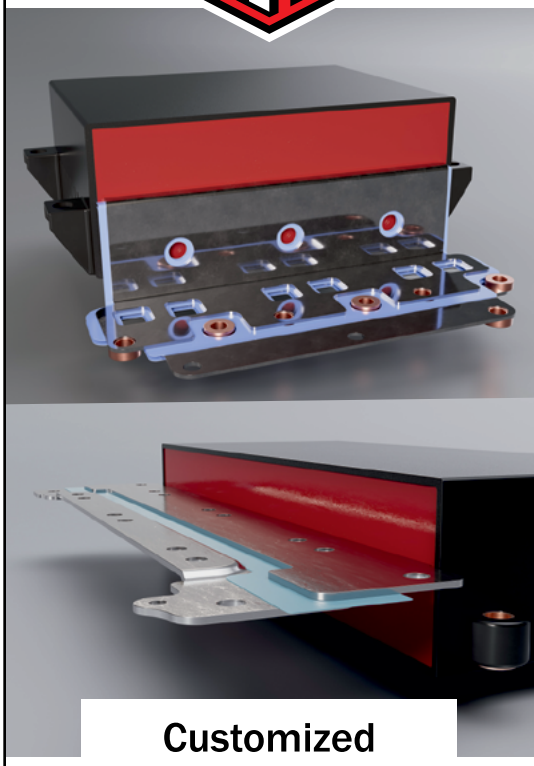

Customized
DC-Link Capacitors

WIMA is presenting a series of DC-LINK capacitors with a sophisticated design for inverter technology:

WIMATec PRO
All-rounder with extremely low self-inductance. Simple design with a wide range of options for adaptation to customer applications.

WIMATec MAX
With significantly reduced self-heating for higher capacitor currents and maximum current path symmetry.

WIMATec ULTRA
With a wide range of connection options for busbars. Optimum cooling through directly connected heat sinks.

WIMATec ULTRA Lite
With modular design for maximum cost efficiency, performance and flexibility.

pcim EUROPE
Nuremberg, 9 - 11 June 2026
Hall 4A / Booth 326

Capacitors Made in Germany !

www.wima.com

Dynamic High Power DC E-Load

ITECH launched the IT8100A/E Series Ultra-Dynamic High Power DC E-Load. Designed for high power density, the IT8100A/E series deliver up to 7.2 kW in a compact 3U chassis (150 V model) and can scale to 1.8 MW through fiber-optic master-slave paralleling, meeting high-voltage and high-current testing requirements. Available in 60 V, 150 V, 600 V, and 1200 V ranges, with standalone power from 2 kW to 86.4 kW, the series features several operating modes – including dynamic, sequence, and advanced loading functions – for performance in applications such as AI server power supplies, power modules, fuel cells, EV charging station, solar array and power electronics. It offers a current slew rate up to 150 A/µs per unit. With 1.5× short-time overloading capability (≤60 s, Ta ≤ 25 °C), it covers transient peak power demands during testing and enables system sizing based on typical operating power rather than peak power, meeting the requirements of power modules, battery packs, and other devices under surge and extreme operating conditions.

www.itechate.com

Discrete Power Solutions

RECOM introduces power ICs and SMD transformers, enabling customers to design their own discrete DC/DC isolated power supplies. The range includes three different topology transformer drivers – flyback, push-pull, and full bridge, integrated and external MOSFET secondary side rectification solutions, and a range of standard subminiature SMD transformers that cover the most common input/output and isolation voltages. The RVPWxxx series flyback power ICs are available with either integrated switches or with a gate drive output for an external MOSFET. These wide input voltage range regulated ICs have three different feedback modes on the same pin: Primary Side Regulation, where the output is regulated by monitoring the primary side waveform to avoid the need for an optocoupler, Secondary Side Regulation, where the output is regulated by optocoupler feedback to maintain the isolation, or Direct DC monitoring for non-isolated applications. The RVPxxx Push-Pull and Full-Bridge transformer drivers are available in DFN2*2 packages. They incorporate all the timing circuits and overcurrent monitoring functions. The heart of any isolated DC/DC converter is the transformer, so RECOM offers a standard range of SMD transformers with isolations from 1.5 kV_{DC} up to 5 kV_{AC} ; custom transformers according to individual specifications are also possible. RECOM also offers the RVSxxx range of secondary side rectification solutions including a fully integrated full bridge rectifier IC in a DFN2*2 package, a self-powered external MOSFET rectifier solution that can operate either high side or low side, and a bidirectional integrated rectifier designed for battery cell charging/discharging.

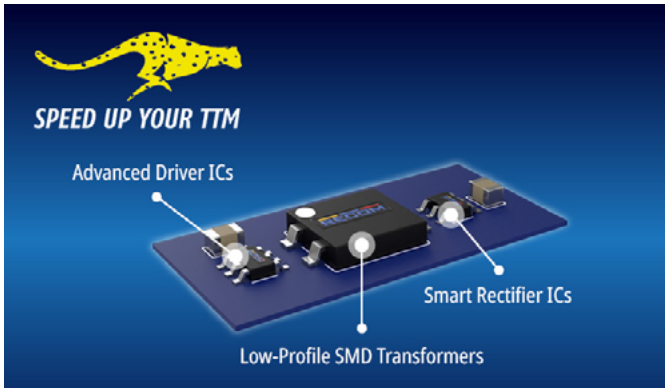

www.recom-power.com

5 kW GaN 3-Phase Inverters for Robotics and Light EVs

Efficient Power Conversion (EPC) introduced the EPC9186HC2 and EPC9186HC3 evaluation boards, two high-performance 3-phase BLDC motor drive inverter platforms designed for applications including robotics, industrial automation, light electric vehicles, electric scooters, forklifts, agricultural machinery, battery-powered mobility systems, and high-power drones. Supporting motor drive systems up to 5 kW, the boards enable engineers to evaluate compact, high-efficiency inverter architectures based on 100 V EPC2361 eGaN® FET technology. The EPC9186HC2 and EPC9186HC3 are based on the EPC9186 platform that was released earlier and have the same hardware architecture. They have another power stage made up of EPC2361 GaN devices that improves conduction performance and allows for higher-current and lower cost operation in motion-control environments. The EPC9186HC2 integrates two EPC2361 eGaN FETs in parallel per switch position, while the EPC9186HC3 uses three devices in parallel, further reducing equivalent on-resistance and improving efficiency at higher load currents. The boards support phase currents up to 150 A_{RMS}, depending on the selected current-sensing configuration, and PWM switching frequencies up to 120 kHz, enabling evaluation of high-density motor drive solutions with fast switching transitions and improved system responsiveness. The inverter platforms operate across a DC input range up to 76 V and feature switching behavior with dv/dt around 6 V/ns, helping reduce torque ripple and acoustic noise in precision motor drive applications. The boards integrate key functions required for three-phase inverter evaluation - including gate drivers, high-bandwidth phase-current sensing, voltage monitoring, housekeeping power supplies, and protection features such as over-current detection and input undervoltage lockout.

www.epc-co.com

Automotive Power Module with integrated MCU and Gate Driver for Three-Phase BLDC Motor Control

Toshiba Electronics Europe begins engineering sample shipments of the AEC-Q100 compliant TB9M030FG, an addition to the SmartMCD™ series that integrates a microcontroller (MCU) and motor driver. The product is suitable for low-speed, sensorless field-oriented control (FOC) of BLDC motors in automotive applications, including electric water pumps, oil pumps, fans, and blowers. Sensorless control of three-phase BLDC motors presents challenges in accurately detecting rotor position at low speeds, creating a strong demand for high-performance sensorless FOC technology capable of delivering stable control from a standstill. The TB9M030FG integrates a 32-bit MCU with an Arm® Cortex®-M0 core, 64 kB flash memory and an additional 12 kB of ROM and 4 kB of RAM. The gate driver controls and drives the N-channel power MOSFETs for three-phase BLDC motor operation. The product also features a vector engine co-processor, a LIN transceiver and a power system that can operate at automotive battery levels. The device is housed in a QFP48 package, measuring 9 mm × 9 mm. Toshiba's sensorless control technology enables position FOC control from zero speed through the low-speed range when used with PM-Synchronous motors, i.e. three-phase BLDC motors with magnetic anisotropy in the rotor ($L_d \neq L_q$), allowing the generation of reluctance torque due to differences in magnetic reluctance within the motor. Compared with the conventional high-frequency injection method, in which the voltage (or current) signal is superimposed and injected into the motor to detect rotor position, this approach eliminates noise caused by harmonic injection and also leads to quieter motor operation.

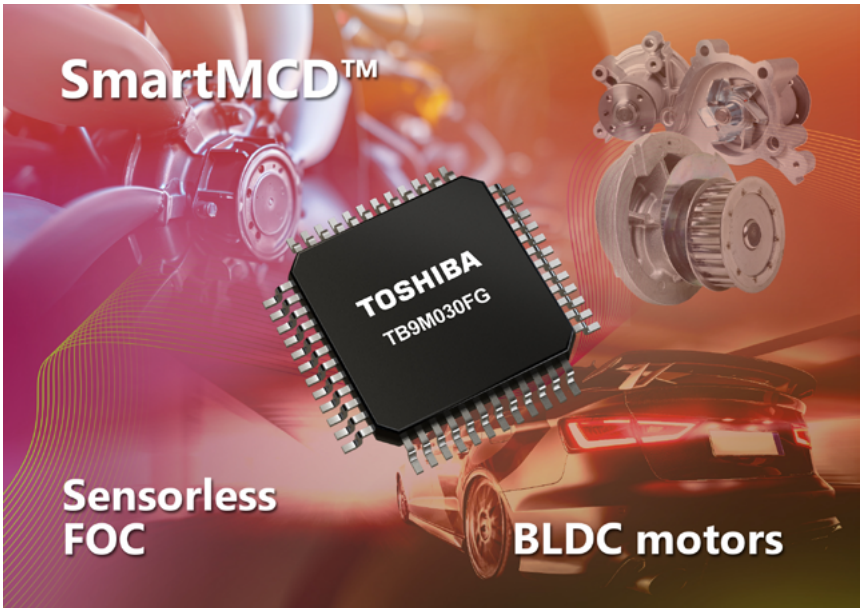

www.toshiba.semicon-storage.com

Power Modules for Traction Inverters

StarPower expands its portfolio with half-bridge and three-phase bridge modules for electric drive systems. The solutions are based on the company's latest chip generation. For example, a family of transfer-molded half-bridge modules designed for traction inverters in power classes starting from 250 kW. These modules are available in both silicon and silicon carbide technologies and utilize the latest Gen3 trench IGBT generation as well as second-generation SiC MOSFETs with conduction losses reaching down to 1.3 mΩ $R_{DS(on)}$ at module level. Si_2N_4 AMB substrates combined with a pin-fin baseplate design enhance heat dissipation. The product range includes 750 V and 1200 V variants, featuring Gen3 IGBT modules rated at 750 A_{rms} and 900 A_{rms}, as well as 450 A_{rms} and 500 A_{rms}. SiC versions are available with $R_{DS(on)}$ values of 1.4 mΩ and 1.0 mΩ, as well as 1.8 mΩ and 1.3 mΩ. In addition, StarPower expands its portfolio of encapsulated three-phase bridge modules for traction inverters in the low- and medium-power range. These modules use SiC MOSFETs, offering losses starting from 2 mΩ $R_{DS(on)}$. The combination of Si_2N_4 AMB substrates and a pin-fin baseplate enhance

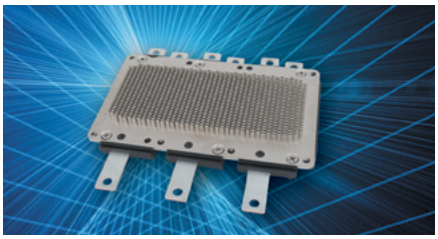

thermal robustness; an integrated current sensor is optionally available. The modules are offered in 750 V and 1200 V versions, including Gen3 IGBT variants rated at 350 A_{rms}, 380 A_{rms}, and 300 A_{rms}. SiC versions are available with $R_{DS(on)}$ values of 2.3 mΩ and 2.0 mΩ, as well as 3.0 mΩ and 2.0 mΩ.

www.starpowereurope.com

Electromagnetic Coils utilizing our tape wound cores provide high precision and reliability for critical applications

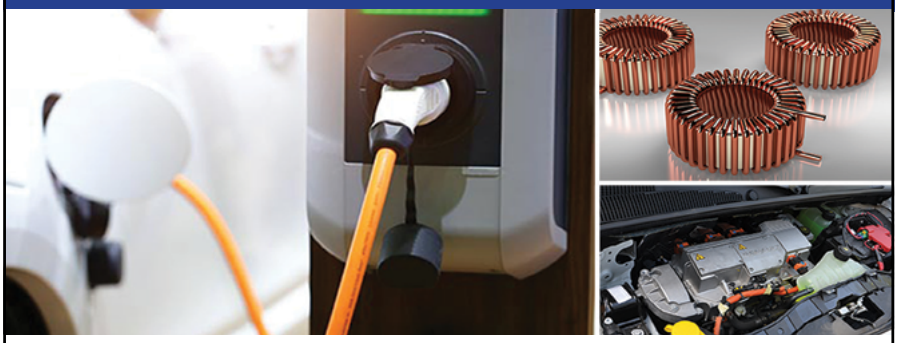

Our coil assemblies meet the stringent specifications and performance requirements that are vital for these applications:

- EV Power & Propulsion Systems
- Aerospace/Military Launching and Defense Systems
- Medical Diagnostic and Monitoring Equipment
- Energy Generation and Distribution Systems
- High-Voltage Power Management Products & Systems

Rely on Magnetic Metals to deliver maximum electromagnetic properties for components used in:

- electric motors,
- transformers,
- generators,
- battery packs,
- EV charging stations,
- power supplies,
- inductors,
- circuit boards,
- sensors
- and more…

Technical and Customer Support

We can customize advanced grades of soft magnetic alloys, enhancing their frequency, permeability and pulse properties to meet your unique requirements.

MADE IN USA

Our competitors' price structure may initially appear lower, but we can guarantee the long-term higher quality that adheres to ANAB ISO 9001:2015, AS9100:9100:2016, ITAR, and USFCR requirements.

Contact Us Today!

75+ YEARS OF CUSTOMER SERVICE

Magnetic Metals Anaheim Division

Phone: (856) 964-7842 Fax: (856) 365-8723
www.magneticmetals.com
© 2025 Magnetic Metals Corporation

SMT Flat-Wire Inductor for Automotive Electronics

Würth Elektronik introduces its WE-SFIA series of flat-wire inductors in 2010, 2013, and 2016 packages. Operating in the temperature range from -40 °C to +180 °C the inductors are available as catalogue components but can also be adapted to meet customer-specific requirements. The WE-SFIA inductors are designed for high-efficiency DC/DC converters in the automotive field, such as single- and multiphase converters, as well as buck and boost converters with high saturation currents of up to 150 A.

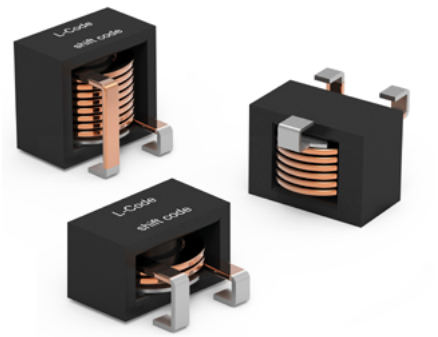

Other filter choke applications include battery management, motor, audio, and infotainment systems. Flat-wire technology used in the chokes offer several advantages: It is mechanically more robust and enables tighter, more even windings as well as improved heat dissipation. Flat-wire windings also offer a larger cross-sectional area, thus reducing electrical resistance. This results in a higher current-carrying capacity, which provides significant advantages in handling transient current peaks. AC losses, such as the skin effect, are also significantly lower in high-frequency applications than in comparable round-wire variants. The flat-wire inductors are available with values from 0.33 µH to 4.7 µH.

www.we-online.de

HV IBC Reference Designs for 800 V_{DC} Architectures in AI Data Centers

Infineon Technologies introduces two high-voltage Intermediate Bus Converter (HV IBC) reference designs to help accelerating the transition to AI server power architectures powered by +/-400 V and 800 V DC. The reference designs address two different architectures: the 800-V_{DC}-to-50-V design serves as an intermediate stage for downstream 48-V IBC modules, while the 800- V_{DC} -to-12-V design enables direct conversion for compact server boards. For custom implementations, the company offers the digital controller XDPP1188-200C, which supports flexible output voltages of 48 V, 24 V, or 12 V. The 800 V_{DC} or +/-400 V to 50 V HV IBC reference design demonstrates more than 98 percent efficiency at full load. Built using Infineon's solution-optimized high-voltage and medium-voltage CoolGaN switches, EiceDRIVER™ gate drivers, and a PSOC™ microcontroller, it consists of two 3 kW 400 V to 50 V converter building blocks, which are configured in an input-series-output-parallel (ISOP) arrangement. The approach scales to 6 kW TDP and supports up to 10.8 kW for 400 µs, using a planar PCB integrated transformer with multiple synchronous rectifier stages and soft switching across all load conditions to reduce EMI. The implementation has a 60 mm x 60 mm x 11 mm form factor and achieves an exceptional 2.5 kW/in³ power density. The second reference design is an ultra-thin HV IBC demo board, which converts an 800 V_{DC} bus voltage directly to a 12 V intermediate rail. The design delivers 6 kW TDP and supports up to 10.8 kW for 400 µs.

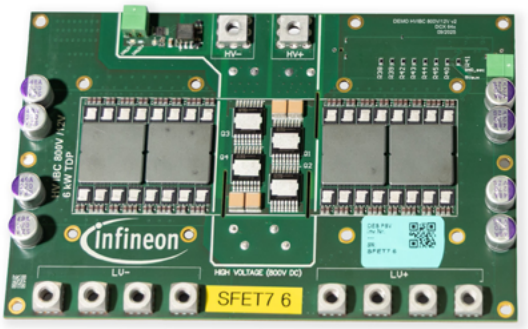

www.infineon.com

Protection for AI Servers and High-End GPUs

Alpha and Omega Semiconductor launched the SmartClamp™ family of protected DrMOS. Designed specifically for the extreme power demands of AI servers, data centers, and high-end graphics cards, the SmartClamp family offers accurate Over Current Protection (OCP) and Negative Current Protection (NCP). The flagship AOZ53228QI provides a special safeguard for multiphase voltage regulators (VRs), preventing catastrophic failures in environments where high peak currents are the norm. Traditional protection methods can suffer from delays; even a mere 50 ns OCP delay can result in a 30 A current runaway, risking permanent damage to the high-side MOSFET - especially when inductor saturation occurs. The SmartClamp family uses current limiting directly within the power stage rather than relying solely on the controller. It provides cycle-by-cycle monitoring utilizing an internal rising-edge current ramp to monitor inductor current in real-time, and it is optimized for industry-standard constant-on-time (COT) and fixed-frequency PWM controllers, as well as the company's own proprietary AOS Advanced Transient Modulator (A2TM) multiphase controllers. Three models for AI servers, data center and high-end graphics cards deliver 60/70/80 A at 18 V while three versions for Gaming and AI PCs provide 55/60/70 A at a voltage of 25 V.

www.aosmd.com

NEW SERIES OF
PLANAR TRANSFORMERS
in the power range from 5 to 25 kW

SIRIO Inductive Components

WHEN YOUR DC/DC CONVERTER HAS:

- working frequency over 100 kHz
- limited ventilation
- harsh industrial environments
- low-height constraint
- high insulation requirements
- cooling via heatsink

SEND US YOUR ELECTRICAL SPECIFICATION TO GET A SAMPLE!

SIRIO ELETTRONICA S.r.l. Via Selve, 2 - 35037 TEOLO (PD) - ITALY Phone: 0039 049 9901090 E-mail: postoffice@sirio-ic.com

Bodo's Wide Bandgap EVENT 2026

December 1 - 2
Hilton Munich Airport

Mark your Calendar!

"Meet the TOP EXPERTS for SiC and GaN!"

December 1
Opening Roundtable & Come Together

December 2
Conference & Tabletop Exhibition

bodoswbg.com

Bodo's Power Systems®

5th Generation SiC MOSFETs

ROHM has developed the latest device of its EcoSiC™ series: the 5th Generation SiC MOSFETs for high-efficiency power applications. This technology is suitable for e. g. xEV traction inverters, onboard chargers (OBCs), DC/DC converters and electric compressors in automotive applications as well as for industrial equipment where it fits into power supplies for AI servers and data centers,

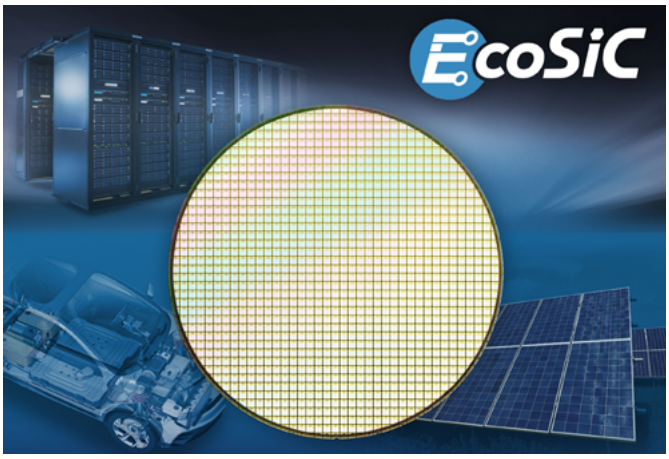

PV inverters, ESS (Energy Storage Systems), UPS (Uninterruptible Power Supplies), eVTOL, AC servos etc. The ON resistance of the 5th Generation SiC is reduced by approximately 30 % during high temperature operation (T_j = 175 °C) compared to conventional 4th Generation products (under the same breakdown voltage and chip size conditions).

www.rohm.com

Advert

TVS Diodes for Automotive Power Protection

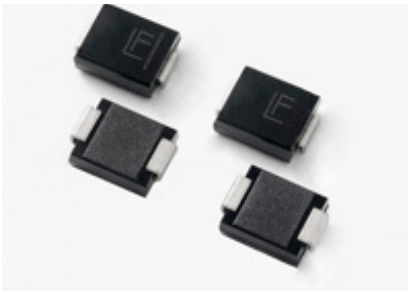

Littlefuse launched its TPSMC, TPSMD, and TP5.0SMDJ high-voltage transient voltage suppression (TVS) diode series, expanding the TP Series portfolio with devices specifically engineered for automotive high-voltage power electronics applications including battery disconnect units (BDUs), high-voltage HVAC systems, and positive temperature coefficient (PTC) heaters. These TVS diodes deliver standoff voltages up to 400 V supporting surge currents up to 300 A and peak pulse power up to 5 kW, while providing a response time of typically less than 1 ps. The devices are AEC-Q101 qualified and PPAP capable for automotive reliability requirements. Integrated in DO-214AB (SMC) surface-mount packages the devices are IEC-61000-4-2 ESD-compliant up to 30 kV.

www.littlefuse.com

Desktop Power Supply for Medical and Industrial Applications

Mascot has introduced the 4320 desktop power supply designed for use across medical, industrial and professional environments. Delivering up to 80 W of output power, it features a universal input range of 90 - 264 V_{AC} and is available with fixed output voltages spanning 12, 16, 24, 48 and 64 V as standard, with a 5 V version and other user-defined outputs available on request. The switching frequency is approximately 65 kHz. Both short-circuit and thermal protection are incorporated to protect critical power supply components from electrical anomalies that have the potential to cause failure or damage, a particularly important attribute in medical and other reliability-critical applications. 4320 is medically certified to IEC 60601-1 edition 3.1 and 3.2, while also meeting IEC 60601-1-11 requirements for home healthcare environments. EMC performance is aligned with IEC/EN 60601-1-2 edition 4.1 for safe and stable operation in crowded electronic environments. In addition, the 4320 complies with IEC 62368-1 and IEC 60335-1, making it suitable for a wide range of household, AV and ICT applications.

The 4320 features a standard 2-pin IEC 60320 (C8) input, with options for 3-pin connectors or fixed mains cords. On the DC side, exchangeable plug solutions are available, supported by standard cord sets or user-specific configurations, enabling straightforward adaptation for different use cases. Furthermore, Mascot offers customisation capabilities for the 4320 series. Accessories for the 4320 series include a wall-mount bracket, 2-pin AC cords, exchangeable DC plugs (individual or in packs) and exchangeable DC push-on terminals.

www.mascot.no

Film Capacitors for High-Frequency Power Electronics

Converter and inverter designs increasingly operate at higher switching frequencies, placing stricter requirements on passive components. Film capacitors with dry plastic dielectrics offer a combination of low losses, high reliability and stable capacitance

over temperature and frequency, making them well suited for DC-link, snubber, coupling, EMC and output filtering applications. A key design factor is the reduction of parasitic elements such as equivalent series inductance (ESL), which directly impacts switching behavior, EMI performance and thermal stress. In this context, self-healing metallized film capacitors provide an additional advantage by improving long-term reliability under dynamic load conditions. To address application-specific challenges, Electronic Concepts Europe applies its PowerPath methodology, focusing on the improvement of geometry, materials and internal design. This enables tailored capacitor solutions that support higher efficiency, reduced component count and improved thermal management.

www.ecicaps.com

High-Voltage Safety Testing Platform

Vitrek launched the V10X electrical safety hipot tester. Designed for automated, connected production environments, the V10X delivers up to 30 kV AC output, and a 100 pA leakage resolution. It provides a single-platform solution for safety testing of appliances, EV components, cable assemblies, power distribution systems, lighting products, and medical electrical equipment. It is designed for connected production environments where safety testing must generate traceable data, integrate with factory networks, and scale with evolving standards. A graphical touchscreen enables test creation, real-time charting, and built-in PDF and CSV report generation, and barcode support is already integrated. Built-in networking, SCPI-compliant automation interfaces, and control of up to 1,600 switch

matrix channels make the system ready for Industry 4.0 production lines. The V10X meets multiple global compliance standards, and is backed by ISO 17025-accredited calibration services.

www.vitrek.com

Copper Conductors for High-Power Transformers and Motors

Hirect now delivers Continuously Transposed Conductors (CTC), Paper Insulated Copper Conductors (PICC), and Enameled Paper Insulated Copper Conductors (EPICC) — all manufactured at Hirect's copper processing plant for transformers, traction motors, and other high-power wound components. The conductors are designed to support key infrastructure segments including power grids, railway rolling stock and catenary power supply systems, and industrial power networks. The continuously transposed conductors (CTC) are aimed for high-efficiency transformers, handling 5 to 63 strands per conductor. Strand dimensions range from 2.5 mm to 12.0 mm in width and 1.0 mm to 5.0 mm in thickness, with transposition pitches adjustable from 25 mm to 200 mm. The PICC

and EPICC (Paper Insulated Conductor) lines accommodate copper widths up to 20 mm and thicknesses up to 8 mm. Overall insulation thickness is precisely controlled between 0.25 mm and 5 mm.

www.hirect.com

Advertising Index

BUILT TO LAST
ENGINEERED TO PERFORM
DESIGNED IN SWITZERLAND

We congratulate *Bodo's Power Systems* to 20 years of promoting *Electronics in Motion and Conversion*!

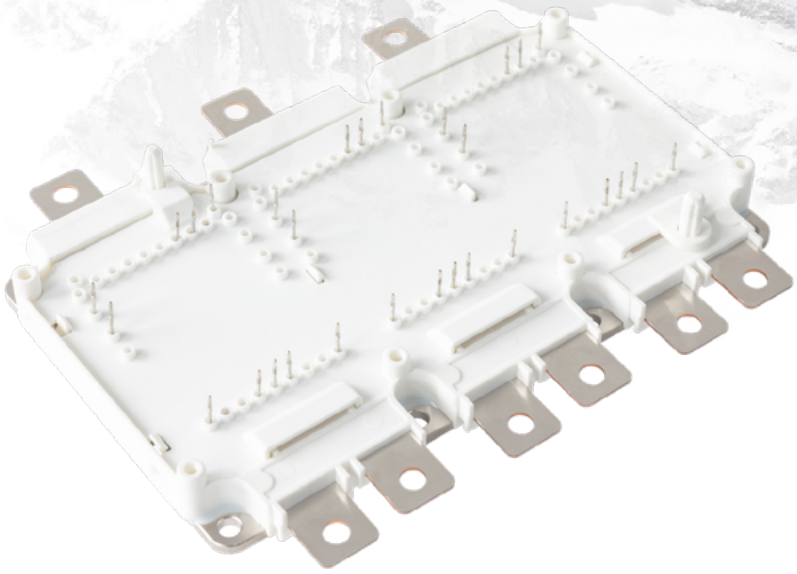

For your applications needing the flexibility: SwissSEM's 1.2 kV EVD-type 6-pack power modules combine advanced chipset technologies with optimized thermal and electrical performance.

Available with automotive optimized *i*25 IGBT/diode chipset and 600 A rating or equipped with the leading-edge *m*23 SiC MOSFET with 2.2 mOhms $R_{DS(on)}$ at 25°C, these modules deliver excellent efficiency and switching performance. The choice is yours!

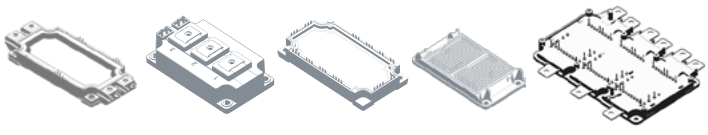

SwissSEM

Ready to optimize your system? Contact us for detailed specifications and technical support or visit our web-page: www.swiss-sem.com

Congratulations to Bodo's Power Systems on its 20th Anniversary. 20 Years of Excellence in connecting innovation with industry. Thanks for your dedication to knowledge sharing and supporting the worldwide power electronics ecosystem. Wishing you many more milestones ahead.
~ Alex Lidow, EPC CEO

GaN Motor Drives for DRONES & HUMANOIDS

EPC33110
100 V, 20 A
Three Phases in 6.5 x 6 mm QFN

https://l.ead.me/EPC91132

epc-co.com

EFFICIENT POWER CONVERSION

pcim
EUROPE

EPC Stand: 9-304